

Electronic Supporting Information for

**Molecular engineering-facilitated AIE-active type-I
photosensitizers for photothermal imaging-guided
photodynamic therapy**

Xiufeng Li, Shasha Zhang, Pengli Gu, Xinyi Zhang and Ju Mei*

Key Laboratory for Advanced Materials, Joint International Research Laboratory of Precision Chemistry and Molecular Engineering, Feringa Nobel Prize Scientist Joint Research Center, School of Chemistry and Molecular Engineering, East China University of Science and Technology, 130 Meilong Road, Shanghai, 200237, China

*E-mail: daisymeiju@ecust.edu.cn

Table of contents

| | |
|---|------|
| 1. Materials and Instruments | S-1 |
| 2. Synthesis | S-2 |
| Scheme S1. Synthetic route to TPAPy and TPAQu. | S-2 |
| Scheme S2. Synthetic route to TPACzPy and TPACzQu. | S-5 |
| 3. Theoretical Calculations | S-8 |
| 4. ROS Generating Ability Test | S-8 |
| 5. Photothermal Properties Measurements | S-9 |
| 6. Nanoparticle Preparation and Characterization | S-9 |
| 7 Studies at Cellular Level | S-10 |
| 8. In-Vivo PDT Studies | S-12 |
| 9. Original Spectra | S-12 |
| Fig. S1. The ¹ H NMR spectrum of compound 3 in CDCl ₃ | S-13 |
| Fig. S2. The ¹³ C NMR spectrum of compound 3 in CDCl ₃ | S-13 |
| Fig. S3. The high-resolution mass spectrum (HRMS) of compound 3 | S-14 |
| Fig. S4. The ¹ H NMR spectrum of compound 8 in CDCl ₃ | S-14 |
| Fig. S5. The ¹³ C NMR spectrum of compound 8 in CDCl ₃ | S-15 |
| Fig. S6. The HRMS of compound 8 | S-15 |
| Fig. S7. The ¹ H NMR spectrum of TPAPy in DMSO- <i>d</i> ₆ | S-16 |
| Fig. S8. The ¹³ C NMR spectrum of TPAPy in DMSO- <i>d</i> ₆ | S-16 |
| Fig. S9. HRMS of TPAPy. | S-17 |
| Fig. S11. The ¹³ C NMR spectrum of compound 9 in CDCl ₃ | S-18 |
| Fig. S12. HRMS of compound 9 | S-18 |
| Fig. S14. The ¹³ C NMR spectrum of TPAQu in DMSO- <i>d</i> ₆ | S-19 |
| Fig. S15. HRMS of TPAQu. | S-20 |
| Fig. S16. The ¹ H NMR spectrum of compound 12 in CDCl ₃ | S-20 |
| Fig. S17. The ¹³ C NMR spectrum of compound 12 in CDCl ₃ | S-21 |
| Fig. S18. HRMS of compound 12 | S-21 |

| | |
|--|------|
| Fig. S19. The ^1H NMR spectrum of compound 13 in CDCl_3 | S-22 |
| Fig. S20. The ^{13}C NMR spectrum of compound 13 in CDCl_3 | S-22 |
| Fig. S21. HRMS of compound 13 | S-23 |
| Fig. S22. The ^1H NMR spectrum of compound 15 in CDCl_3 | S-23 |
| Fig. S23. The ^{13}C NMR spectrum of compound 15 in CDCl_3 | S-24 |
| Fig. S24. HRMS of compound 15 | S-24 |
| Fig. S25. The ^1H NMR spectrum of compound 16 in CDCl_3 | S-25 |
| Fig. S26. The ^1H NMR spectrum of compound 17 in CDCl_3 | S-25 |
| Fig. S27. The ^{13}C NMR spectrum of compound 17 in CDCl_3 | S-26 |
| Fig. S28. HRMS of compound 17 | S-26 |
| Fig. S29. The ^1H NMR spectrum of TPACzPy in $\text{DMSO}-d_6$ | S-27 |
| Fig. S30. The ^{13}C NMR spectrum of TPACzPy in $\text{DMSO}-d_6$ | S-27 |
| Fig. S31. HRMS of TPACzPy..... | S-28 |
| Fig. S32. The ^1H NMR spectrum of compound 18 in CDCl_3 | S-28 |
| Fig. S33. The ^{13}C NMR spectrum of compound 18 in CDCl_3 | S-29 |
| Fig. S34. HRMS of compound 18 | S-29 |
| Fig. S35. The ^1H NMR spectrum of TPACzQu in $\text{DMSO}-d_6$ | S-30 |
| Fig. S36. The ^{13}C NMR spectrum of TPACzQu in $\text{DMSO}-d_6$ | S-30 |
| Fig. S37. HRMS of TPACzQu..... | S-31 |
| Table S1. Theoretically calculated energy levels and energy gaps of TPAPy..... | S-31 |
| Table S2. Theoretically calculated energy levels and energy gaps of TPAQu..... | S-31 |
| Table S3. Theoretically calculated energy levels and energy gaps of TPACzPy .. | S-32 |
| Table S4. Theoretically calculated energy levels and energy gaps of TPACzQu.. | S-32 |
| Fig. S38. The dihedral angles of a) TPAPy, b) TPAQu, c) TPACzPy, and d) TPACzQu..... | S-32 |
| Fig. S39. The normalized UV-Vis spectra of a) TPAPy, b) TPAQu, c) TPACzPy, and d) TPACzQu in different solvents with various polarities..... | S-33 |
| Fig. S40. PL spectra of a) TPAPy, b) TPAQu, c) TPACzPy and d) TPACzQu in different solvents with various polarities..... | S-34 |
| Fig. S41. The UV-Vis spectra of a) TPAPy, b) TPAQu, c) TPACzPy, and d) TPACzQu in the solid state..... | S-35 |
| Fig. S42. The UV-Vis spectra of a) TPAPy, b) TPAQu, c) TPACzPy, and d) TPACzQu in the DMSO/toluene mixtures with different toluene fractions (f_{TS})..... | S-36 |
| Fig. S43. PL spectra of a) TPAPy, b) TPAQu, c) TPACzPy, and d) TPACzQu in the DMSO/toluene mixtures with different f_{TS} | S-37 |
| Fig. S44. PL spectra of a) DCFH+TPAPy, b) TPAPy, c) DCFH+TPAQu, d) TPAQu, e) DCFH+TPACzPy, f) TPACzPy, g) DCFH+TPACzQu, h) TPACzQu, and g) DCFH+RB in the DMSO/PBS ($v/v = 2/98$) mixture under the irradiation of white light for different time..... | S-38 |
| Fig. S45. PL spectra of DHR123 in the presence of a) TPAPy and d) TPAQu in the DMSO/PBS ($v/v = 2/98$) mixture under the white-light irradiation with different time. PL spectra of HPF in the presence of b) TPAPy and e) TPAQu in the DMSO/PBS ($v/v = 2/98$) mixture under the white-light irradiation with different time. The UV-Vis spectra of ABDA in the presence of c) TPAPy and f) TPAQu after being irradiated by white light..... | S-38 |

| | |
|---|------|
| for different time. | S-39 |
| Fig. S46. PL spectra of DHR123 in the presence of a) TPACzPy and d) TPACzQu in the DMSO/PBS (v/v = 2/98) mixture under the white-light irradiation with different time. PL spectra of HPF in the presence of b) TPACzPy and e) TPACzQu in the DMSO/PBS (v/v = 2/ 98) mixture under the white-light irradiation with different time. The UV-Vis spectra of ABDA in the presence of c) TPACzPy and f) TPACzQu after being irradiated by white light for different time. | S-39 |
| Fig. S47. The temperature variation of the solid-state a) TPAPy and c) TPAQu under the irradiation of a 660 nm-laser (0.70 W/cm ²). The temperature profiles of the solid-state b) TPAPy and d) TPAQu under the irradiation of a 660 nm-laser (0.70 W/cm ²) in six ON/OFF cycles. | S-40 |
| Fig. S48. The temperature variation of the solid-state a) TPACzPy and c) TPACzQu under the irradiation of a 660 nm-laser (0.70 W/cm ²). The temperature profiles of the solid-state b) TPACzPy and d) TPACzQu under the irradiation of a 660 nm-laser (0.70 W/cm ²) in six ON/OFF cycles. | S-41 |
| Fig. S49. The UV-Vis spectra of a) TPAPy and c) TPAQu solutions at different concentrations. The linear relationship between the absorbance and concentration of b) TPAPy and d) TPAQu. | S-42 |
| Fig. S50. The UV-Vis spectra of a) TPACzPy and c) TPACzQu solutions at different concentrations. The linear relationship between absorbance and concentration of b) TPACzPy and d) TPACzQu. | S-43 |
| Fig. S51. Photothermal behaviors of a) TPAPy, b) TPAQu, and c) TPACzQu NPs at different concentrations (660 nm, 1.47 W/cm ²). Photothermal behaviors of d) TPAPy, e) TPAQu, and f) TPACzQu NPs at different power densities (660 nm, 200 µg/mL).44 | |
| Fig. S52. Photothermal images of TPAPy NPs, TPAQu NPs, and TPACzQu NPs (at different concentrations) when irradiated with 660 nm laser for 8 minutes (1.47 W/cm ²). | S-44 |
| Fig. S53. Photothermal images of TPAPy NPs, TPAQu NPs and TPACzQu NPs when irradiated with 660 nm laser (at different power densities) for 8 minutes (200 µg/mL). | S-45 |
| Fig. S54. The Photothermal stability of a) TPAPy, b) TPAQu, c) TPACzPy, and d) TPACzQu (660 nm, 1.16 W/cm ² , 200 µg/mL). | S-46 |
| Fig. S55. Intracellular ROS, O ₂ ^{•-} , ·OH and ¹ O ₂ detection of TPACzPy NPs (4T1 cells), accessed by DCFH-DA, DHR123, HPF, and SOSG, respectively | S-47 |
| Fig. S56. a) The temperature difference between the mice injected with TPACzPy NPs and PBS for 20 h using 660 nm laser at the tumor site for two minutes. b, c) Blood biochemistry indices (aspartate aminotransferase (AST) and blood urea nitrogen (BUN) of the mice obtained at day 7 after treatment. | S-47 |
| Fig. S57. Photographs of 4T1 tumor-bearing mice in different groups on day 0, 2 and 7 during the treatment process. | S-48 |
| Reference | S-48 |

1. Materials and Instruments

1.1 Materials

1,4-Benzenediacetonitrile, palladium acetate, 4,4'-dimethoxydiphenylamine, potassium hexafluorophosphate and ultra-dry tetrahydrofuran (THF) are Adamas-beta-branded and purchased from Shanghai Titan Technology Co., Ltd. *p*-Bromobenzaldehyde was purchased from Energy Chemical. Ethyl bromide and ethyl iodide were purchased from Shanghai Aladdin Biochemical Technology Co., Ltd. 4-Pyridine formaldehyde was purchased from Shanghai Darui Fine Chemicals Co., Ltd. 4-Quinoline formaldehyde was purchased from Bide Pharmatech. Ltd. Tri-*tert*-butylphosphine was purchased from Shanghai Maclean Co., Ltd., and ultra-dry *N,N*-dimethylformamide (DMF) was purchased from Shanghai Merrell Chemical Technology Co., Ltd. 2,7-Dibromocarbazole was purchased from Shanghai Haohong Scientific Co., Ltd. Cesium carbonate, potassium *tert*-butoxide, sodium chloride and sodium sulfate are GENERAL-REAGENT-branded, and purchased from Shanghai Titan Technology Co., Ltd. *N*-formylpiperidine and *n*-butyllithium (*n*-BuLi) were purchased from J&K Scientific Co. Ltd. Dimethyl sulfoxide (DMSO) used for spectroscopic testing is chromatographically pure and was purchased from Alfa Aesar Chemical Co., Ltd. (China).

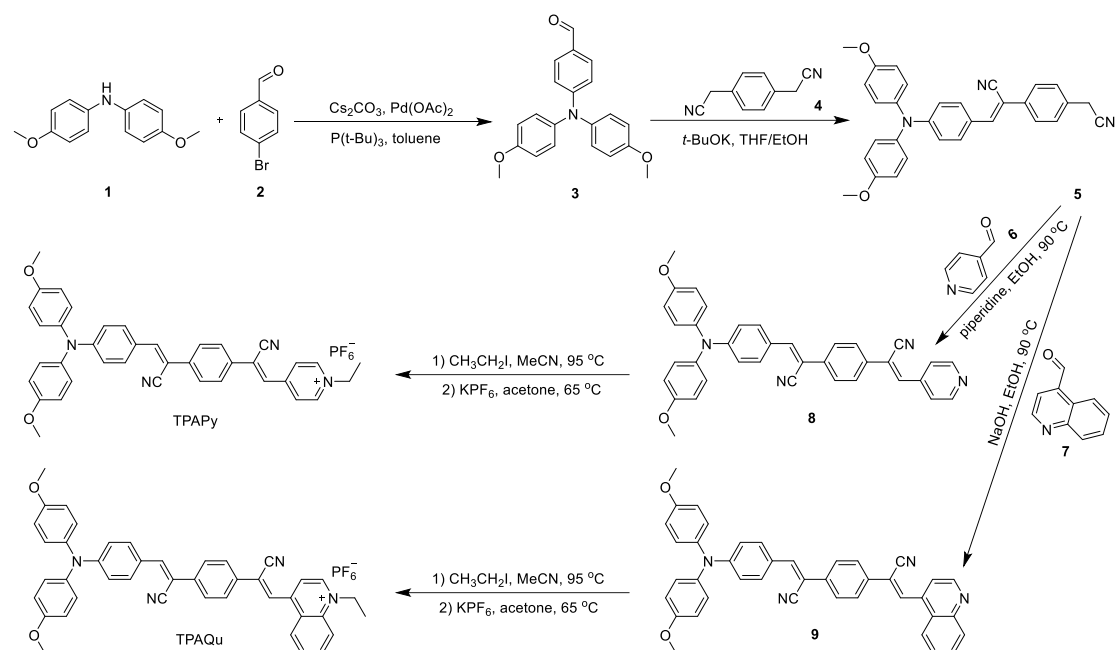
The biological chemical reagents including dihydrorhodamine 123 (DHR 123) were obtained from KGI Biotechnology Co., Ltd., Jiangsu. The ROS (reactive oxygen species) indicators 2',7'-dichlorodihydrofluorescein diacetate (DCFH-DA) and hydroxyphenyl fluorescein (HPF) were purchased from Shanghai Chuangsai Technology Co., Ltd. Singlet oxygen sensor green (SOSG) and Calcein-AM/PI were purchased from Shanghai Beyotime Biotechnology Co., Ltd. 9,10-Anthracene diylbis(methylene) dimalonic acid (ABDA) was purchased from J&K Scientific Co. Ltd. Cell Counting Kit-8 (CCK-8) was obtained Wenzhou Puno Biotechnology Co., Ltd. Fetal bovine serum (FBS) and penicillin-streptomycin were purchased from Gibco. Roswell Park Memorial Institute 1640 (RPMI 1640) and phosphate buffered saline (PBS, 10 mM, pH = 7.4) were obtained from Bioagrio.

1.2 Instruments

¹H NMR and ¹³C NMR spectra were measured on a Bruker AV 400, AVANCE III 400 or Ascend 600 spectrometer. High-resolution mass spectrometry (HRMS) was measured on a Xevo G2 TOF MS spectrometer. UV-Vis absorption spectra were measured on a Shimadzu UV-600 spectrophotometer. Photoluminescence (PL) spectra were recorded on the Edinburgh FLS-1000 or the PE LS-55 spectrofluorometer. The particle size analysis was performed on a Malvern Zetasizer Nano ZSE. Transmission electron microscope (TEM) images were obtained on the JEM 1400. The photothermal properties were studied with a 660 nm laser (MW-GX-660/1300 mW) and the photothermal images were taken with an infrared thermal imager (E6, FLIR Inc.). The 660 nm light source for the photothermal properties evaluation at the cellular level is a LED array (LED-II). White-light source for ROS-generation evaluation of AIEgens in solutions is from commercial LED lamps (KM-S059N), while that used for cellular experiments is from a 96-hole LED array (HC-TG030011-WH). A Xenon lamp irradiator was used for the in-vivo therapeutic effect assessment (CXE-350). Confocal laser scanning microscopy (CLSM) images were obtained on a STELLARIS 8 Leica confocal scanning microscope (STELLARIS 5,

Germany). The in-vivo imaging of mice were performed with a Living Image system and the relative fluorescence intensity was analyzed by Living Image 4.3.1 software (Caliper).

2. Synthesis



Scheme S1. Synthetic route to TPAPy and TPAQu.

2.1 Synthesis of compound 3

Under the N₂ atmosphere, a mixture of compound 1 (1.15 g, 5.00 mmol), compound 2 (1.39 g, 7.50 mmol), Cs₂CO₃ (2.45 g, 7.50 mmol), Pd(OAc)₂ (56 mg, 0.25 mmol), and P(*t*-Bu)₃ (0.5 mL, 0.50 mmol) in 25 mL toluene was stirred at 110 °C for 6 h. After being cooled to room temperature, the reaction mixture was diluted with dichloromethane (50 mL) and washed with water (50 mL) for three times. The organic phase was separated and dried over anhydrous Na₂SO₄, filtered, and concentrated under reduced pressure. The resulting crude mixtures were purified by column chromatography on silica gel (petroleum ether/ethyl acetate, 5/1 in volume ratio) to give the compound 3 as a yellow solid with a yield of 80.5%. ¹H NMR (400 MHz, CDCl₃) δ (TMS, ppm): 9.75 (s, 1H), 7.62 (t, *J* = 5.6 Hz, 2H), 7.17–7.09 (m, 4H), 6.92–6.87 (m, 4H), 6.85 (d, *J* = 8.8 Hz, 2H), 3.81 (s, 6H). ¹³C NMR (100 MHz, CDCl₃) δ (TMS, ppm): 190.31, 157.33, 154.08, 138.84, 131.44, 128.08, 127.79, 116.77, 115.08, 55.50. HRMS (ESI, *m/z*): [M+H]⁺ calcd. for C₂₁H₂₀NO₃⁺ 334.1438, found 334.1435.

2.2 Synthesis of compound 5

A two-necked bottle equipped with a magnetic stir bar was charged with compound 4 (187 mg, 1.20 mmol) and 10 mL THF. Compound 3 (333 mg, 1.00 mmol) was dissolved in 15 mL THF and potassium *tert*-butanol (56 mg, 0.50 mmol) was dissolved in 5 mL ethanol, which were added to a constant pressure dropping funnel. Under the N₂ atmosphere, the reaction system is heated to 60 °C, with the mixture of compound 3 and potassium *tert*-butanol being dripped into the reaction flask via the constant pressure dropping funnel. Half an hour after the end of the dripping, the reaction was immediately terminated with

dilute hydrochloric acid. After being cooled to room temperature, the reaction mixture was diluted with dichloromethane (80 mL) and washed with saturated saline solution (100 mL) for three times. The organic phase was separated, collected, and dried over anhydrous Na₂SO₄, filtered, and concentrated under reduced pressure, affording crude product of compound **5** which will be used for the next step without further purification.

2.3 Synthesis of compound **8**

A 100 mL round-bottom flask equipped with a magnetic stir bar was charged with compound **5** (235 mg, 0.50 mmol), compound **6** (94 μ L, 1.00 mmol), and piperidine (100 μ L, 1.00 mmol), to which 15 mL ethanol was added, and the resulted reaction mixture was heated for 12 h at 90 °C. Filtered while hot, collected the filter residue, and got a crude product. The resulting crude mixtures were purified by column chromatography on silica gel (petroleum ether/ethyl acetate = 3/1 (v/v)) to give the compound **8** as an orange-red solid with a yield of 86.6%. ¹H NMR (400 MHz, CDCl₃) δ (TMS, ppm): 8.76 (d, *J* = 6.0 Hz, 2H), 7.81–7.69 (m, 8H), 7.50 (d, *J* = 15.4 Hz, 2H), 7.18–7.08 (m, 4H), 6.95–6.82 (m, 6H), 3.82 (s, 6H). ¹³C NMR (100 MHz, CDCl₃) δ (TMS, ppm): 157.08, 151.32, 150.47, 142.93, 139.11, 138.52, 137.25, 132.86, 131.18, 127.78, 126.82, 126.16, 124.17, 122.78, 118.68, 117.76, 116.69, 115.84, 115.00, 104.60, 55.53. HRMS (ESI, *m/z*): [M+H]⁺ calcd. for C₃₇H₂₉N₄O₂⁺ 561.2285, found: 561.2282.

2.4 Synthesis of TPAPy

Under the N₂ atmosphere, a mixture of compound **8** (200 mg, 0.36 mmol) and ethyl iodide (144 μ L, 1.80 mmol) in 10 mL of acetonitrile was stirred at 95 °C for 6 h. After being cooled to room temperature, the solvents were removed by vacuum distillation to obtain the reaction intermediates. Then added 10 mL of acetone to dissolve them, and transferred them into a two-necked flask, to which 3 mL of saturated aqueous solution of potassium hexafluorophosphate was added afterwards. After 2 hours of reflux and being cooled to room temperature, the reaction mixture was diluted with dichloromethane (50 mL) and washed with saturated saline solution (50 mL) for three times. The organic phase was collected and concentrated under reduced pressure to obtain a crude product. The resulting crude mixtures were purified by the alumina column chromatography (dichloromethane/methanol = 3/1, v/v) and then further purified by the recrystallization with ethanol to give TPAPy as black solid with a yield of 86.6%. ¹H NMR (400 MHz, DMSO-*d*₆) δ (TMS, ppm): 9.20 (d, *J* = 6.9 Hz, 2H), 8.48 (d, *J* = 6.8 Hz, 2H), 8.39 (s, 1H), 8.04 (s, 1H), 7.95 (dd, *J*₁ = 19.2 Hz, *J*₂ = 8.8 Hz, 4H), 7.85 (d, *J* = 9.1 Hz, 2H), 7.26–7.12 (m, 4H), 7.07–6.94 (m, 4H), 6.76 (d, *J* = 9.0 Hz, 2H), 4.65 (q, *J* = 7.3 Hz, 2H), 3.77 (s, 6H), 1.59 (t, *J* = 7.3 Hz, 3H). ¹³C NMR (150 MHz, DMSO-*d*₆) δ (TMS, ppm): 157.42, 151.55, 149.27, 145.40, 144.23, 138.82, 137.68, 136.61, 132.17, 131.78, 128.53, 127.91, 127.19, 126.44, 124.16, 119.22, 118.95, 116.81, 116.52, 115.71, 103.68, 56.76, 55.78, 16.53. HRMS (ESI, *m/z*): [M-PF₆]⁺ calcd. for C₃₉H₃₃N₄O₂⁺ 589.2598, found 589.2601.

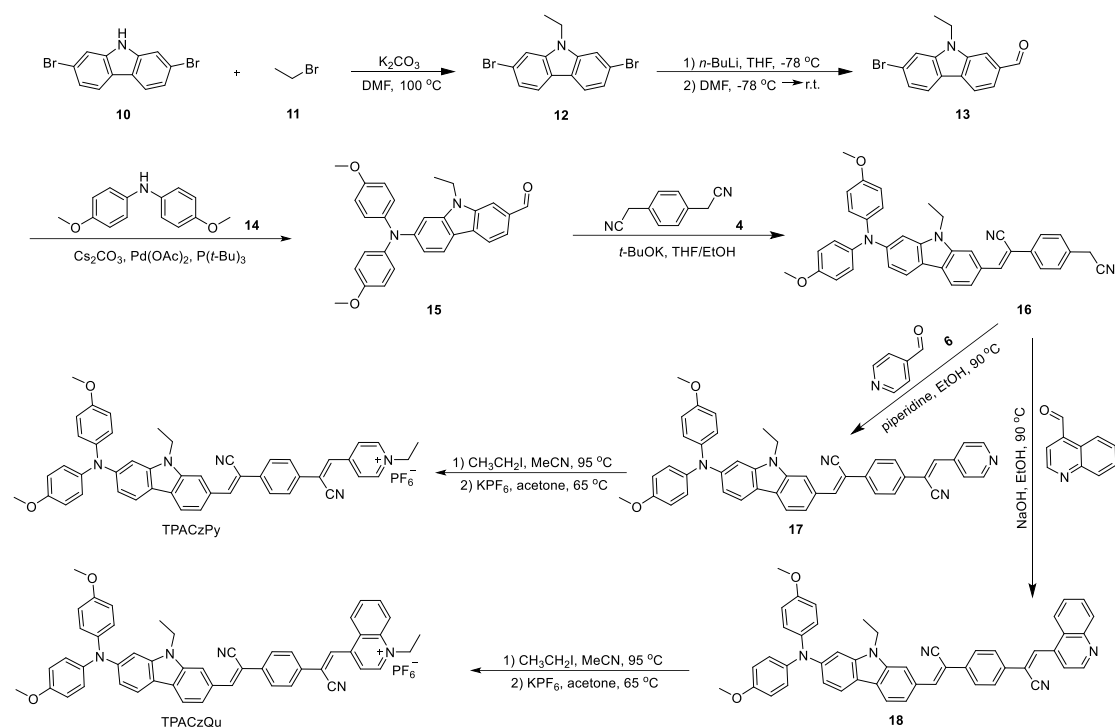
2.5 Synthesis of compound **9**

A 100 mL round-bottom flask equipped with a magnetic stir bar was charged with compound **5** (235 mg, 0.50 mmol), compound **7** (314 mg, 2.00 mmol), sodium hydroxide (20 mg, 0.50 mmol), to which 15 mL ethanol was added, and the reaction mixture was

heated 12 h at 90 °C. The reaction was immediately terminated with dilute hydrochloric acid. After being cooled to room temperature, the reaction mixture was diluted with dichloromethane (80 mL) and washed with saturated saline solution (100 mL) for three times to obtain a crude product. The resulting crude mixtures were purified by column chromatography on silica gel (hexane/ethyl acetate = 3/1, v/v) to give the compound **9** as a red solid with a yield of 56.3%. ¹H NMR (400 MHz, CDCl₃) δ (TMS, ppm): 9.06 (d, *J* = 4.5 Hz, 1H), 8.26 (d, *J* = 10.2 Hz, 2H), 8.01 (d, *J* = 8.2 Hz, 1H), 7.93 (d, *J* = 4.4 Hz, 1H), 7.84 (d, *J* = 8.4 Hz, 3H), 7.78 (dd, *J*₁ = 8.7 Hz, *J*₂ = 3.8 Hz, 4H), 7.67 (q, *J* = 7.0 Hz, 1H), 7.51 (d, *J* = 6.8 Hz, 1H), 7.14 (d, *J* = 8.8 Hz, 4H), 6.95–6.83 (m, 6H), 3.83 (s, 6H). ¹³C NMR (100 MHz, CDCl₃) δ (TMS, ppm): 157.08, 151.33, 150.19, 142.95, 139.11, 137.30, 136.86, 132.75, 131.20, 130.10, 127.79, 127.64, 126.95, 126.21, 126.05, 124.18, 123.24, 120.16, 117.76, 115.01, 104.61, 55.54. HRMS (ESI, *m/z*): [M+H]⁺ calcd. for C₄₁H₃₁N₄O₂⁺ 611.2442, found 611.2439.

2.6 Synthesis of TPAQu

Under the N₂ atmosphere, a mixture of compound **9** (305 mg, 0.50 mmol) and ethyl iodide (800 μL, 10.00 mmol) in 10 mL of acetonitrile was stirred at 95 °C temperature for 24 h. After being cooled to room temperature, the solvents were removed by vacuum distillation to obtain the reaction intermediates. 10 mL of acetone was added to dissolve the reaction intermediates, and the resulted mixture was transferred to a two-necked flask. Then 5 mL of saturated aqueous solution of potassium hexafluorophosphate was added. After 4 hours of reflux and being cooled to room temperature, the reaction mixture was diluted with dichloromethane (50 mL) and washed with saturated saline solution (50 mL) for three times. The organic phase was collected and concentrated under reduced pressure to give the crude product. The resulting crude mixtures were purified by the alumina column chromatography (dichloromethane/methanol = 100/1, v/v) and washed with ethanol at 85 °C. TPAQu were obtained as black solids with a yield of 41.5% after hot filtration. ¹H NMR (400 MHz, DMSO-*d*₆) δ (TMS, ppm): 9.69 (d, *J* = 6.3 Hz, 1H), 8.99 (s, 1H), 8.70 (d, *J* = 9.0 Hz, 2H), 8.60 (d, *J* = 6.1 Hz, 1H), 8.42–8.23 (m, 1H), 8.15–8.08 (m, 3H), 8.07 (s, 1H), 7.95 (d, *J* = 8.6 Hz, 2H), 7.87 (d, *J* = 9.0 Hz, 2H), 7.18 (t, *J* = 11.2 Hz, 4H), 7.00 (d, *J* = 8.9 Hz, 4H), 6.77 (d, *J* = 8.9 Hz, 2H), 5.14 (q, *J* = 7.2 Hz, 2H), 3.77 (d, *J* = 6.1 Hz, 6H), 1.74–1.57 (m, 3H). ¹³C NMR (150 MHz, DMSO-*d*₆) δ (TMS, ppm): 157.42, 151.53, 150.59, 149.34, 144.16, 138.84, 137.86, 137.57, 136.25, 135.90, 132.16, 131.77, 130.72, 128.53, 128.26, 128.08, 128.00, 126.32, 124.19, 122.04, 121.13, 119.94, 119.00, 116.83, 116.40, 115.71, 103.80, 55.79, 53.82, 15.64. HRMS (ESI, *m/z*): [M-PF₆]⁺ calcd. for C₄₃H₃₅N₄O₂⁺ 639.2755, found 639.2756.



Scheme S2. Synthetic route to TPACzPy and TPACzQu.

2.7 Synthesis of compound 12

Under the N₂ atmosphere, a mixture of compound **10** (650 mg, 2.00 mmol) and anhydrous potassium carbonate (829 mg, 6.00 mmol) in 15 mL of ultra-dry DMF was stirred at 80 °C temperature for 1 h. Compound **11** (447 μ L, 6.00 mmol) was added to the reaction system using a syringe and the mixture was heated and kept stirring at 100 °C for 6 h. After being cooled to room temperature, the reaction mixture was decanted into 100 mL of ultrapure water and extracted with ethyl acetate (100 mL) for three times. The organic phase was collected and dried over Na₂SO₄, filtered, and concentrated under reduced pressure. The resulting crude mixture was purified by the column chromatography on silica gel (petroleum ether/ethyl acetate = 20/1, v/v) to give the compound **12** as a white solid with a yield of 88.9%. ¹H NMR (400 MHz, CDCl₃) δ (TMS, ppm): 7.89 (d, *J* = 8.3 Hz, 2H), 7.54 (d, *J* = 1.5 Hz, 2H), 7.34 (dd, *J*₁ = 8.3, *J*₂ = 1.6 Hz, 2H), 4.27 (q, *J* = 7.2 Hz, 2H), 1.42 (t, *J* = 7.2 Hz, 3H). ¹³C NMR (100 MHz, CDCl₃) δ (TMS, ppm): 140.88, 122.56, 121.56, 121.39, 119.72, 111.82, 37.84, 13.73. HRMS (NSI, *m/z*) [M+H]⁺ calcd. for C₁₄H₁₂BrN⁺ 351.9331, found 351.9332.

2.8 Synthesis of compound 13

Under strict anhydrous and oxygen-free conditions, compound **12** (1.05 g, 3.00 mmol) was added into a 100 mL round-bottom flask and dissolved with 40 mL ultrapure THF and then cooled to -78 °C. A solution of *n*-butyllithium (1.38 mL, 3.30 mmol) was added dropwise. After stirring at -78 °C for 2 h, anhydrous DMF (0.35 mL, 4.50 mmol) was added. After further stirring at -78 °C for 1 h, the mixture was warmed to room temperature and stirred for 6 h. Then dilute hydrochloric acid was slowly added to the reaction mixture under stirring to quench the reaction. The solvent was removed under reduced pressure and extracted with dichloromethane and water. The organic phase was collected and dried over Na₂SO₄

to afford the crude product. The resulting crude mixture was purified by the silica-gel column chromatography (hexane/ethyl acetate = 10/1, v/v) to give the compound **13** as a light-yellow oil with a yield of 48.9%. ¹H NMR (400 MHz, CDCl₃) δ (TMS, ppm): 10.16 (s, 1H), 8.21–8.14 (m, 1H), 8.03–7.92 (m, 2H), 7.75 (dt, *J*₁ = 4.1 Hz, *J*₂ = 2.1 Hz, 1H), 7.61 (d, *J* = 1.4 Hz, 1H), 7.38 (dd, *J*₁ = 8.3 Hz, *J*₂ = 1.5 Hz, 1H), 4.39 (q, *J* = 7.2 Hz, 2H), 1.46 (t, *J* = 7.2 Hz, 3H). ¹³C NMR (100 MHz, CDCl₃) δ (TMS, ppm): 191.40, 141.36, 138.73, 133.12, 126.58, 121.87, 121.56, 120.76, 120.51, 119.88, 119.60, 111.07, 108.50, 36.90, 12.83. HRMS (DART, *m/z*): [M+H]⁺ calcd. for C₁₅H₁₃BrNO⁺ 302.0175, found 302.0175.

2.9 Synthesis of compound 15

Under the atmosphere of N₂, a mixture of compound **13** (301 mg, 1.00 mmol), compound **15** (343 mg, 1.50 mmol), Cs₂CO₃ (487 mg, 1.50 mmol), Pd(OAc)₂ (11 mg, 0.05 mmol), and P-*t*(Bu)₃ (100 μL, 0.10 mmol) in 20 mL toluene was stirred at 110 °C for 6 h. After being cooled to room temperature, the reaction mixture was diluted with dichloromethane (100 mL) and washed with water (100 mL) for three times. The organic phase was collected and dried over Na₂SO₄, filtered, and concentrated under reduced pressure. The resulting crude mixture was purified by the silica-gel column chromatography (hexane/ethyl acetate = 1/10, v/v) to give the compound **15** as a light-yellow solid with a yield of 67.2%. ¹H NMR (400 MHz, CDCl₃) δ (TMS, ppm): 10.10 (s, 1H), 8.03 (d, *J* = 7.9 Hz, 1H), 7.88 (d, *J* = 9.3 Hz, 2H), 7.68 (d, *J* = 7.9 Hz, 1H), 7.13 (d, *J* = 8.9 Hz, 4H), 6.94–6.81 (m, 6H), 4.22 (q, *J* = 7.1 Hz, 2H), 3.82 (s, 6H), 1.33 (t, *J* = 7.2 Hz, 3H). ¹³C NMR (100 MHz, CDCl₃) δ (TMS, ppm): 191.55, 155.00, 148.43, 140.05, 138.86, 131.50, 127.76, 125.71, 120.83, 118.22, 114.71, 113.72, 107.25, 98.84, 54.47, 36.50, 12.77. HRMS (NSI, *m/z*): [M+H]⁺ calcd. for C₂₉H₂₇N₂O₃⁺ 451.2016, found 451.2014.

2.10 Synthesis of compound 16

A two-necked reaction bottle equipped with a magnetic stir bar was charged with compound **4** (187 mg, 1.20 mmol), 2.5 mL ethanol and 7.5 mL THF. Compound **3** (333 mg, 1.00 mmol) was dissolved in 15 mL THF and potassium *tert*-butanol (56 mg, 0.50 mmol) was dissolved in 5 mL ethanol, which were added to a constant pressure dropping funnel. Under the N₂ atmosphere, the reaction system is heated to 60 °C, and the dropping funnel is opened to slowly drip the mixture of compound **3** and potassium *tert*-butanol into the reaction flask. Half an hour after the end of the dripping, the reaction was immediately terminated with dilute hydrochloric acid. After being cooled to room temperature, the reaction mixture was diluted with dichloromethane (100 mL) and washed with saturated saline solution (100 mL) for three times. The organic phase was collected and concentrated under reduced pressure. The resulting crude mixture was purified by the column chromatography on silica gel (petroleum ether/ethyl acetate/dichloromethane = 10/1/2, v/v/v) and was washed by methanol to give the compound **16** as an orange-yellow solid with a yield of 46.2%. ¹H NMR (400 MHz, CDCl₃) δ (TMS, ppm): 8.10 (s, 1H), 7.97 (d, *J* = 7.6 Hz, 1H), 7.86 (s, 1H), 7.73 (d, *J* = 8.4 Hz, 3H), 7.59 (d, *J* = 8.1 Hz, 1H), 7.44 (t, *J* = 13.0 Hz, 2H), 7.26–7.01 (m, 4H), 6.91 (t, *J* = 28.8 Hz, 6H), 4.21 (q, *J* = 7.1 Hz, 2H), 3.80 (t, *J* = 11.4 Hz, 8H), 1.37 (t, *J* = 7.2 Hz, 3H).

2.11 Synthesis of compound 17

A 100 mL round-bottom flask equipped with a magnetic stir bar was charged with compound **16** (294 mg, 0.50 mmol), compound **6** (94 μ L, 1.00 mmol), and piperidine (100 μ L, 1.00 mmol), to which 15 ml ethanol was added. The resulting reaction mixture was heated 12 h at 90 °C. Filtered while hot, collected the filter residue, and got the crude product. The resulting crude mixture was purified by column chromatography on silica gel (petroleum ether/ethyl acetate = 3/1, v/v) to give the compound **17** as a scarlet solid with a yield of 83.3%. ¹H NMR (400 MHz, CDCl₃) δ (TMS, ppm): 8.78 (s, 2H), 8.13 (s, 1H), 7.98 (d, *J* = 8.1 Hz, 1H), 7.89–7.71 (m, 8H), 7.62 (d, *J* = 8.1 Hz, 1H), 7.53 (s, 1H), 7.13 (d, *J* = 8.8 Hz, 4H), 6.88 (t, *J* = 9.8 Hz, 6H), 4.22 (q, *J* = 7.0 Hz, 2H), 3.82 (s, 6H), 1.37 (t, *J* = 7.1 Hz, 3H). ¹³C NMR (100 MHz, CDCl₃) δ (TMS, ppm): 155.96, 149.05, 144.82, 142.91, 141.22, 140.09, 138.52, 137.16, 133.24, 129.01, 126.95, 126.64, 126.51, 126.16, 122.10, 121.43, 119.57, 118.60, 116.61, 116.19, 114.74, 108.50, 107.21, 100.18, 55.53, 37.55, 13.77. HRMS (ESI, *m/z*) [M+H]⁺ calcd. for C₄₅H₃₆N₅O₂⁺ 678.2864, found 678.2851.

2.12 Synthesis of TPACzPy

Under the N₂ atmosphere, a mixture of compound **17** (338 mg, 0.50 mmol) and ethyl iodide (200 μ L, 2.50 mmol) in 15 mL of acetonitrile was stirred at 95 °C for 6 h. The following specific synthesis and purification procedures referred to those of TPAPy. TPACzPy was afforded as black solids with a yield of 73.6%. ¹H NMR (400 MHz, DMSO-*d*₆) δ (TMS, ppm): 9.19 (d, *J* = 6.6 Hz, 2H), 8.46 (d, *J* = 6.4 Hz, 2H), 8.40 (s, 1H), 8.34 (s, 1H), 8.16 (s, 1H), 8.12 (d, *J* = 8.2 Hz, 1H), 8.06–7.92 (m, 5H), 7.86 (d, *J* = 8.4 Hz, 1H), 7.09 (d, *J* = 8.9 Hz, 4H), 6.94 (d, *J* = 9.0 Hz, 4H), 6.91 (s, 1H), 6.82–6.62 (m, 1H), 4.64 (q, *J* = 7.2 Hz, 2H), 4.22 (d, *J* = 6.8 Hz, 2H), 3.77 (s, 6H), 1.58 (t, *J* = 7.3 Hz, 3H), 1.27 (t, *J* = 7.1 Hz, 3H). ¹³C NMR (150 MHz, DMSO-*d*₆) δ (TMS, ppm): 155.14, 148.10, 147.98, 144.90, 144.28, 141.67, 139.86, 138.84, 136.31, 135.76, 131.57, 128.61, 126.89, 126.09, 126.00, 125.75, 124.50, 121.20, 119.94, 119.01, 118.07, 117.79, 115.42, 114.90, 114.36, 113.17, 109.67, 105.71, 98.74, 55.69, 54.65, 36.39, 15.44, 12.88. HRMS (ESI, *m/z*): [M–PF₆]⁺ calcd. for C₄₇H₄₀N₅O₂⁺ 706.3177, found 706.3177.

2.13 Synthesis of compound 18

A 100 mL round-bottom flask equipped with a magnetic stir bar was charged with compound **16** (294 mg, 0.50 mmol), 4-quinolinecarboxaldehyde (314 mg, 2.00 mmol) and sodium hydroxide (20 mg, 0.50 mmol), to which 15 mL ethanol was added. The resulting reaction mixture was heated 12 h at 90 °C. The reaction was immediately terminated with dilute hydrochloric acid. After being cooled to room temperature, the reaction mixture was diluted with dichloromethane (80 mL) and washed with saturated saline solution (100 mL) for three times to generate the crude product. The resulting crude mixture was purified by column chromatography on silica gel (hexane/ethyl acetate = 3/1, v/v) to give the compound **18** as a black solid with a yield of 52.2%. ¹H NMR (400 MHz, CDCl₃) δ (TMS, ppm): 9.00 (t, *J* = 6.7 Hz, 1H), 8.23–8.14 (m, 2H), 8.07 (s, 1H), 7.93 (t, *J* = 9.0 Hz, 2H), 7.87 (t, *J* = 5.5 Hz, 1H), 7.81–7.73 (m, 6H), 7.64–7.52 (m, 2H), 7.18 (s, 1H), 7.04 (dd, *J*₁ = 16.8, *J*₂ = 8.9 Hz, 4H), 6.86–6.74 (m, 6H), 4.15 (q, *J* = 7.1 Hz, 2H), 3.74 (d, *J* = 8.5 Hz, 6H), 1.30 (t, *J* = 7.1 Hz, 3H). ¹³C NMR (100 MHz, CDCl₃) δ (TMS, ppm): 154.92, 149.21, 147.99, 147.35, 143.69, 141.85, 140.16, 139.03, 137.93, 136.11, 135.99, 132.15, 129.47, 129.01, 127.97, 126.57, 126.26, 125.98, 125.61, 125.46, 125.08, 124.97, 122.16, 121.05, 120.38,

119.11, 118.51, 117.59, 116.69, 115.44, 115.14, 113.70, 113.64, 107.47, 106.17, 99.10, 54.48, 36.49, 12.72. HRMS (ESI, m/z): $[M+H]^+$ calcd. for $C_{49}H_{38}N_5O_2^+$ 728.3020, found 728.3002.

2.14 Synthesis of TPACzQu

Under the N_2 atmosphere, a mixture of compound **18** (364 mg, 0.50 mmol) and ethyl iodide (800 μ L, 10.00 mmol) in 10 mL of acetonitrile was stirred at 95 °C for 24 h. The following specific synthesis and purification procedures referred to those of TPAPy. TPACzQu was afforded as black solids with a yield of 46.3%. 1H NMR (400 MHz, $DMSO-d_6$) δ (TMS, ppm): 9.69 (d, $J = 6.3$ Hz, 1H), 9.01 (s, 1H), 8.76–8.67 (m, 2H), 8.60 (d, $J = 6.1$ Hz, 1H), 8.36 (dd, $J_1 = 14.2$ Hz, $J_2 = 5.9$ Hz, 2H), 8.18 (s, 2H), 8.16–8.10 (m, 3H), 8.04 (d, $J = 8.6$ Hz, 2H), 7.99 (d, $J = 8.6$ Hz, 1H), 7.87 (d, $J = 8.3$ Hz, 1H), 7.16–7.04 (m, 4H), 6.98–6.92 (m, 4H), 6.92 (d, $J = 1.6$ Hz, 1H), 6.73 (dd, $J_1 = 8.6$ Hz, $J_2 = 1.8$ Hz, 1H), 5.13 (q, $J = 7.0$ Hz, 2H), 4.22 (d, $J = 6.9$ Hz, 2H), 3.77 (s, 6H), 1.67 (t, $J = 7.2$ Hz, 3H), 1.27 (t, $J = 7.1$ Hz, 3H). ^{13}C NMR (150 MHz, $DMSO-d_6$) δ (TMS, ppm): 156.19, 150.38, 149.21, 149.04, 145.88, 142.70, 140.93, 139.86, 137.80, 137.24, 136.24, 136.01, 132.57, 130.72, 129.69, 128.30, 128.02, 127.05, 126.65, 125.50, 122.23, 121.92, 121.06, 120.98, 120.01, 119.87, 118.90, 116.39, 115.96, 115.42, 114.25, 110.73, 106.93, 99.82, 55.71, 53.78, 37.44, 15.63, 13.94. HRMS (ESI, m/z): $[M-PF_6]^-$ calcd. for $C_{51}H_{42}N_5O_2^+$ 756.3333, found 756.3330.

3. Theoretical calculation method

Gaussian 16 c01^{S1} was used to carry out the theoretical calculation of the compounds. Firstly, the ground-state geometries of TPAPy, TPAQu, TPACzPy and TPACzQu were optimized with the B3LYP/6-311G(d) basis set, and then the highest occupied molecular orbital (HOMO) and the lowest unoccupied molecular orbital (LUMO) energy levels were calculated using the B3LYP/6-311G(d) basis set as well. Time-dependent density functional theory (TD-DFT) calculations of their excited states were performed based on the PBE0/6-311G(d) basis set.

4. ROS generating ability test

4.1 Measurement of total ROS production

Firstly, DCFH-DA was activated. Specific steps: 2 mL of aqueous solution of sodium hydroxide (10^{-2} M) was mixed with 0.5 mL of ethanol solution of DCFH-DA (10^{-3} M). The mixed solution was stirred in the dark at room temperature for 30 minutes. Then the above solution was added to 10 mL of ultrapure water to obtain the activated DCFH-DA solution (40 μ M, DCFH), which was stored in a refrigerator at 4 °C with airtight and light-free. 5 mL of test samples of TPAPy, TPAQu, TPACzPy, or TPACzQu (in the mixture of $DMSO/PBS = 2/98$, v/v) in the presence of DCFH were prepared, respectively. The concentration of the AIE compound is 10 μ M, while that of the DCFH is 40 μ M. White-light source with a power density of 10 mW/cm² was used to irradiate the test samples for different time, and the fluorescence intensity at 525 nm was recorded using a fluorescence spectrometer at an excitation wavelength of 488 nm to indicate the generation of total ROS.

4.2 Detection of 1O_2 by ABDA

To further distinguish the types of ROS generated by the AIE compounds, ABDA was used

to evaluate the ability of singlet-oxygen generation under light irradiation. Prepare 3 mL of test solution of the AIE compound (10 μM) in the presence of ABDA (50 μM), which was then exposed to the white-light irradiation for different time. Correspondingly recorded the absorbance of ABDA at 378 nm.

4.3 Detection of $\text{O}_2^{\cdot-}$ by DHR123

3 mL of test solution of the AIE compound (in DMSO/PBS = 2/98, v/v) in the presence of DHR123 was prepared, where the [AIE compound] = 10 μM ; [DHR123] = 10 μM . The test solutions were subjected to the irradiation of white light with a power of 10 mW/cm^2 for different time. The corresponding fluorescence intensities at 520–530 nm with the excitation at 490 nm were recorded using a fluorescence spectrometer to indicate the generation of $\text{O}_2^{\cdot-}$.

4.4 Detection of $\cdot\text{OH}$ by HPF

3 mL of test solution of the AIE compound (DMSO/PBS = 2/98, v/v) in the presence of HPF was prepared, where the [AIE compound] = 10 μM ; [HPF] = 10 μM . The test solutions are then irradiated with white light at a power of 10 mW/cm^2 for different time. The fluorescence intensities at 515–525 nm were measured using a fluorescence spectrometer with the excitation of 480 nm to indicate the generation of $\cdot\text{OH}$.

5. Photothermal properties measurements

5.1 Evaluation of the photothermal properties of the solid-state AIE compounds

Add 2 mg of the solid compound to a 1 mL-centrifuge tube. Under the irradiation of a 660 nm laser with a power density of 0.7 W/cm^2 , a photothermal imager was used to record the temperature changes during continuous irradiation for 5 minutes, as well as the temperature rise and decrease curves before and after irradiation, repeating this process for 6 cycles.

5.2 Assessment of the photothermal properties of the AIE NPs

For the evaluation of the photothermal properties of AIE NPs at the same power density but at different concentrations: Dilute the prepared nanoparticles to 20, 50, 100, 200, and 500 $\mu\text{g}/\text{mL}$, and an infrared thermal imager was utilized to record the temperature changes during continuous irradiation by a 660 nm laser for 8 minutes with a power density of 1.47 W/cm^2 .

For the evaluation of the photothermal properties of AIE NPs at different power densities but at the same concentration: An infrared thermal imager was used to record the temperature changes of AIE NPs over 8 minutes under the irradiation of a 660 nm laser at different power densities (0.18, 0.49, 0.82, 1.16, and 1.47 W/cm^2) with a concentration of 200 $\mu\text{g}/\text{mL}$. Heating-cooling cycle test: An infrared thermal imager was utilized to record the temperature changes of AIE NPs (200 $\mu\text{g}/\text{mL}$) under the irradiation of a 660 nm laser at a power density of 1.16 W/cm^2 , both before and after illumination, and repeat this process for 5 cycles.

6. Nanoparticle preparation and characterization

6.1 Preparation of nanoparticles

1 mg TPACzPy and 5 mg polyether F127 were added into a 5 mL centrifuge tube, then 0.8 mL DMSO was added. The mixture was sonicated for 1 min using a cell disruptor (output power of 60%, JY88-IIN) to completely dissolve the components. To a sample tube equipped with a magnetic stirring bar and containing 10 mL of ultrapure water, the above solution was slowly dropped using a syringe. The mixed solution was transferred to a dialysis bag which was then placed in a 500 mL beaker for dialysis. The dialysis took about 24 hours, with the ultrapure water being replaced every 4–6 hours. Ultrafiltration centrifugation was performed on the dialyzed solution, and the specific concentration of the nanoparticle solution was determined by measuring the standard curve using a UV-vis absorption spectrometer. The obtained TPACzPy NPs was stored in a refrigerator at 4 °C.

6.2 Size and shape of nanoparticles

Dynamic light scattering (DLS) was used to monitor the size of the TPACzPy NPs prepared in the aqueous solution, and their morphologies were observed by the TEM.

7 Studies at cellular level

7.1 Cell culture

4T1 cells were cultured in the RPMI 1640 medium, which was supplemented with 10% FBS and 1% penicillin-streptomycin in a 5 % CO₂ humidity incubator at 37 °C.

7.2 Cytotoxicity assay

4T1 cells were inoculated into 96-well plates at a density of 8000 cells per well for 24 h. The cells were then cultured with different concentrations of TPACzPy NPs (0, 1, 2, 5, 10, 15, 20, 30 µg/mL) for 2 h. Afterwards, these cells were divided into two groups, where one group of the 4T1 cells was irradiated with white light (72 mW/cm²) for 30 min, and the other group of cells was not illuminated. Then all the cells were incubated for another 12 h. After the cells being rinsed with PBS, 100 µL of CCK-8 solution was added to each well. The 4T1 cells were put into the cell incubator in the dark for 2 h and the absorbance was then measured at 450 nm. Cell survival rate was calculated as follows: Cell survival rate = (treated group OD–blank group OD)/(untreated group OD–blank group OD) × 100 %.

7.3 Intracellular ROS detection of TPACzPy NPs at different irradiation time

Approximately 1.0×10^5 of 4T1 cells were seeded into 35 mm-glass-bottom confocal petri dishes and incubated with the RPMI 1640 medium for 24 h. 4T1 cells were first cultured with different concentration of TPACzPy NPs (0, 20 µg/mL) for 2 h. After being irradiated with white light (72 mW/cm²) for different time (0, 5, 10, 15, 30 min), the 4T1 cells were rinsed with PBS and cultured with DCFH-DA (20 µM) for 0.5 h. Then the 4T1 cells were further rinsed, and fresh PBS was added to the dishes. The confocal petri dishes were then observed using CLSM, with $\lambda_{\text{ex}} = 480$ nm and $\lambda_{\text{em}} = 490\text{--}550$ nm.

7.4 Intracellular total ROS detection

Approximately 1.0×10^5 of 4T1 cells were seeded into 35 mm-glass-bottom confocal petri dishes and incubated with the RPMI 1640 medium for 24 h. The cells were divided into four groups: a) DCFH-DA, b) TPACzPy NPs+light, c) TPACzPy NPs+DCFH-DA, and d)

TPACzPy NPs+DCFH-DA+light. Aspirate the old cell culture medium of each group. For Group a, 1 mL of complete phenol red-free medium was added. For Groups b, c, and d, 1 mL of complete phenol red-free medium containing TPACzPy NPs was added. All groups were incubated in the dark for 2 h. Cells in Groups b and d were irradiated with a white-light source (400–800 nm, 72 mW/cm²) for 20 minutes. Aspirate the old cell culture medium, and for Group b, 1 mL of basic phenol red-free medium was added, while the other groups received 1 mL of basic phenol red-free medium containing DCFH-DA. The cells were further incubated in the dark for 0.5 hours. Ultimately, the 4T1 cells of all groups were rinsed, with fresh PBS added. The confocal petri dishes were then observed using CLSM, where $\lambda_{\text{ex}} = 480 \text{ nm}$, $\lambda_{\text{em}} = 490\text{--}550 \text{ nm}$, [TPACzPy NPs] = 20 $\mu\text{g/mL}$, [DCFH-DA] = 20 μM .

7.5 Intracellular O₂^{•-} detection

Approximately 1.0×10^5 of 4T1 cells were seeded into 35 mm-glass-bottom confocal petri dishes and incubated with the RPMI 1640 medium for 24 h. The cells were divided into four groups: a) DHR123, b) TPACzPy NPs+light, c) TPACzPy NPs+DHR123, d) TPACzPy NPs+DHR123+light. The specific operations are the same with Section 7.4 except the DCFH-DA was replaced by DHR 123. The confocal petri dishes were observed using CLSM, where $\lambda_{\text{ex}} = 480 \text{ nm}$, $\lambda_{\text{em}} = 500\text{--}550 \text{ nm}$, [TPACzPy NPs] = 20 $\mu\text{g/mL}$, [DHR123] = 20 μM .

7.6 Intracellular •OH detection

Approximately 1.0×10^5 of 4T1 cells were seeded into 35 mm-glass-bottom confocal petri dishes and incubated with the RPMI 1640 medium for 24 h. The cells were divided into four groups: a) HPF, b) TPACzPy NPs+light, c) TPACzPy NPs+HPF, d) TPACzPy NPs+HPF+light. The specific operations are the same with Section 7.4 except the DCFH-DA was replaced by HPF. The confocal petri dishes were observed using CLSM, where $\lambda_{\text{ex}} = 495 \text{ nm}$, $\lambda_{\text{em}} = 490\text{--}600 \text{ nm}$, [TPACzPy NPs] = 20 $\mu\text{g/mL}$, [HPF] = 20 μM .

7.7 Intracellular ¹O₂ detection

Approximately 1.0×10^5 of 4T1 cells were seeded into 35-mm glass-bottom confocal petri dishes and incubated with the RPMI 1640 medium for 24 h. The cells were divided into four groups: a) SOSG, b) TPACzPy NPs+light, c) TPACzPy NPs+SOSG, d) TPACzPy NPs+SOSG+light. The specific operations are the same with Section 7.4 except the DCFH-DA was replaced by SOSG. The confocal petri dishes were observed using CLSM, where $\lambda_{\text{ex}} = 480 \text{ nm}$, $\lambda_{\text{em}} = 490\text{--}550 \text{ nm}$, [TPACzPy NPs] = 20 $\mu\text{g/mL}$, [SOSG] = 20 μM .

7.8 Live/dead cell staining assays

4T1 cells were inoculated into 96-well plates at a density of 8000 cells per well for 24 h. The cells were divided into four groups: a) PBS, b) PBS+light, c) TPACzPy NPs, d) TPACzPy NPs+light. A white-light source (400–800 nm, 72 mW/cm²) was used to irradiate the cells of group b and d for 30 minutes. 4T1 cells were cultured with TPACzPy NPs or PBS for 2 h and were then irradiated with white-light source. The cells were then further cultured in the cell incubator for 6 h. The original culture medium was discarded. The cells were rinsed with PBS for three times, and were incubated with the Calcein-AM/PI kit for 30 min to detect cell viability. Then the 4T1 cells were rinsed and added with fresh PBS. The cells were observed with CLSM. Calcein-AM: $\lambda_{\text{ex}} = 495 \text{ nm}$, $\lambda_{\text{em}} = 510\text{--}550 \text{ nm}$, PI: λ_{ex}

= 535 nm, λ_{em} = 580–630 nm, [TPACzPy NPs] = 20 $\mu\text{g}/\text{mL}$, [AM] = 10 μM , [PI] = 30 μM .

8. In-vivo PDT studies

8.1 Establishment of tumor models

Female BALB/c mice (4–6 weeks old, 16 g) were purchased from Charles River Ltd. Co (Zhejiang). A 4T1 tumor model was successfully established by subcutaneous injection of 50 μL (5×10^5 cells) of cell suspension into the right upper limb of mice. Tumor growth was monitored daily, with the length and width of the tumor measured with vernier calipers. The tumor volume was calculated by $V = (\text{tumor length}) \times (\text{tumor width})^2 / 2$. The relative tumor volume was calculated as V/V_0 , where V_0 is the tumor volume before the treatment. When tumors grow to a certain size, 4T1 tumor-bearing mice were further used for the photothermal imaging and photodynamic therapy studies. All the animal-related experiments were conducted with the approval of Institutional Animal Care and Use Committee of Shanghai Jiao Tong University (Assigned approval no: A2023066-002).

8.2 In-vivo photothermal imaging

Female BALB/c mice bearing tumors (100–200 mm^3) were randomly divided into three groups ($n = 3$). PBS, TPACzPy, and TPACzPy NPs were injected through the tail vein at a dose of 10 mg/kg . At 0, 20, 28, 42, 48 h after injection, mice were anesthetized with isoflurane, and the real-time photothermal imaging was performed respectively, for two minutes, with the photothermal images recorded every 20 s.

8.3 In-vivo study of the anti-tumor effect of the TPACzPy NPs

Female BALB/c mice bearing tumors (about 50 mm^3) were randomly divided into four groups ($n = 5$): a) PBS; b) PBS+light; c) TPACzPy NPs; d) TPACzPy NPs+light. On every day during the treatment, the mice of group c and d were intravenously injected with TPACzPy NPs, while the mice of group a and b were treated with PBS by intravenous injection. The mice of group b and d were irradiated with a xenon lamp (400–1000 nm, 150 mW/cm^2) for 15 minutes at 20 hours after tail-vein injection of the TPACzPy NPs or PBS. Body weight and tumor size of all the mice were monitored daily for eight days. Finally, the major organs of the mice, such as liver, spleen, heart, lung, and kidney, were dissected and fixed in 4% paraformaldehyde solution for histological examination to further investigate the biocompatibility of TPACzPy NPs.

8.4 Histological analysis

After the end of treatment, the sections of tumors and major organs (heart, liver, spleen, lungs, and kidneys) were further stained with H&E and subjected to the histological analysis.

8.5 Biochemical parameters

After the end of treatment, about 500 μL of orbital blood was collected from each group of mice. The automatic biochemical analyzer was used to analyze the two important liver and kidney function indexes, namely glutamic oxaloacetic transaminase (AST) and blood urea nitrogen (BUN).

9. Original spectra

9.1 The characterization spectra

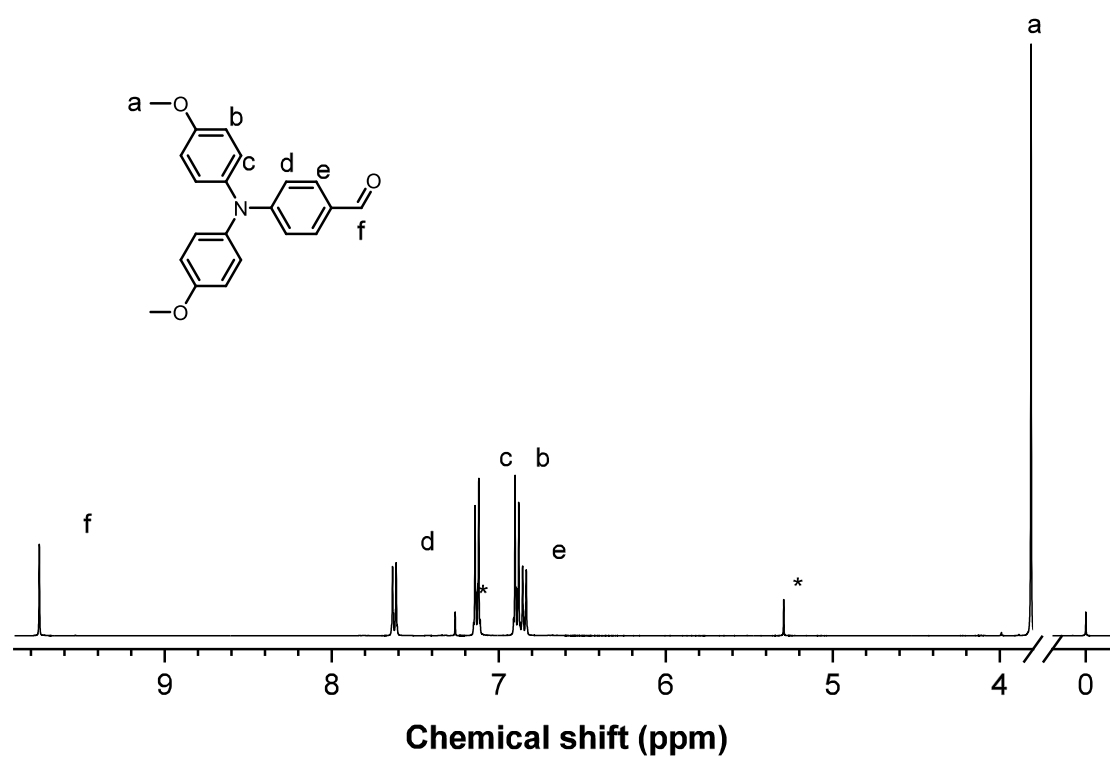


Fig. S1. The ^1H NMR spectrum of compound **3** in CDCl_3 .

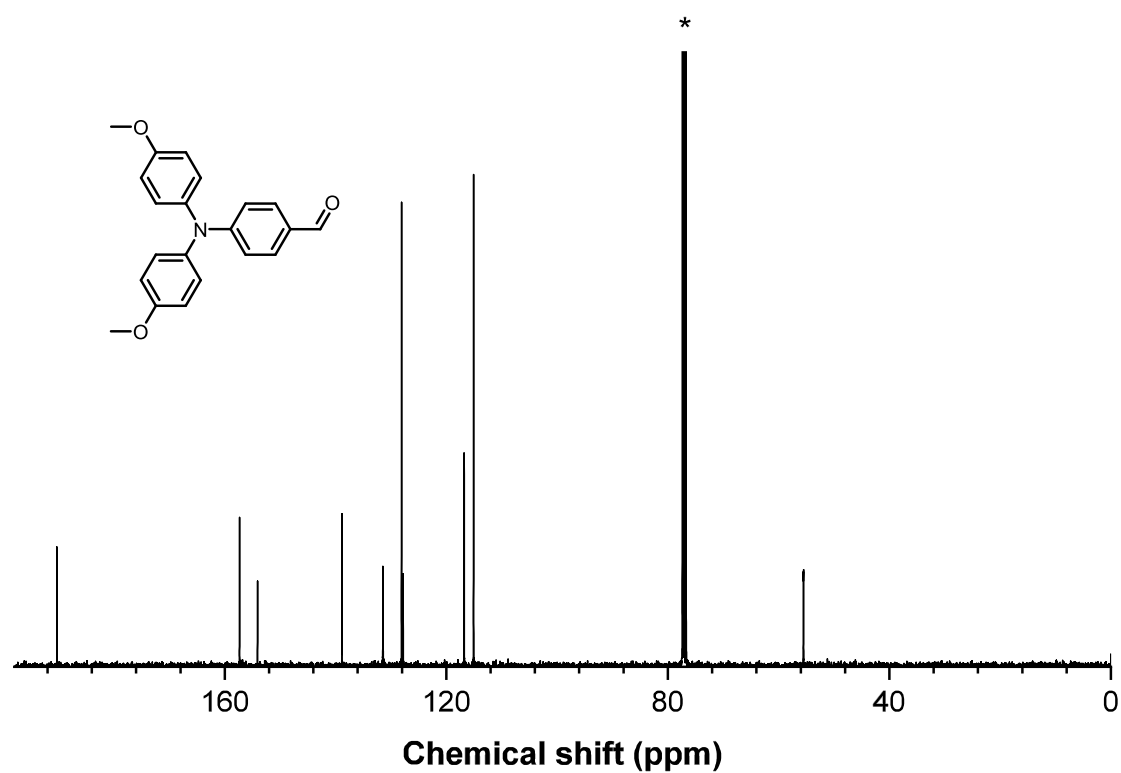
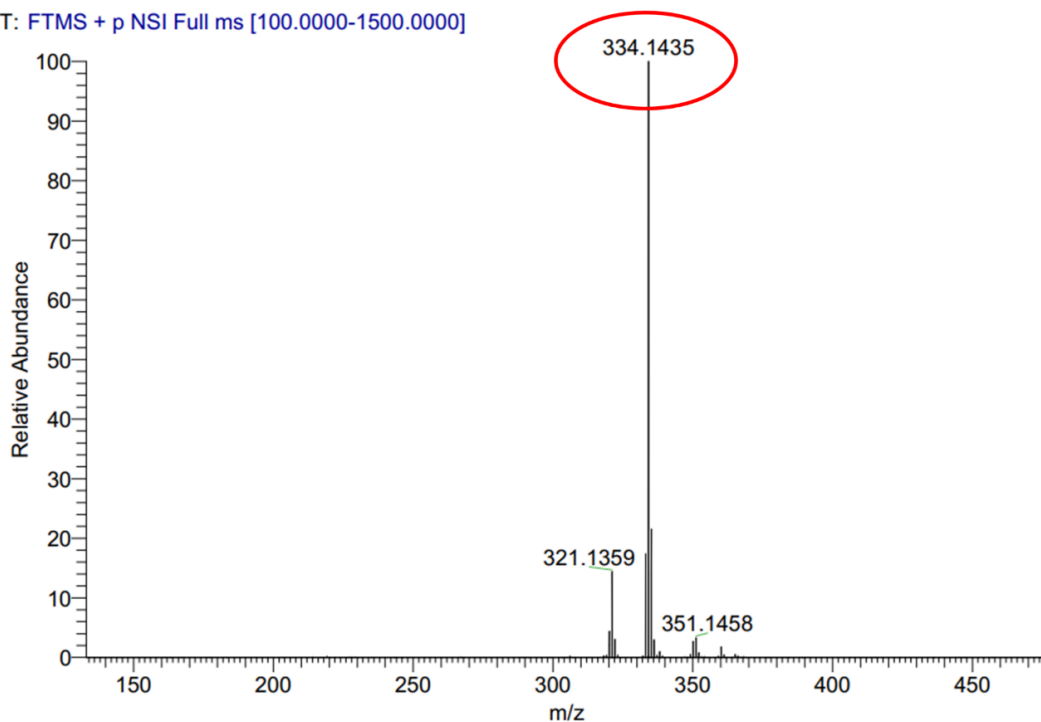


Fig. S2. The ^{13}C NMR spectrum of compound **3** in CDCl_3 .

T: FTMS + p NSI Full ms [100.0000-1500.0000]



zss-074#79 RT: 0.18

T: FTMS + p NSI Full ms [100.0000-1500.0000]

m/z= 326.61-335.78

| m/z | Intensity | Relative | Theo. Mass | Delta (ppm) | Composition |
|----------|---------------|----------|------------|-------------|--|
| 334.1435 | 12692553728.0 | 100.00 | 334.1438 | -0.28 | C ₂₁ H ₂₀ O ₃ N |

Fig. S3. The high-resolution mass spectrum (HRMS) of compound 3.

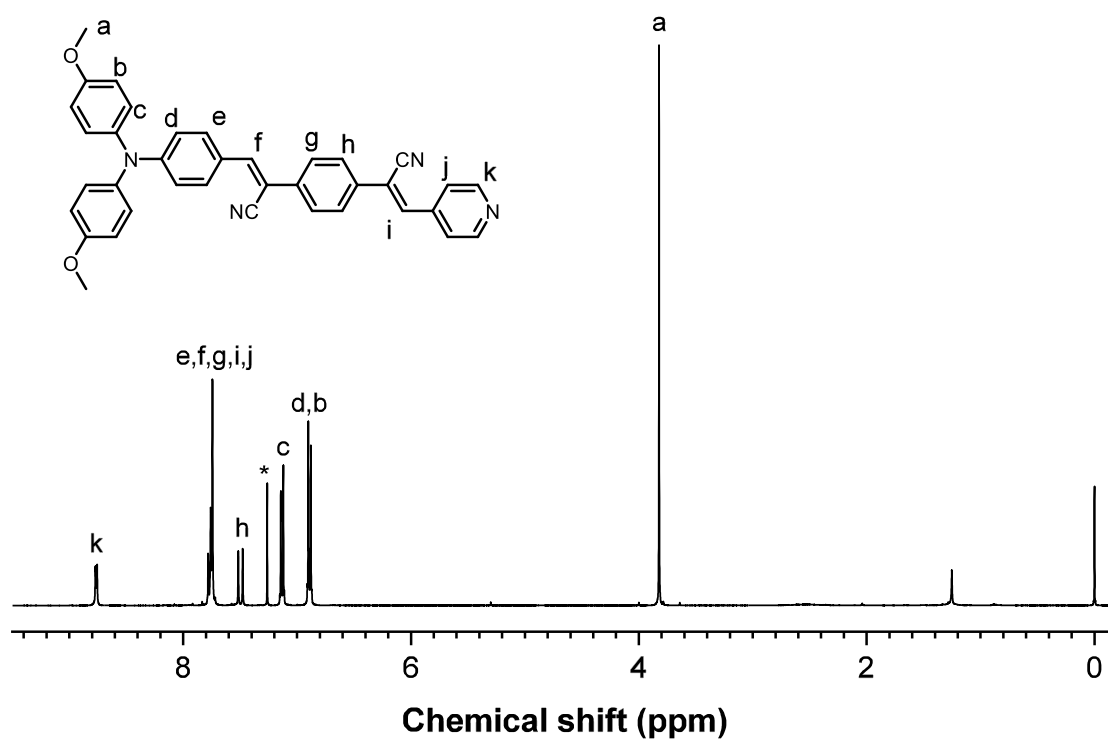


Fig. S4. The ¹H NMR spectrum of compound 8 in CDCl₃.

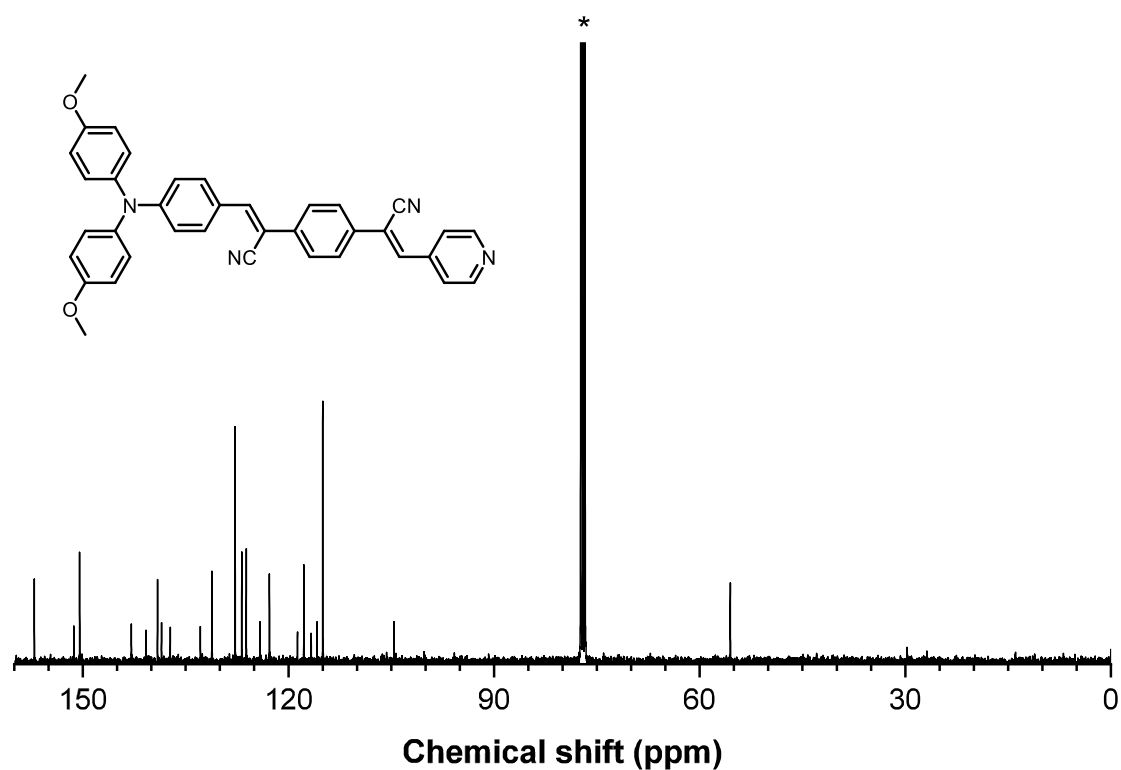
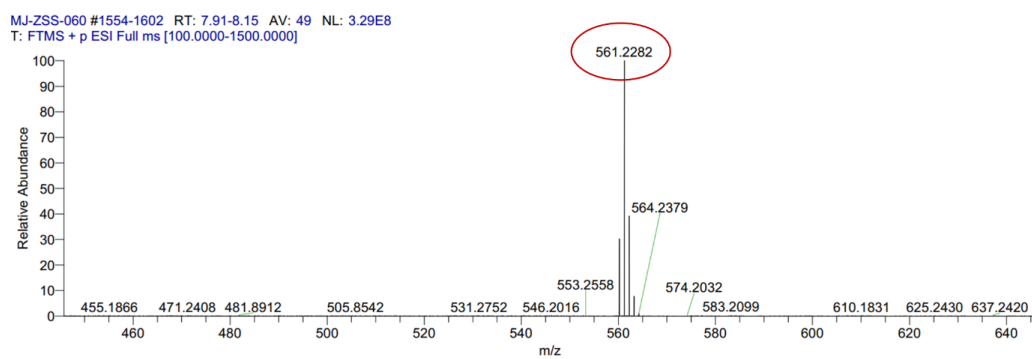


Fig. S5. The ^{13}C NMR spectrum of compound **8** in CDCl_3 .



MJ-ZSS-060#1561-1600 RT: 7.94-8.14 AV: 40
T: FTMS + p ESI Full ms [100.0000-1500.0000]
m/z= 559.37-562.99

| m/z | Intensity | Relative | Theo. Mass | Delta (ppm) | Composition |
|----------|-------------|----------|------------|-------------|--|
| 561.2282 | 341445120.0 | 100.00 | 561.2285 | -0.29 | $\text{C}_{37}\text{H}_{29}\text{O}_2\text{N}_4$ |

Fig. S6. The HRMS of compound **8**.

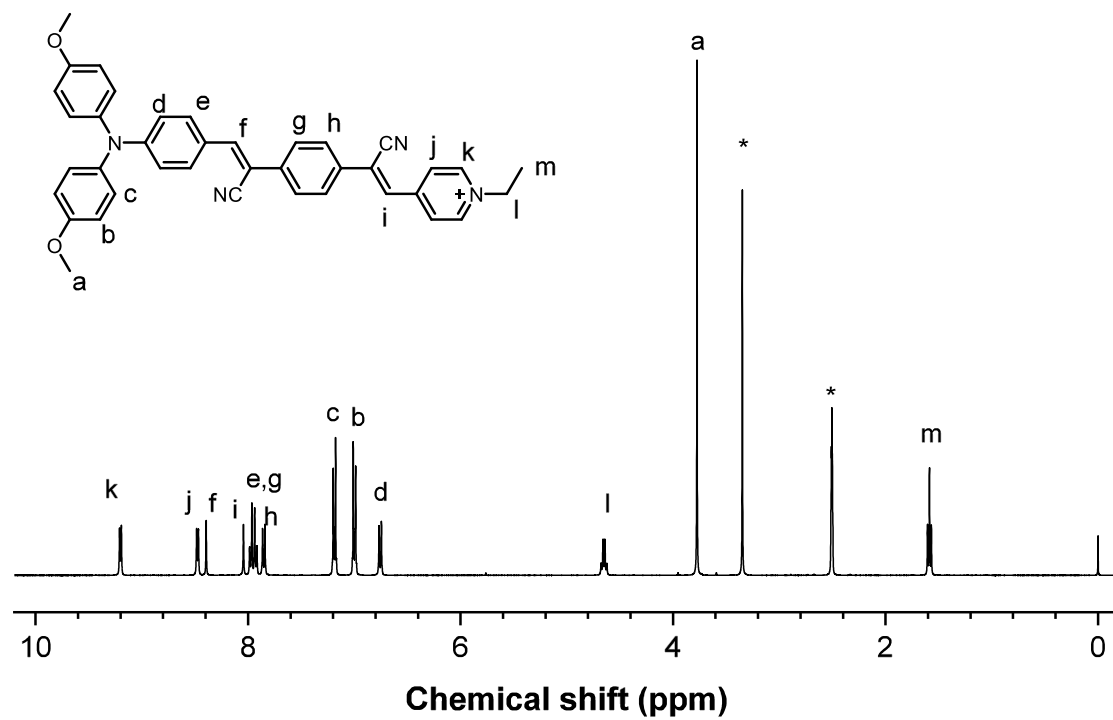


Fig. S7. The ^1H NMR spectrum of TPAPy in $\text{DMSO-}d_6$.

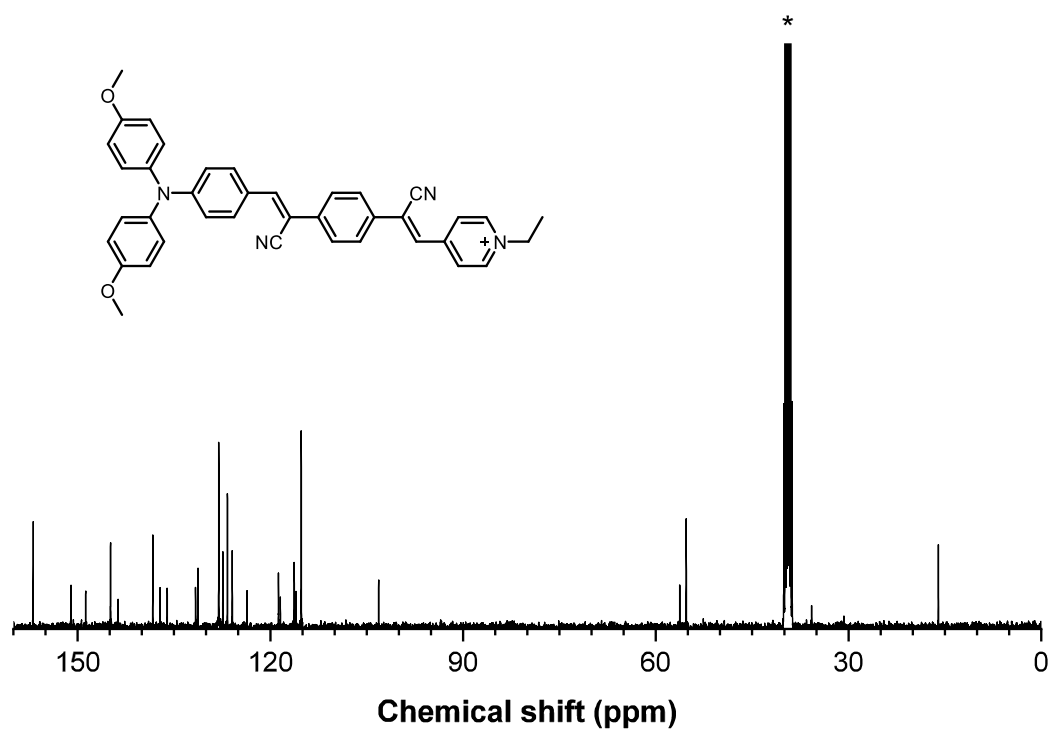
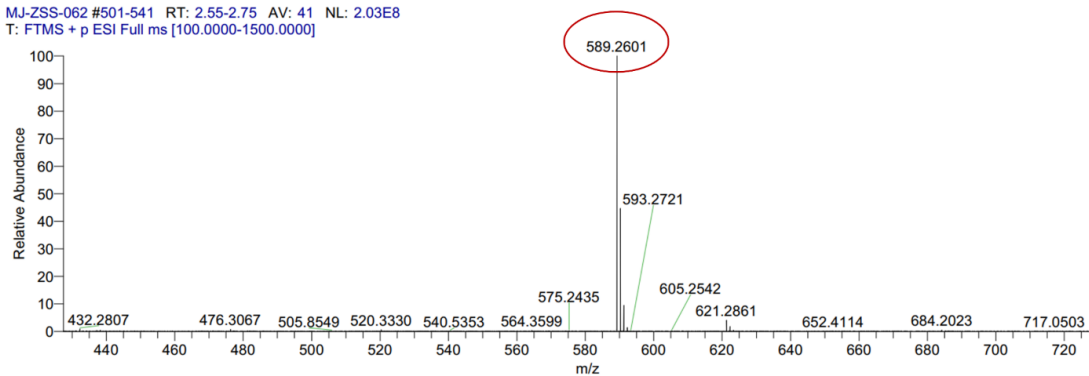


Fig. S8. The ^{13}C NMR spectrum of TPAPy in $\text{DMSO-}d_6$.

MJ-ZSS-062 #501-541 RT: 2.55-2.75 AV: 41 NL: 2.03E8
T: FTMS + p ESI Full ms [100.0000-1500.0000]



MJ-ZSS-062#501-541 RT: 2.55-2.75 AV: 41
T: FTMS + p ESI Full ms [100.0000-1500.0000]
m/z= 587.60-590.97

| m/z | Intensity | Relative | Theo. Mass | Delta (ppm) | Composition |
|----------|-------------|----------|------------|-------------|---|
| 589.2601 | 208858976.0 | 100.00 | 589.2598 | 0.30 | C ₃₉ H ₃₃ O ₂ N ₄ |

Fig. S9. HRMS of TPAPy.

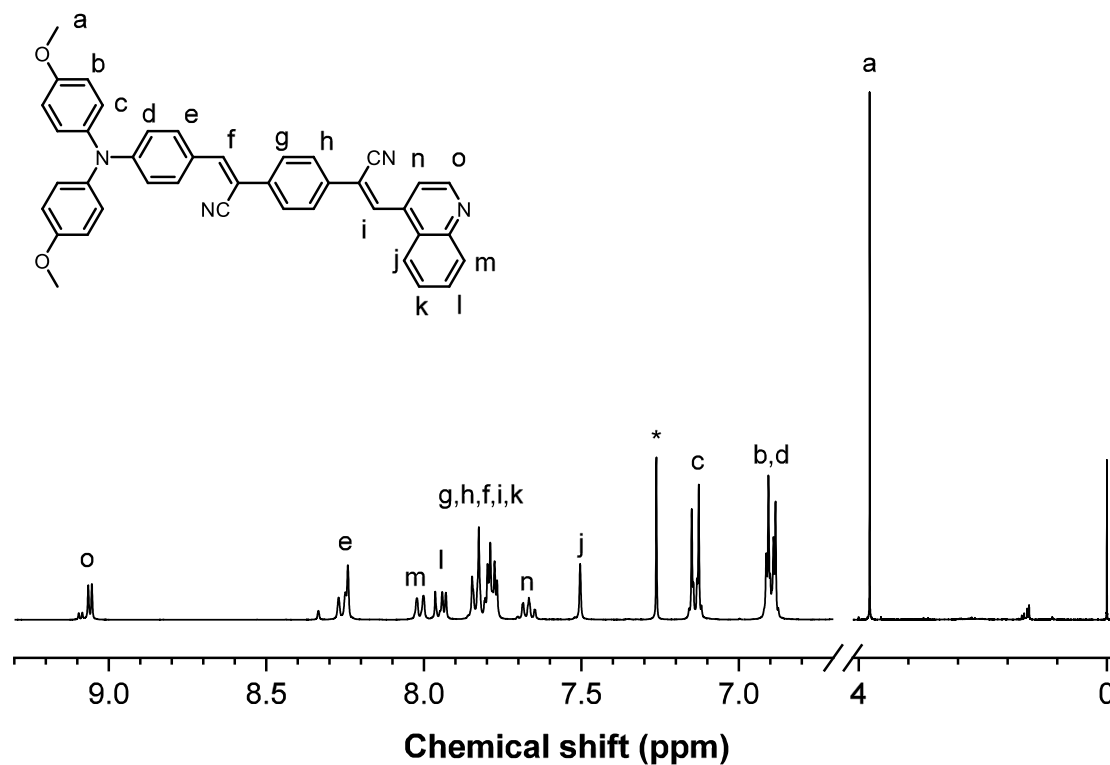


Fig. S10. The ¹H NMR spectrum of compound **9** in CDCl₃.

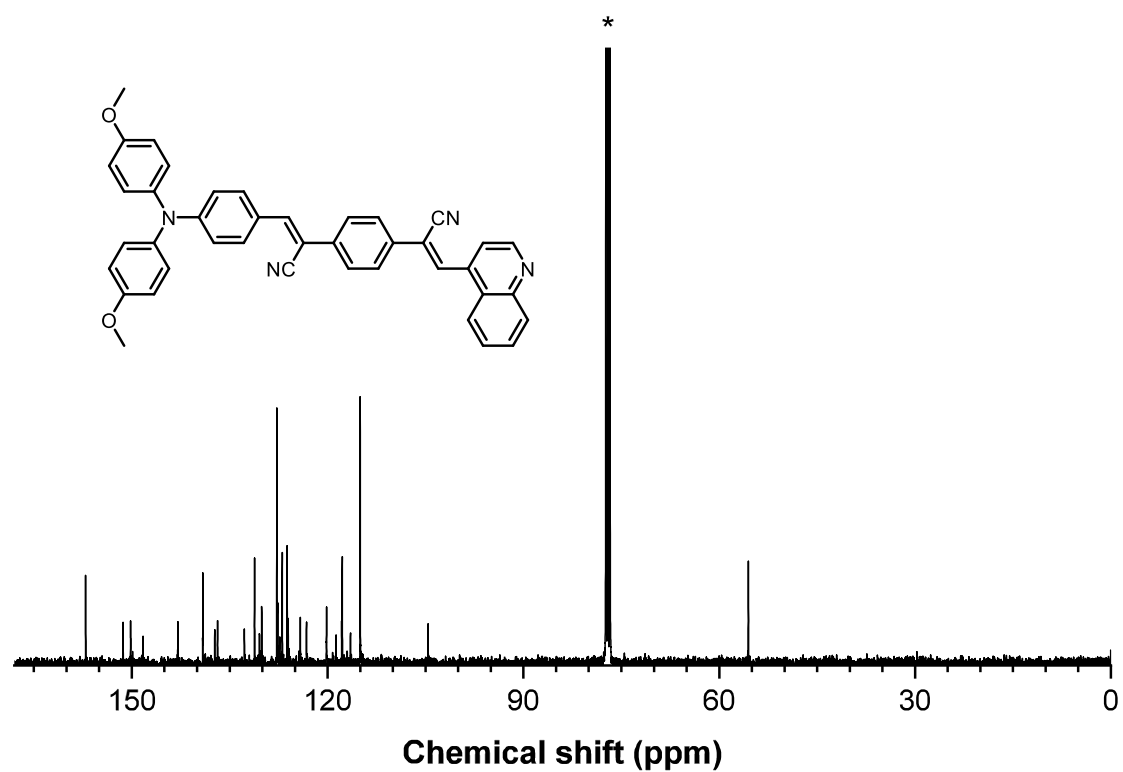
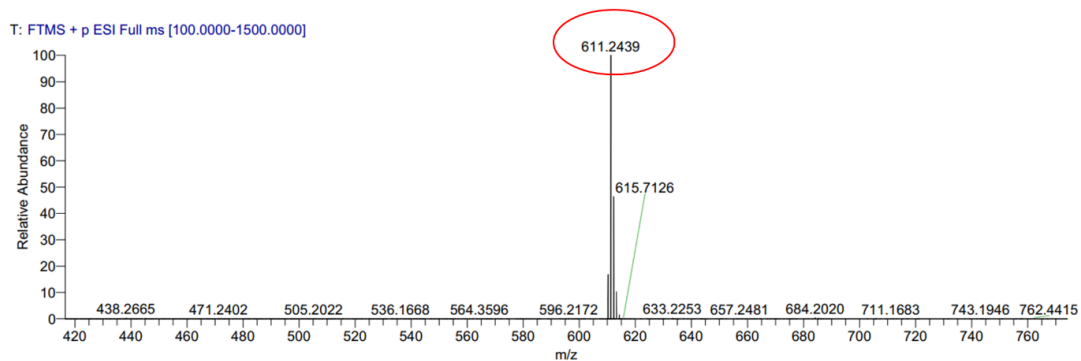


Fig. S11. The ^{13}C NMR spectrum of compound **9** in CDCl_3 .



MJ-ZSS-061#1910-1945 RT: 9.72-9.90 AV: 36
T: FTMS + p ESI Full ms [100.0000-1500.0000]
m/z = 608.90-613.36

| m/z | Intensity | Relative | Theo. Mass | Delta (ppm) | Composition |
|----------|-------------|----------|------------|-------------|--|
| 611.2439 | 295547936.0 | 100.00 | 611.2442 | -0.29 | $\text{C}_{41}\text{H}_{31}\text{O}_2\text{N}_4$ |

Fig. S12. HRMS of compound **9**.

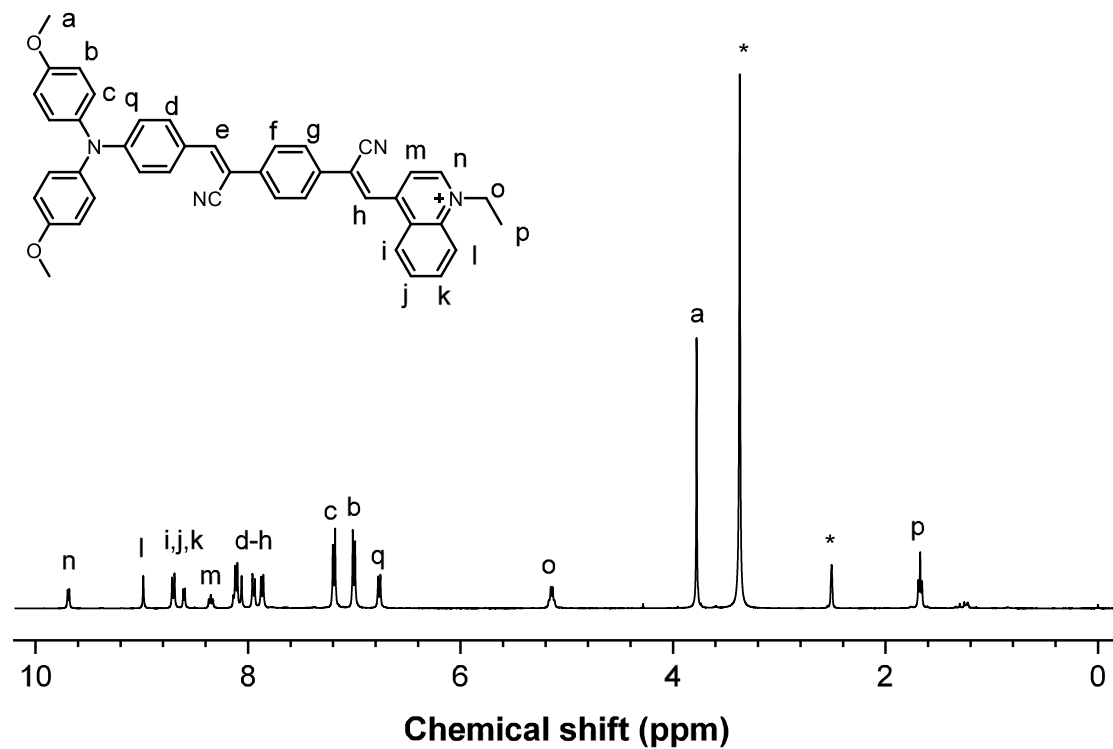


Fig. S13. The ^1H NMR spectrum of TPAQu in $\text{DMSO-}d_6$.

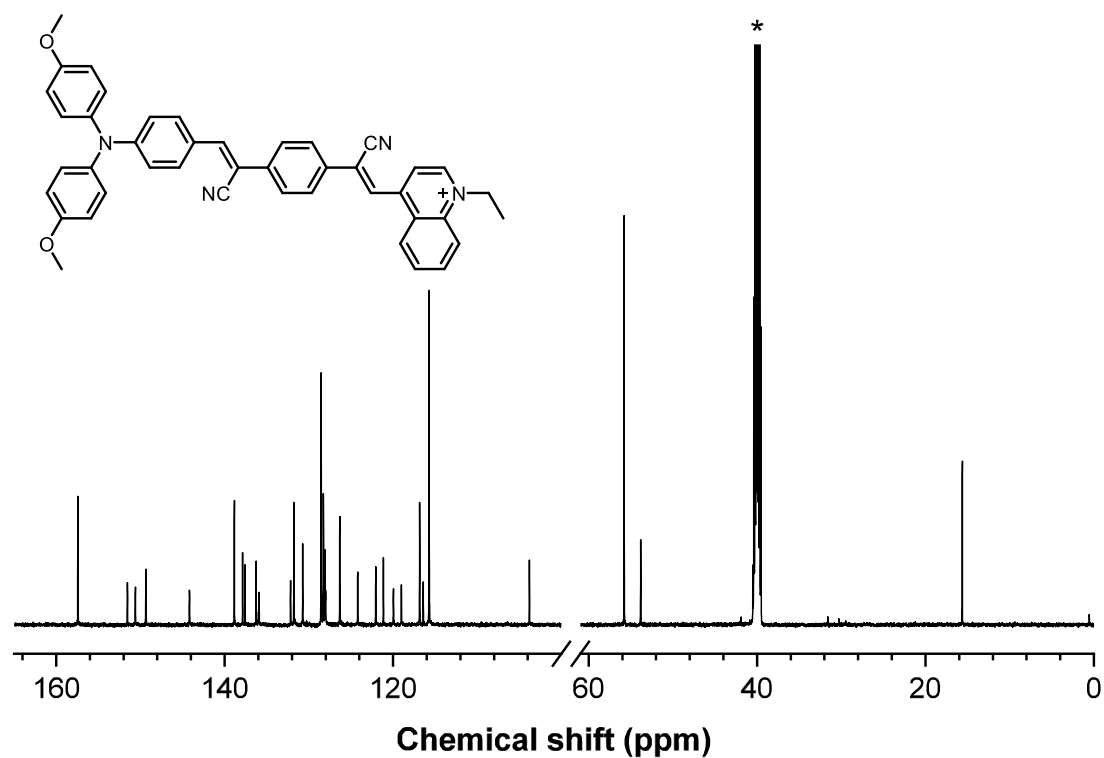
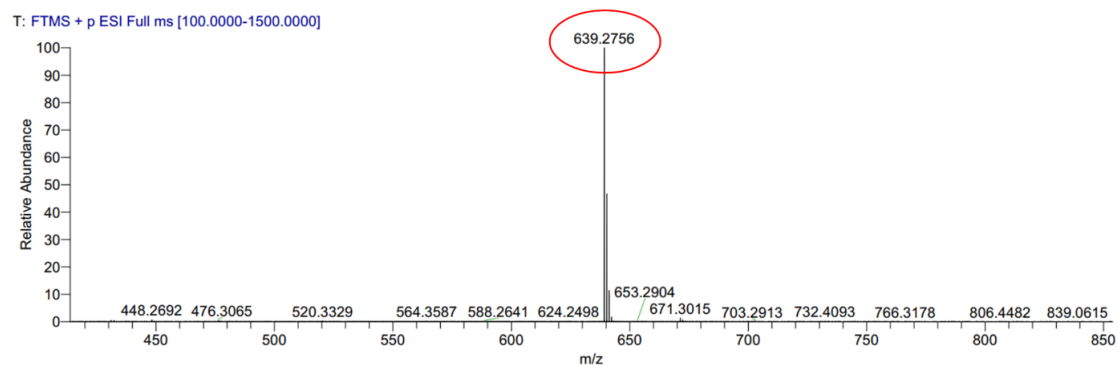


Fig. S14. The ^{13}C NMR spectrum of TPAQu in $\text{DMSO-}d_6$.



MJ-ZSS-063#508-555 RT: 2.58-2.82 AV: 48

T: FTMS + p ESI Full ms [100.0000-1500.0000]

m/z = 633.16-645.39

| m/z | Intensity | Relative | Theo. Mass | Delta (ppm) | Composition |
|----------|-------------|----------|------------|-------------|---|
| 639.2756 | 355640064.0 | 100.00 | 639.2755 | 0.10 | C ₄₃ H ₃₅ O ₂ N ₄ |

Fig. S15. HRMS of TPAQu.

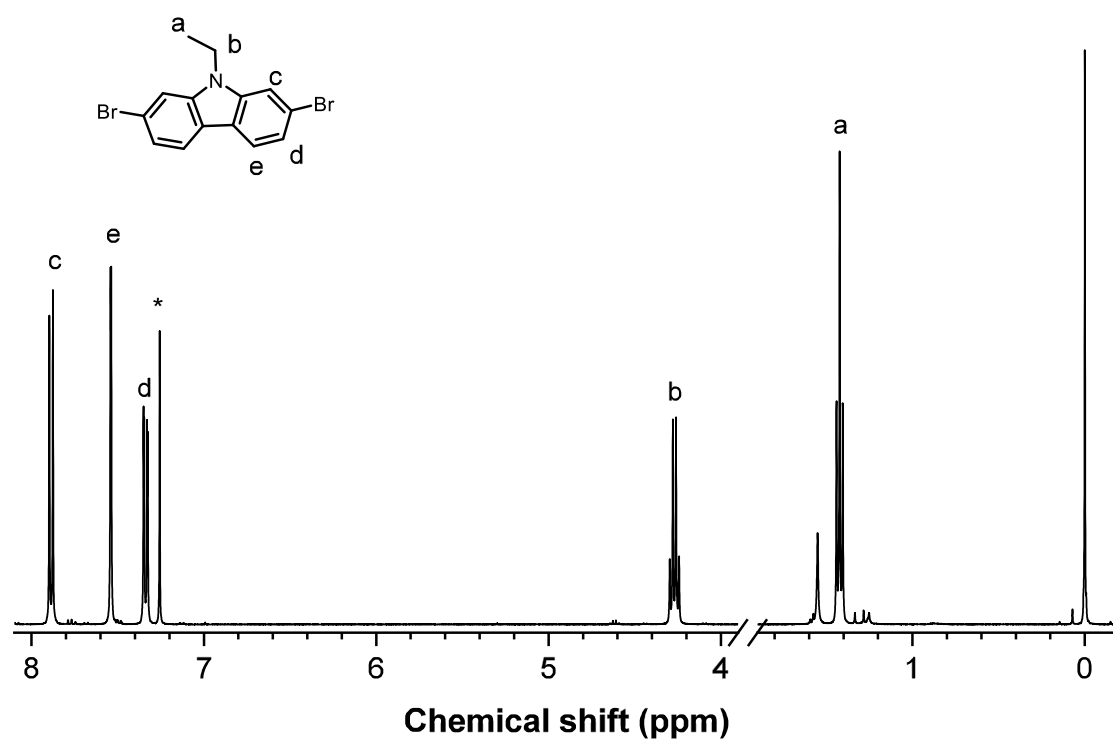


Fig. S16. The ¹H NMR spectrum of compound 12 in CDCl₃.

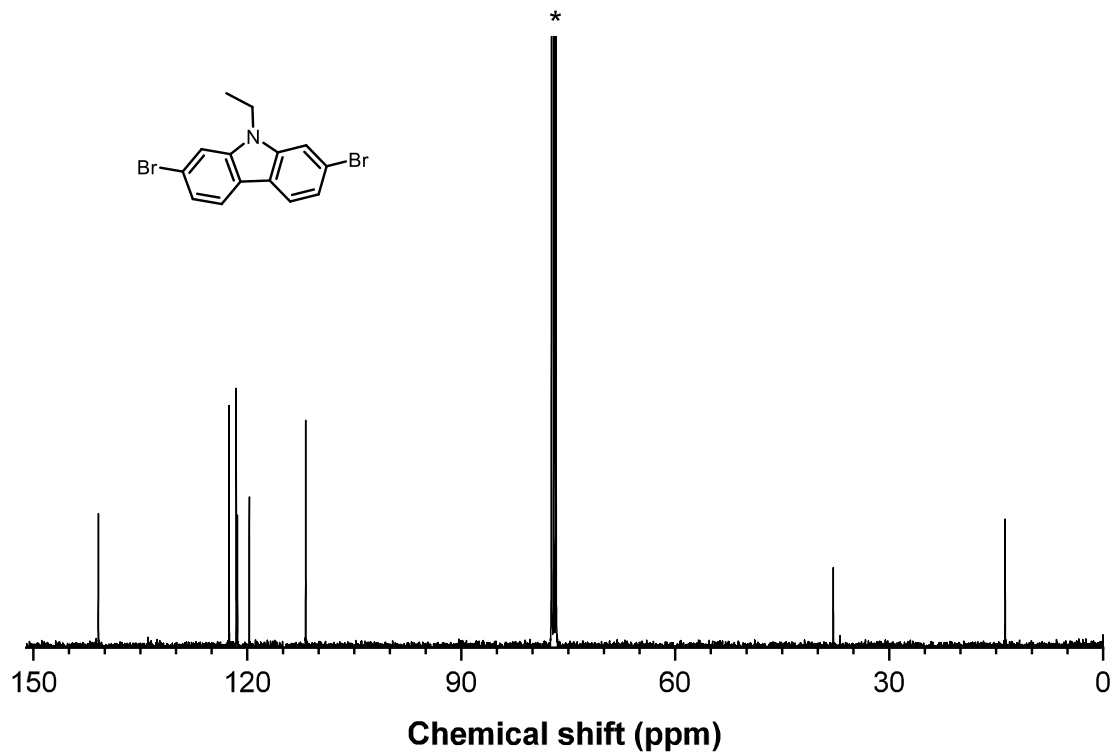
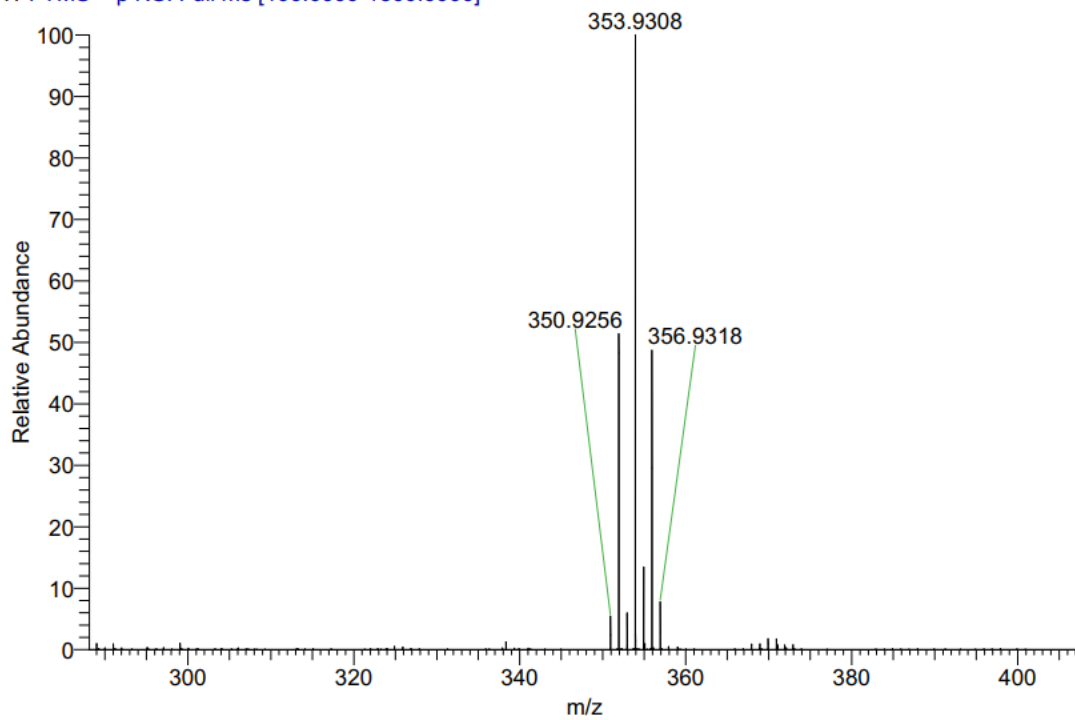


Fig. S17. The ^{13}C NMR spectrum of compound **12** in CDCl_3 .

T: FTMS + p NSI Full ms [100.0000-1500.0000]



zss-071#88 RT: 0.20

T: FTMS + p NSI Full ms [100.0000-1500.0000]

m/z= 351.35-352.51

| m/z | Intensity | Relative | Theo. Mass | Delta (ppm) | Composition |
|----------|--------------|----------|------------|-------------|--|
| 351.9332 | 1579010816.0 | 100.00 | 351.9331 | 0.13 | $\text{C}_{14}\text{H}_{12}\text{NBr}_2$ |

Fig. S18. HRMS of compound **12**.

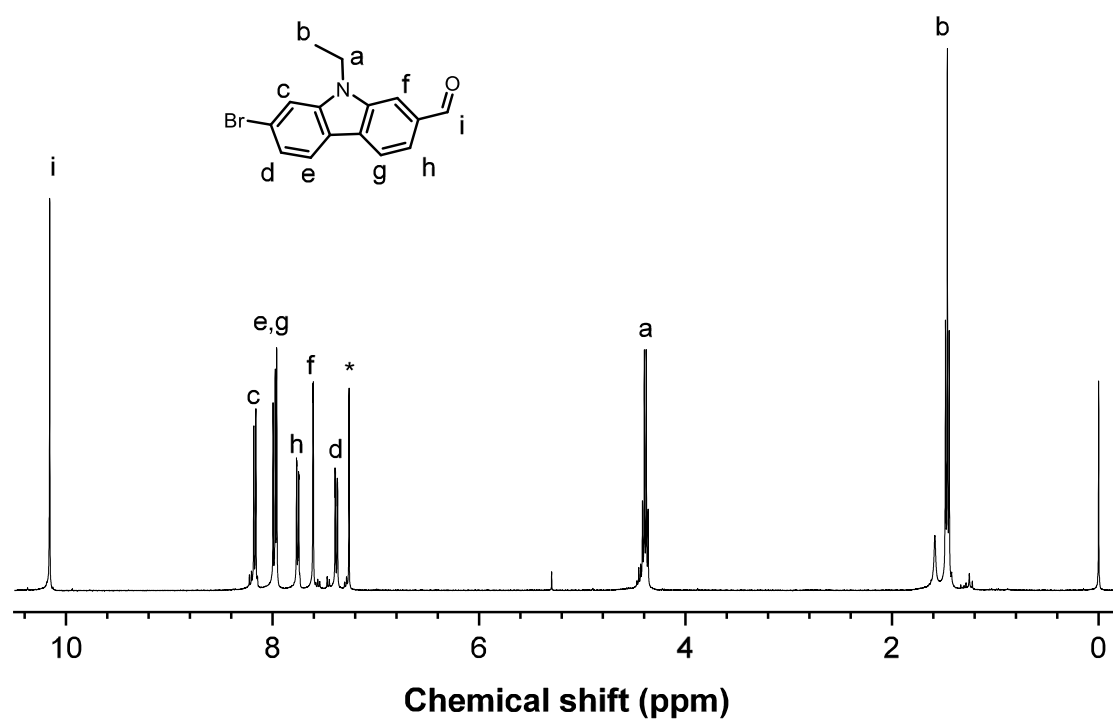


Fig. S19. The ¹H NMR spectrum of compound **13** in CDCl₃.

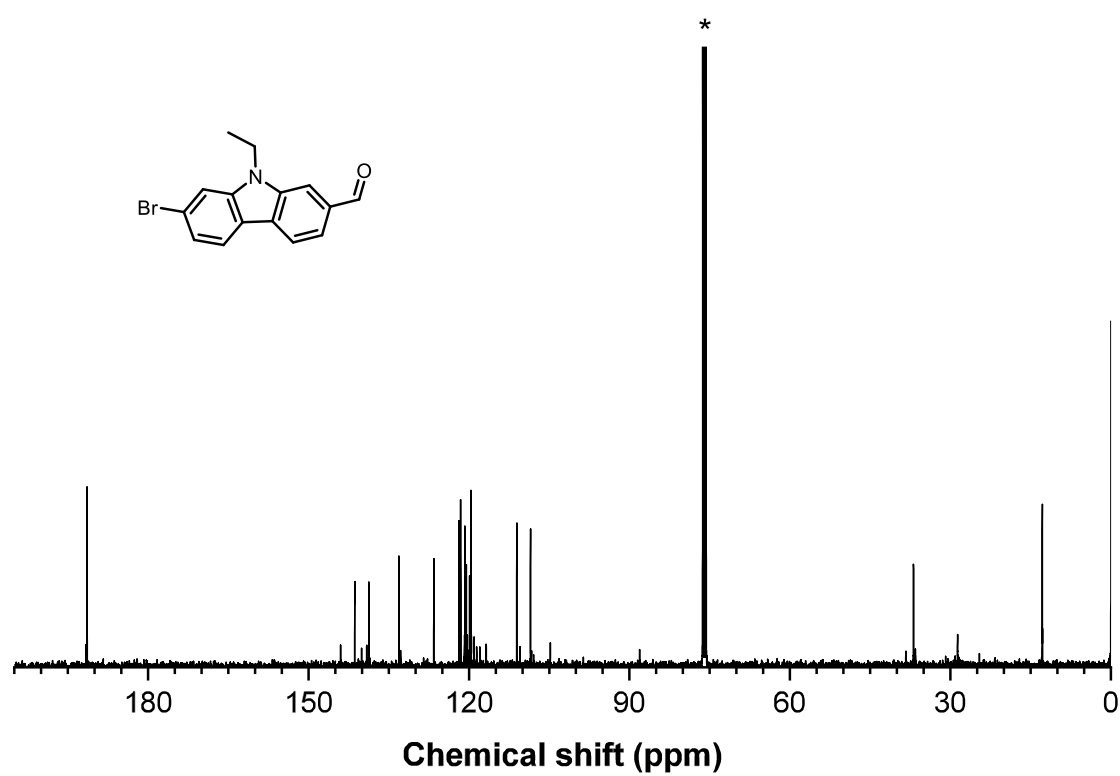
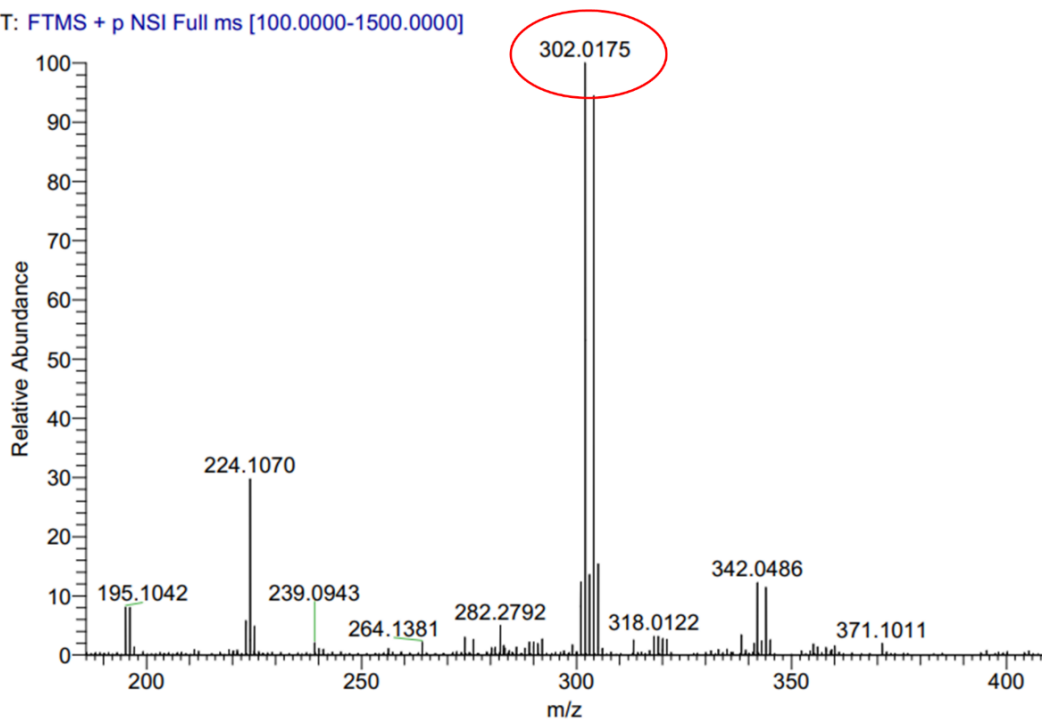


Fig. S20. The ¹³C NMR spectrum of compound **13** in CDCl₃.

T: FTMS + p NSI Full ms [100.0000-1500.0000]



zss-072#86 RT: 0.19

T: FTMS + p NSI Full ms [100.0000-1500.0000]

m/z= 299.74-304.92

| m/z | Intensity | Relative | Theo. Mass | Delta (ppm) | Composition |
|----------|-------------|----------|------------|-------------|--------------------------------------|
| 302.0175 | 978101952.0 | 100.00 | 302.0175 | -0.05 | C ₁₅ H ₁₃ ONBr |

Fig. S21. HRMS of compound 13.

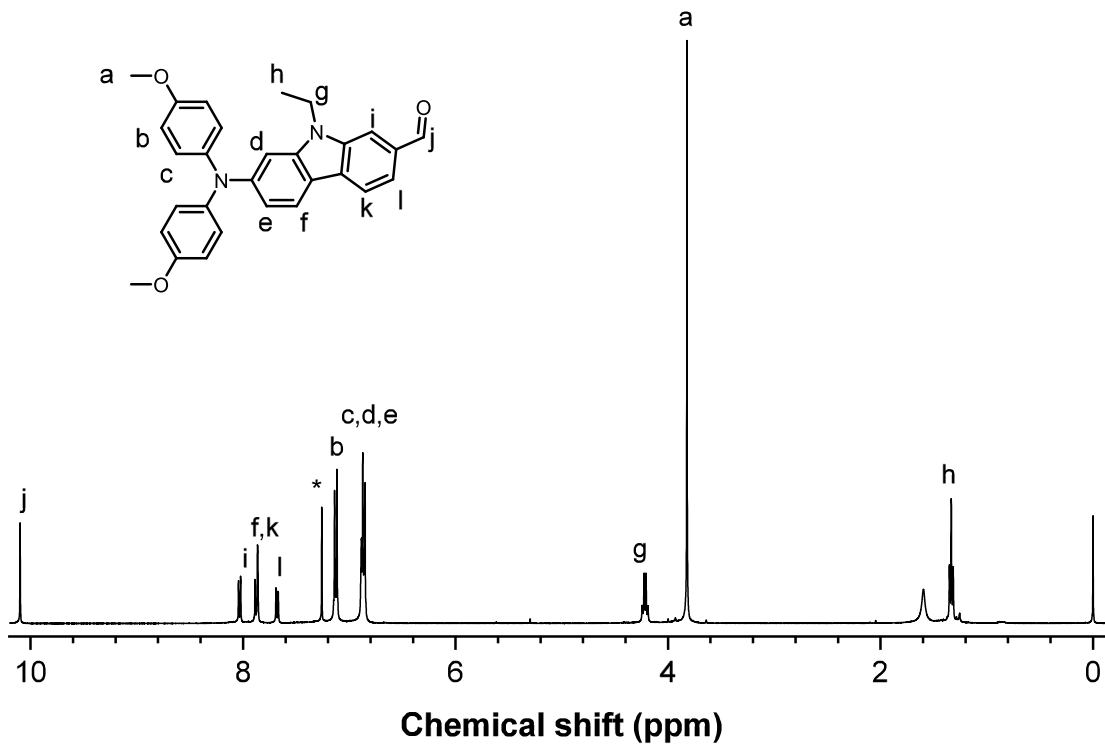


Fig. S22. The ¹H NMR spectrum of compound 15 in CDCl₃.

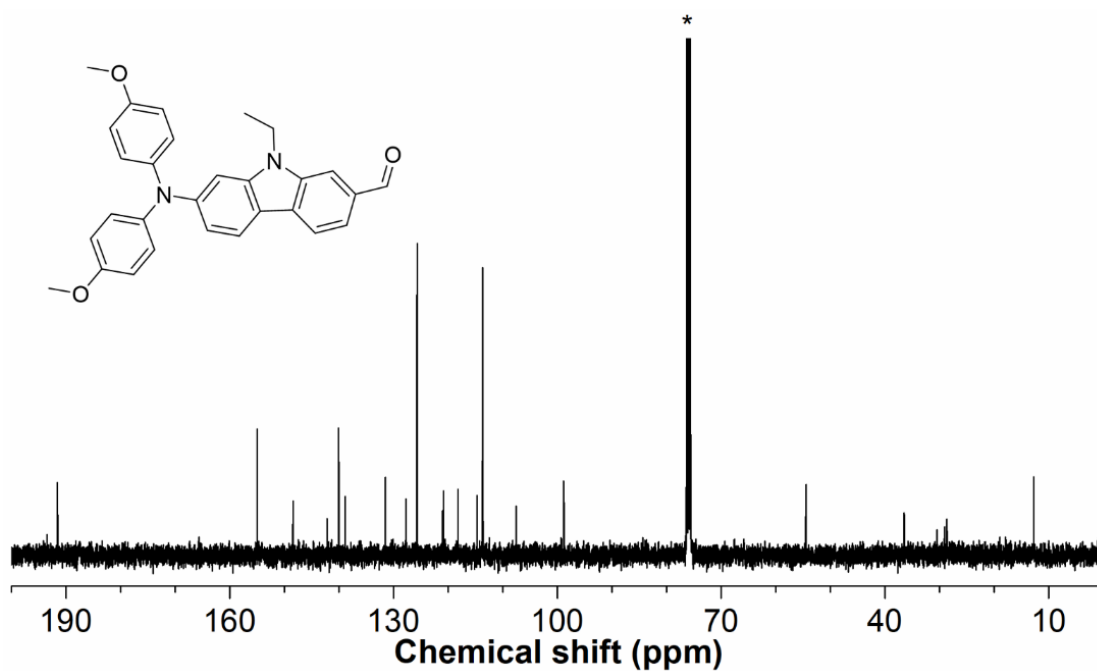
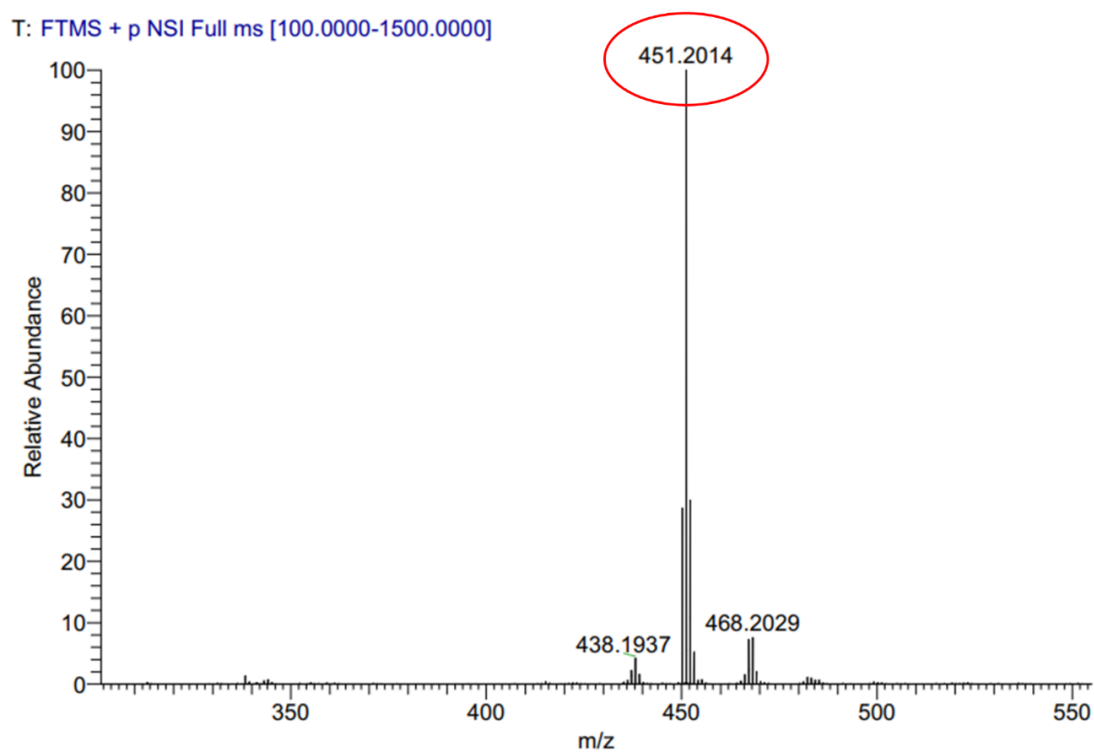


Fig. S23. The ^{13}C NMR spectrum of compound **15** in CDCl_3 .



zss-073#86 RT: 0.20

T: FTMS + p NSI Full ms [100.0000-1500.0000]

m/z = 450.00-460.97

| m/z | Intensity | Relative | Theo. Mass | Delta (ppm) | Composition |
|----------|--------------|----------|------------|-------------|--|
| 451.2014 | 7303992832.0 | 100.00 | 451.2016 | -0.20 | $\text{C}_{29}\text{H}_{27}\text{O}_3\text{N}_2$ |

Fig. S24. HRMS of compound **15**.

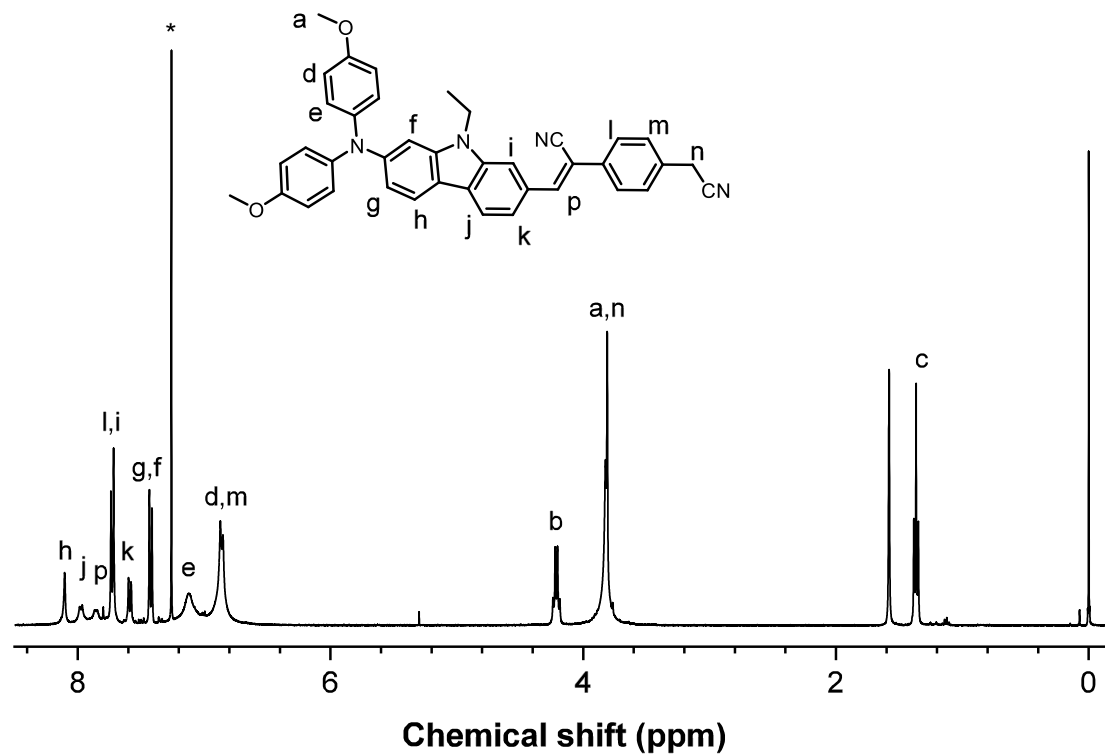


Fig. S25. The ^1H NMR spectrum of compound **16** in CDCl_3 .

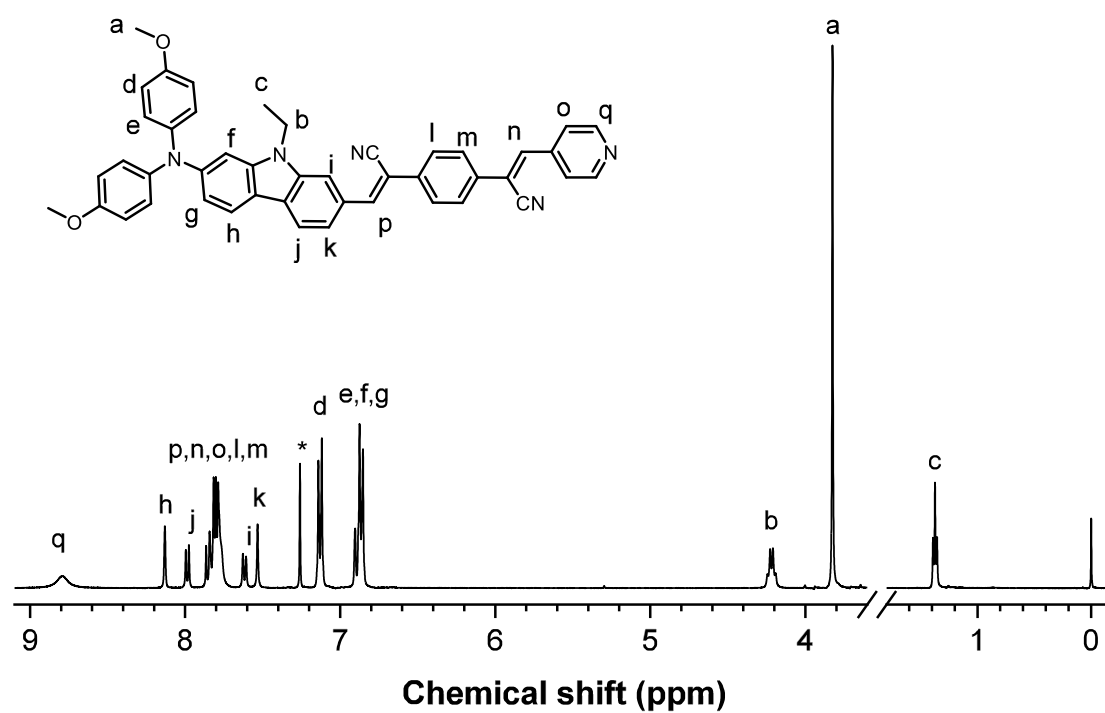


Fig. S26. The ^1H NMR spectrum of compound **17** in CDCl_3 .

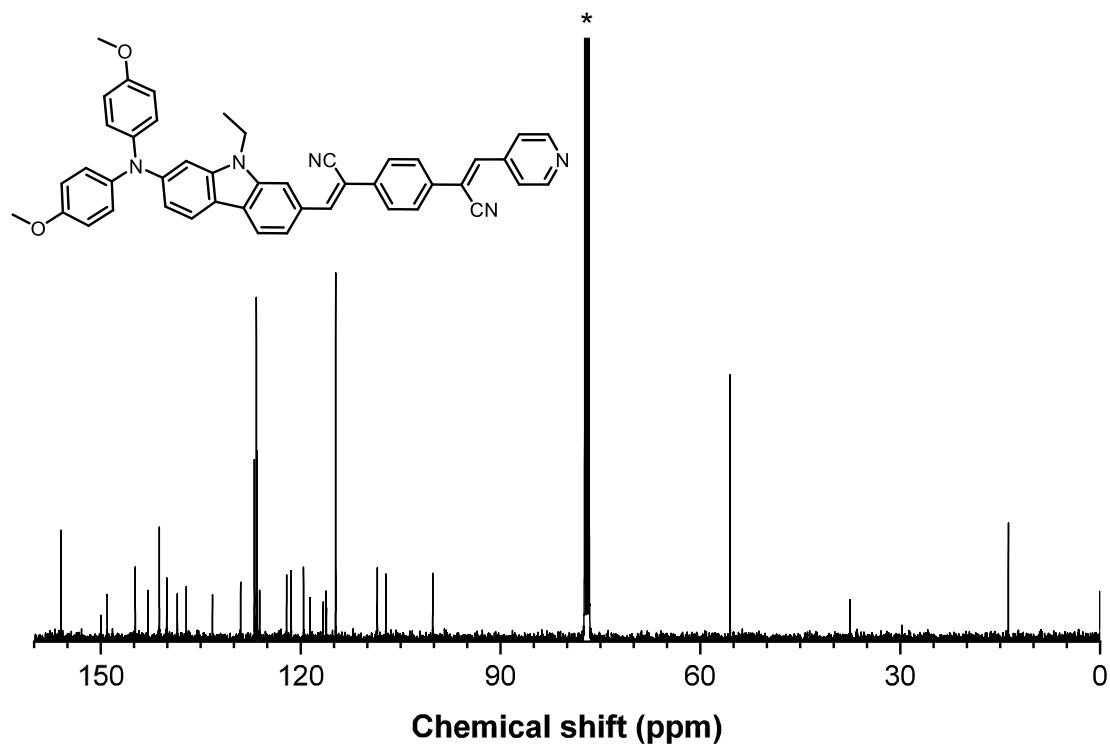


Fig. S27. The ^{13}C NMR spectrum of compound **17** in CDCl_3 .

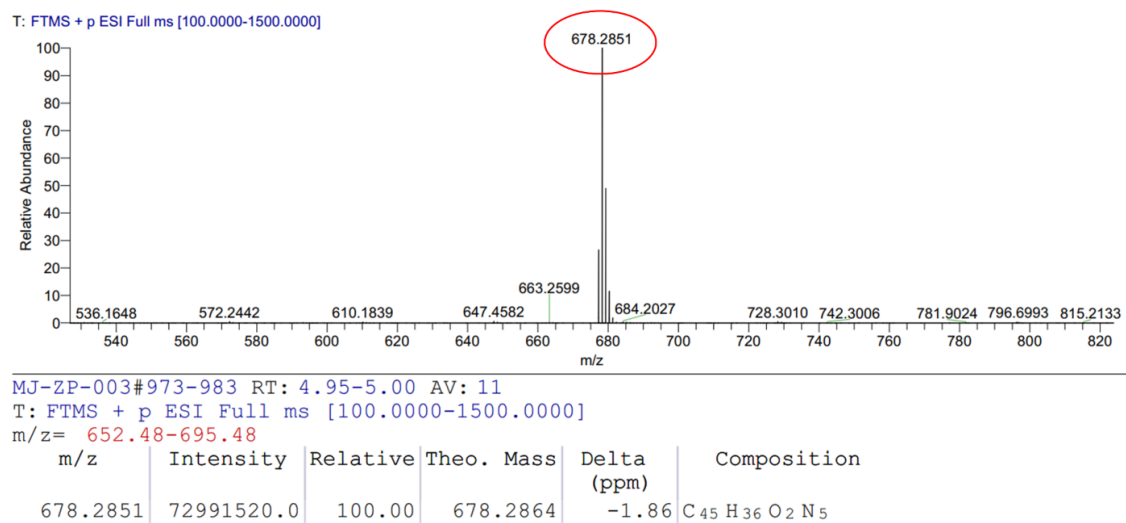


Fig. S28. HRMS of compound **17**.

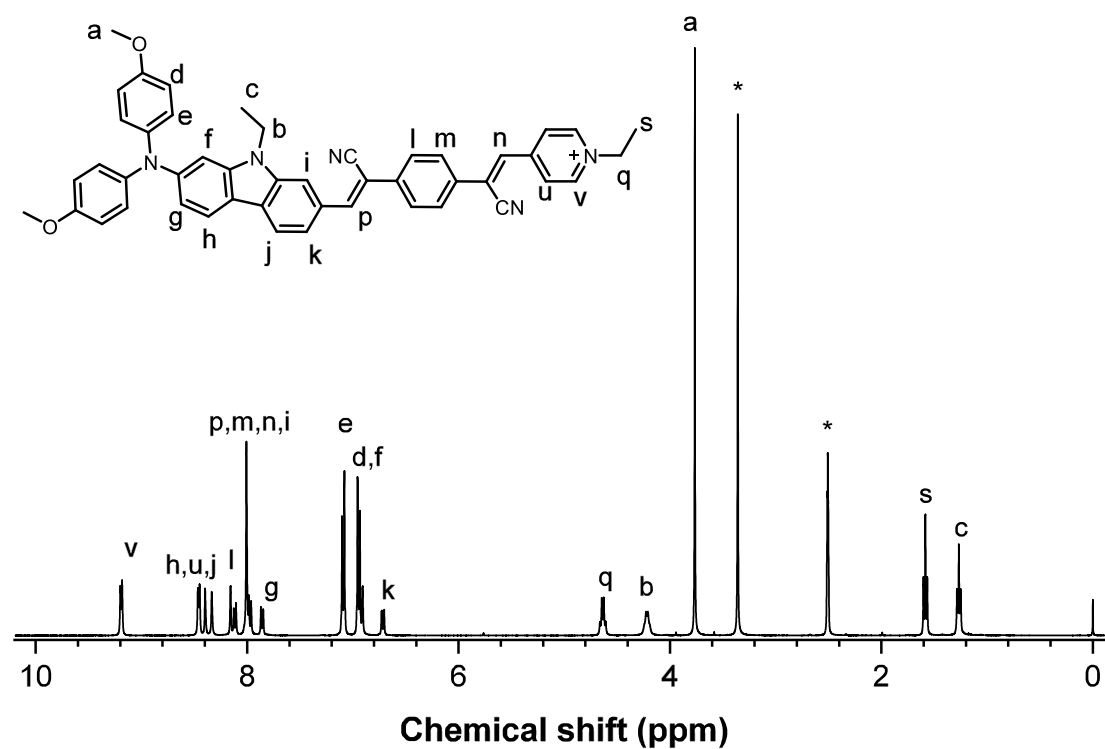


Fig. S29. The ^1H NMR spectrum of TPACzPy in $\text{DMSO-}d_6$.

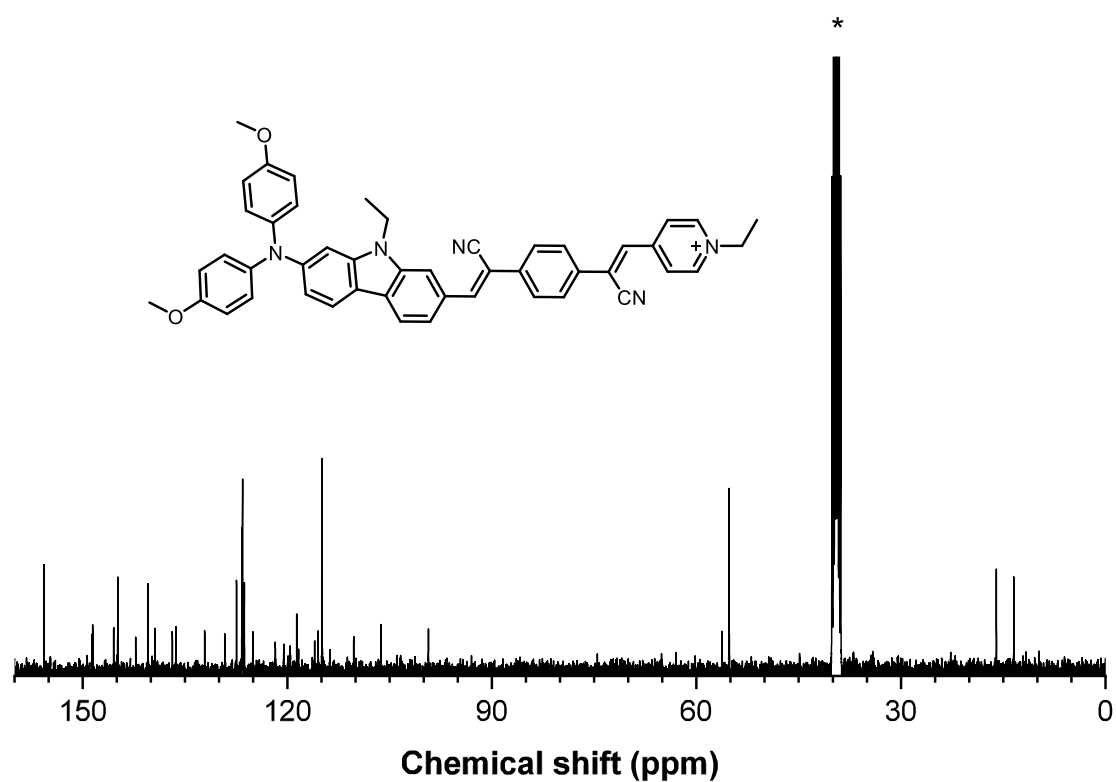
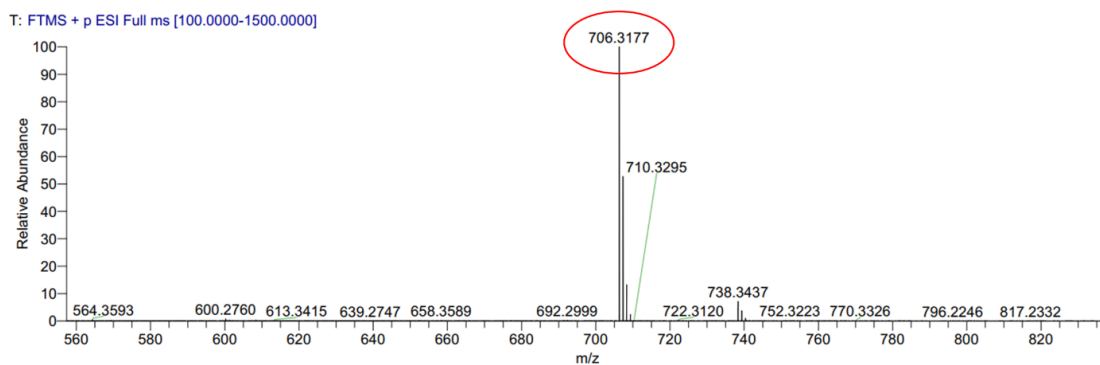


Fig. S30. The ^{13}C NMR spectrum of TPACzPy in $\text{DMSO-}d_6$.



MJ-ZSS-064#497-545 RT: 2.53-2.77 AV: 49

T: FTMS + p ESI Full ms [100.0000-1500.0000]

m/z = 704.67-708.29

| m/z | Intensity | Relative | Theo. Mass | Delta (ppm) | Composition |
|----------|-------------|----------|------------|-------------|---|
| 706.3177 | 151973600.0 | 100.00 | 706.3177 | 0.04 | C ₄₇ H ₄₀ O ₂ N ₅ |

Fig. S31. HRMS of TPACzPy.

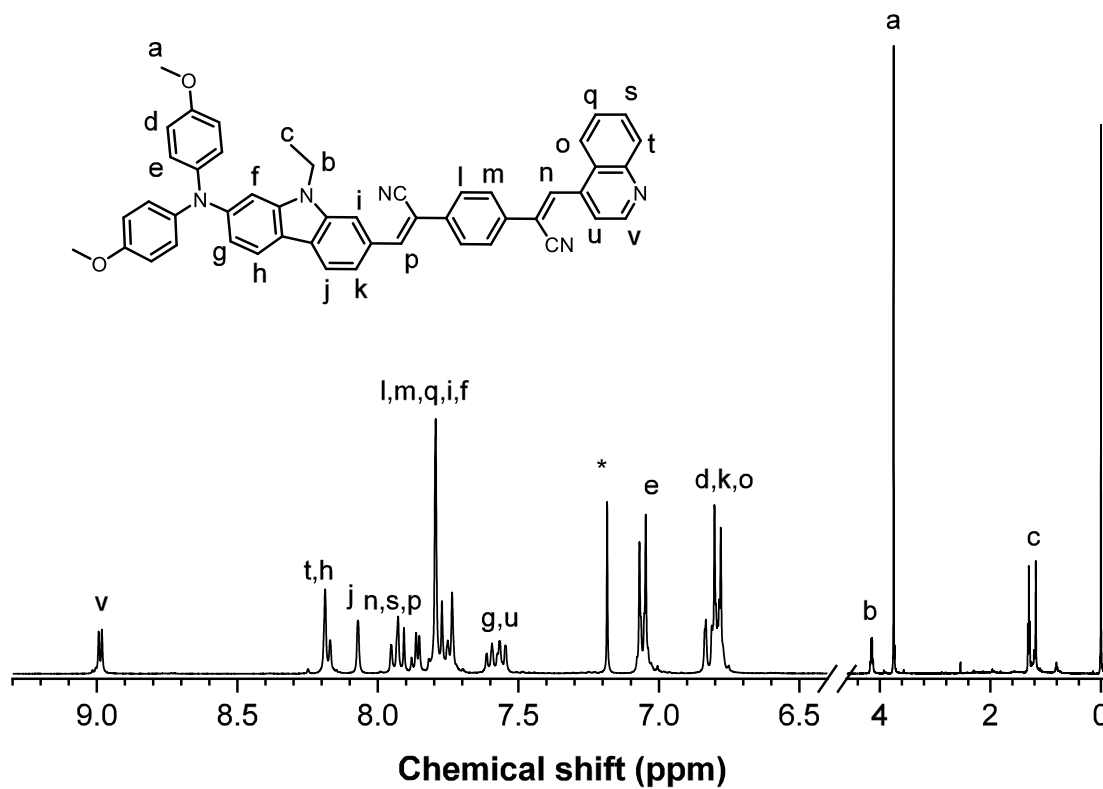


Fig. S32. The ¹H NMR spectrum of compound 18 in CDCl₃.

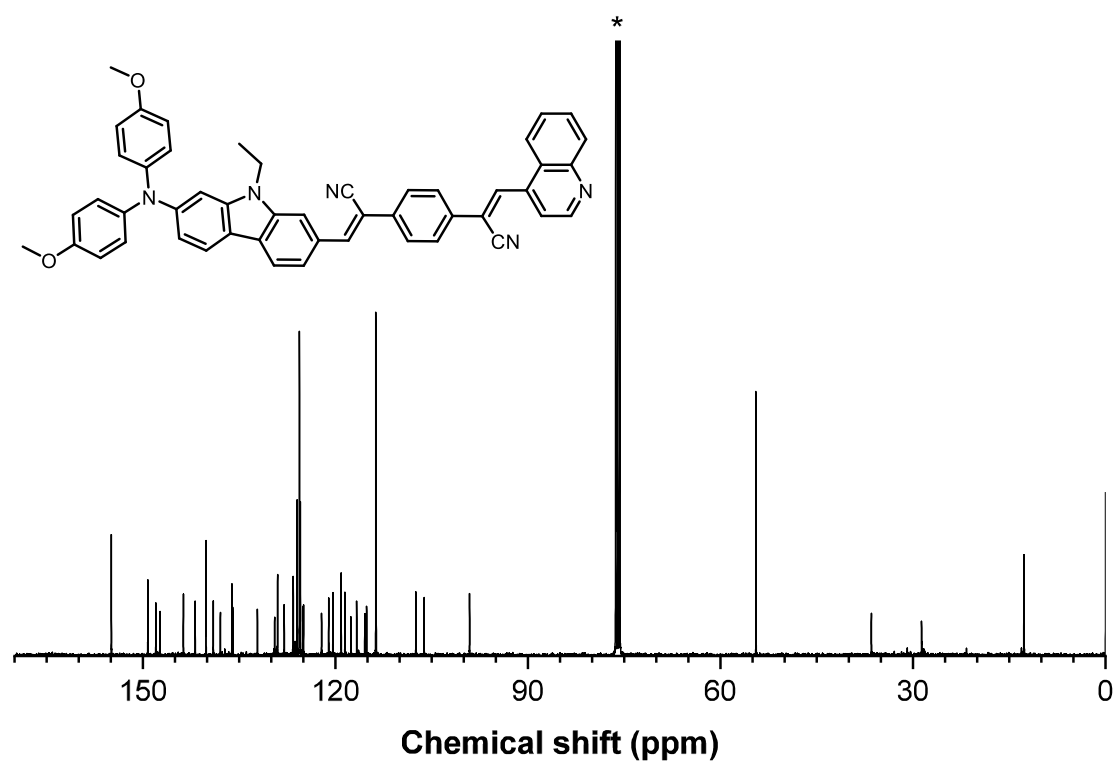
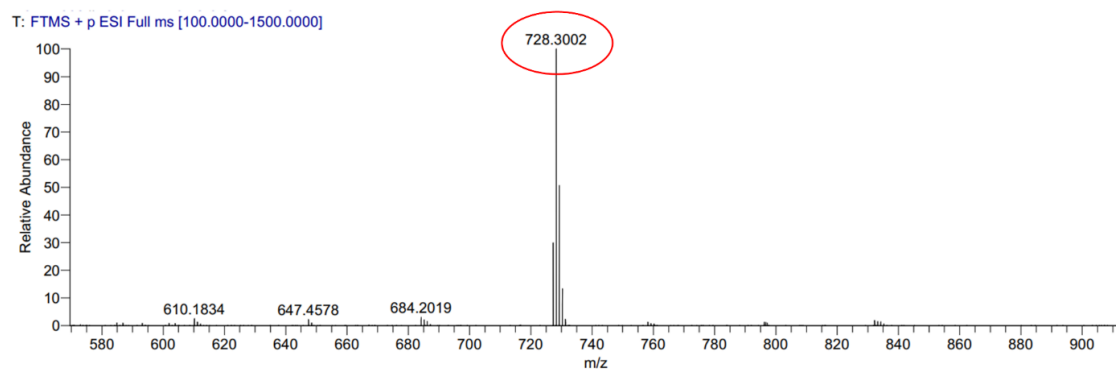


Fig. S33. The ^{13}C NMR spectrum of compound **18** in CDCl_3 .



MJ-ZP-003#46-83 RT: 0.23-0.42 AV: 38

T: FTMS + p ESI Full ms [100.0000-1500.0000]

m/z = 720.19-737.57

| m/z | Intensity | Relative | Theo. Mass | Delta (ppm) | Composition |
|----------|------------|----------|------------|-------------|--|
| 728.3002 | 11640662.0 | 100.00 | 728.3020 | -2.50 | $\text{C}_{49}\text{H}_{38}\text{O}_2\text{N}_5$ |

Fig. S34. HRMS of compound **18**.

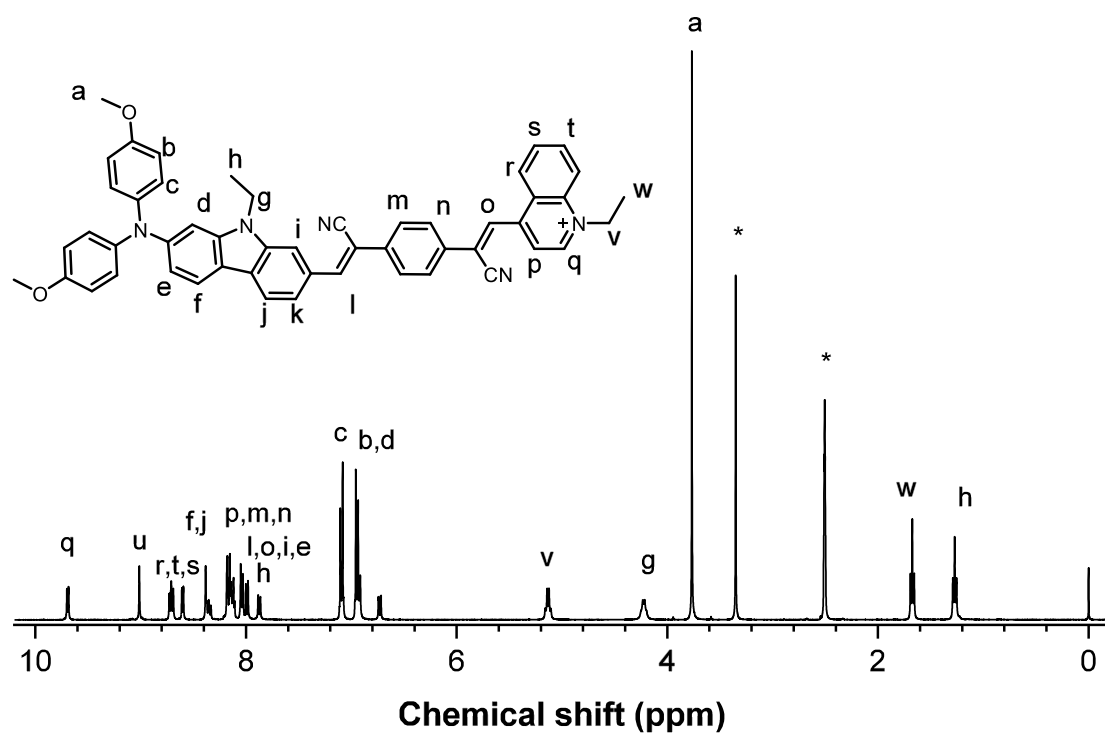


Fig. S35. The ^1H NMR spectrum of TPACzQu in $\text{DMSO-}d_6$.

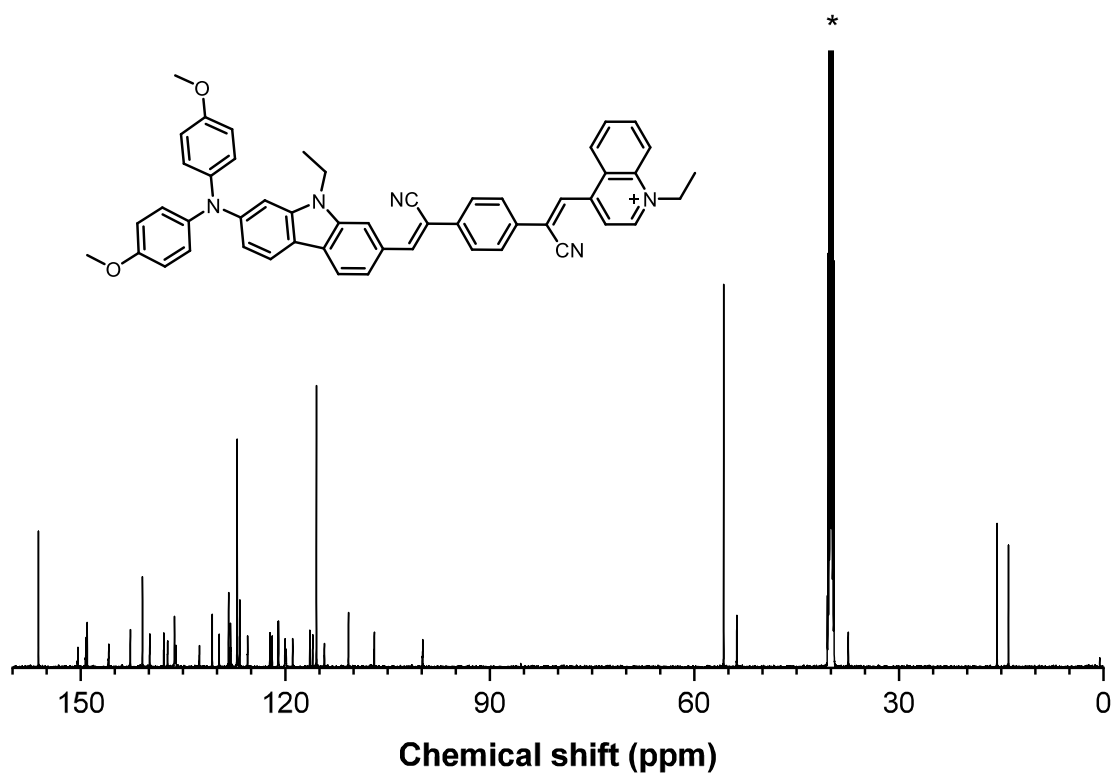


Fig. S36. The ^{13}C NMR spectrum of TPACzQu in $\text{DMSO-}d_6$.

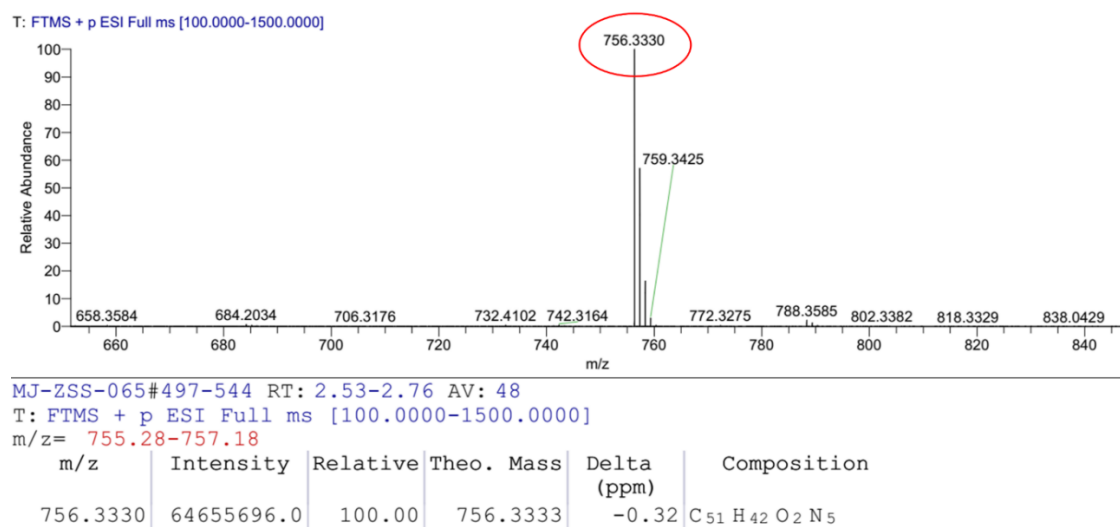


Fig. S37. HRMS of TPACzQu.

9.2 The calculation results and measurement spectra

Table S1. Theoretically calculated energy levels and energy gaps of TPAPy.

| S _n | Energy (eV) | T _n | Energy (eV) | S ₁ /T _n | $\Delta E_{S_1-T_n}$ (eV) |
|----------------|-------------|----------------|-------------|--------------------------------|---------------------------|
| S ₁ | 1.20 | T ₁ | 0.46 | S ₁ /T ₁ | 0.74 |
| S ₂ | 2.04 | T ₂ | 1.47 | S ₁ /T ₂ | -0.27 |
| S ₃ | 2.09 | T ₃ | 1.91 | S ₁ /T ₃ | -0.71 |
| S ₄ | 2.58 | T ₄ | 2.04 | S ₁ /T ₄ | -0.84 |
| S ₅ | 2.79 | T ₅ | 2.18 | S ₁ /T ₅ | -0.98 |

Table S2. Theoretically calculated energy levels and energy gaps of TPAQu.

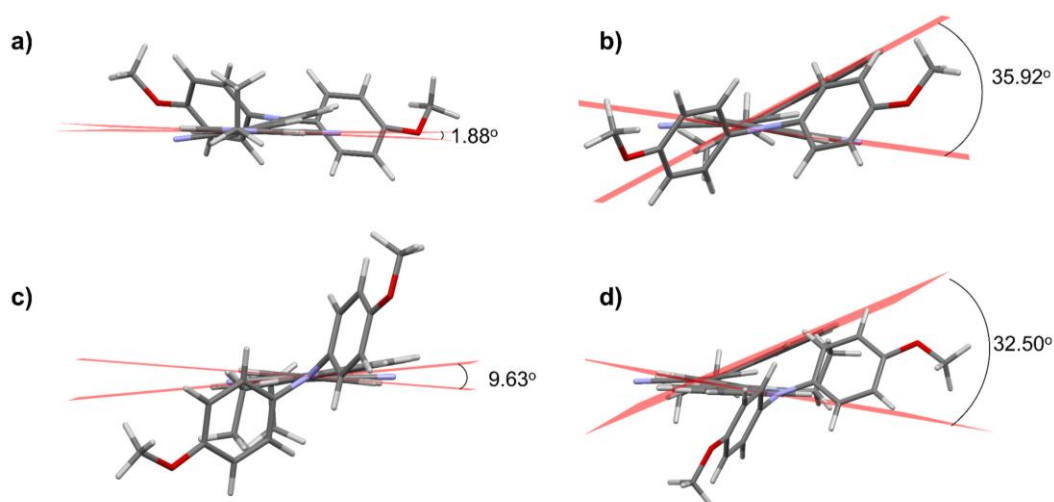
| S _n | Energy (eV) | T _n | Energy (eV) | S ₁ /T _n | $\Delta E_{S_1-T_n}$ (eV) |
|----------------|-------------|----------------|-------------|--------------------------------|---------------------------|
| S ₁ | 1.12 | T ₁ | 0.43 | S ₁ /T ₁ | 0.69 |
| S ₂ | 1.95 | T ₂ | 1.42 | S ₁ /T ₂ | -0.30 |
| S ₃ | 2.05 | T ₃ | 1.85 | S ₁ /T ₃ | -0.73 |
| S ₄ | 2.46 | T ₄ | 2.00 | S ₁ /T ₄ | -0.88 |
| S ₅ | 2.77 | T ₅ | 2.09 | S ₁ /T ₅ | -0.97 |

Table S3. Theoretically calculated energy levels and energy gaps of TPACzPy.

| S_n | Energy (eV) | T_n | Energy (eV) | S_1/T_n | $\Delta E_{S_1-T_n}$ (eV) |
|-------|-------------|-------|-------------|-----------|---------------------------|
| S_1 | 1.49 | T_1 | 0.30 | S_1/T_1 | 1.19 |
| S_2 | 1.63 | T_2 | 1.10 | S_1/T_2 | 0.39 |
| S_3 | 1.99 | T_3 | 1.72 | S_1/T_3 | -0.23 |
| S_4 | 2.07 | T_4 | 2.02 | S_1/T_4 | -0.53 |
| S_5 | 2.17 | T_5 | 2.17 | S_1/T_5 | -0.68 |

Table S4. Theoretically calculated energy levels and energy gaps of TPACzQu.

| S_n | Energy (eV) | T_n | Energy (eV) | S_1/T_n | $\Delta E_{S_1-T_n}$ (eV) |
|-------|-------------|-------|-------------|-----------|---------------------------|
| S_1 | 1.46 | T_1 | 0.32 | S_1/T_1 | 1.14 |
| S_2 | 1.60 | T_2 | 1.06 | S_1/T_2 | 0.40 |
| S_3 | 1.99 | T_3 | 1.99 | S_1/T_3 | -0.53 |
| S_4 | 2.03 | T_4 | 2.03 | S_1/T_4 | -0.57 |
| S_5 | 2.08 | T_5 | 2.08 | S_1/T_5 | -0.62 |

**Fig. S38.** The dihedral angles of a) TPAPy, b) TPAQu, c) TPACzPy, and d) TPACzQu.

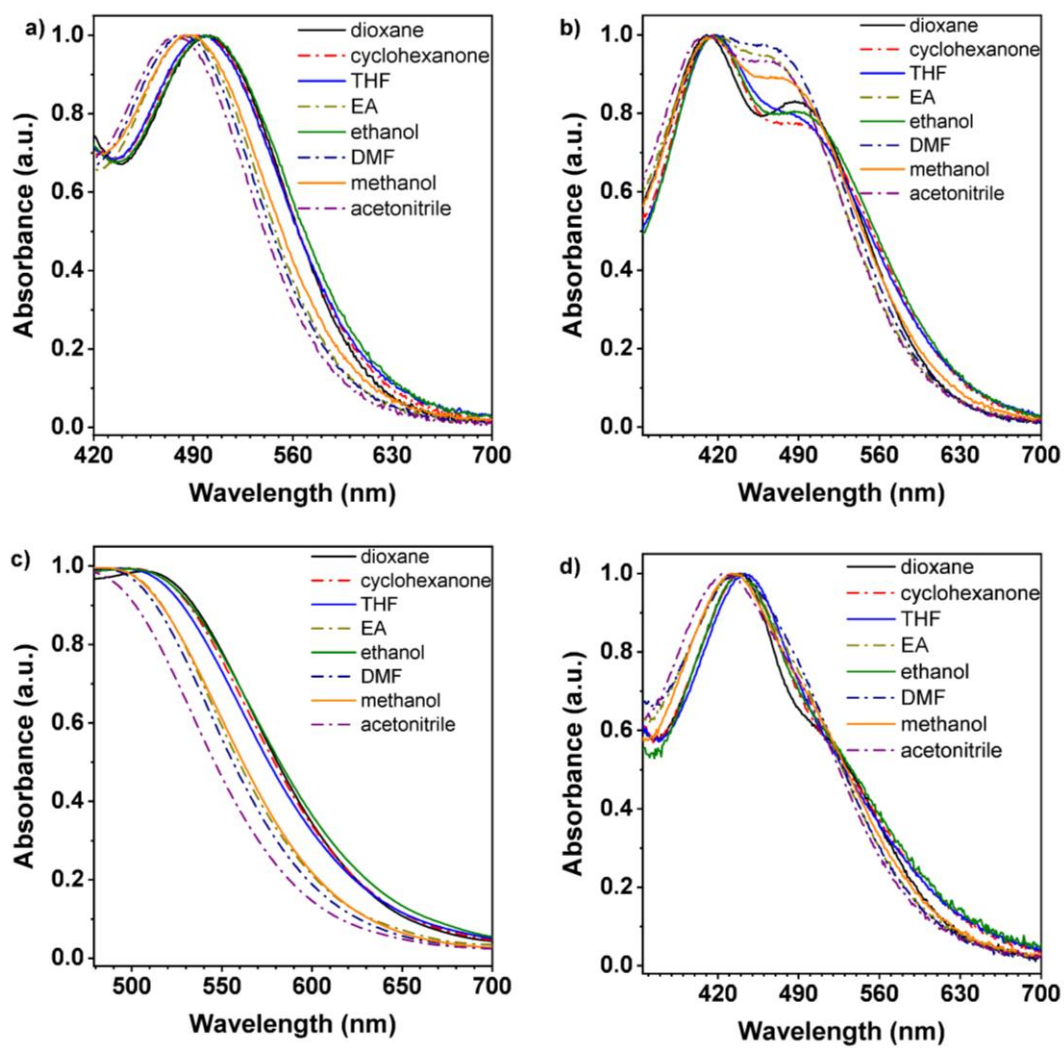


Fig. S39. The normalized UV-Vis spectra of a) TPAPy, b) TPAQu, c) TPACzPy, and d) TPACzQu in different solvents with various polarities. $c = 10 \mu\text{M}$.

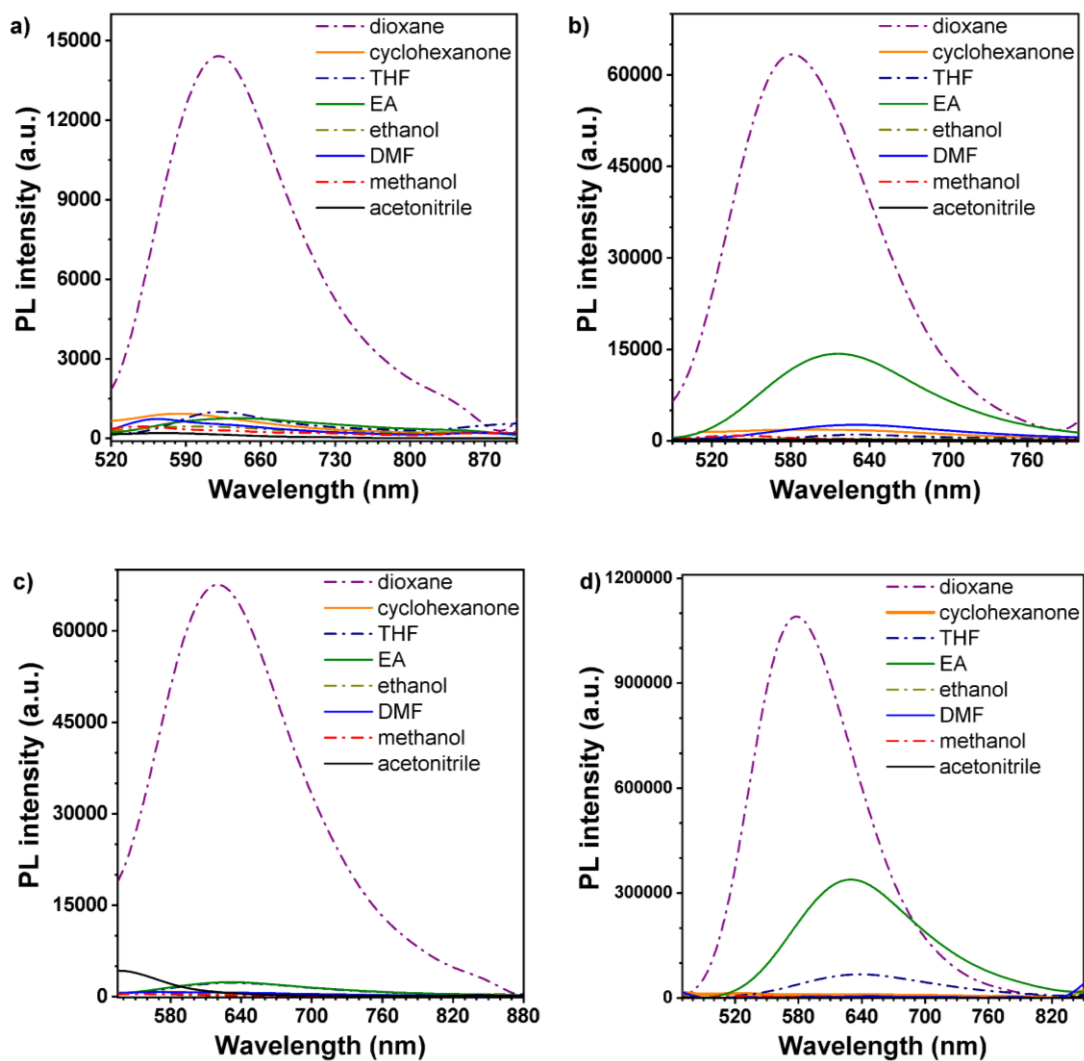


Fig. S40. PL spectra of a) TPAPy, b) TPAQu, c) TPACzPy and d) TPACzQu in different solvents with various polarities. TPAPy: $\lambda_{\text{ex}} = 500$ nm, TPAQu: $\lambda_{\text{ex}} = 410$ nm, TPACzPy: $\lambda_{\text{ex}} = 515$ nm, TPACzQu: $\lambda_{\text{ex}} = 440$ nm. $c = 10$ μM .

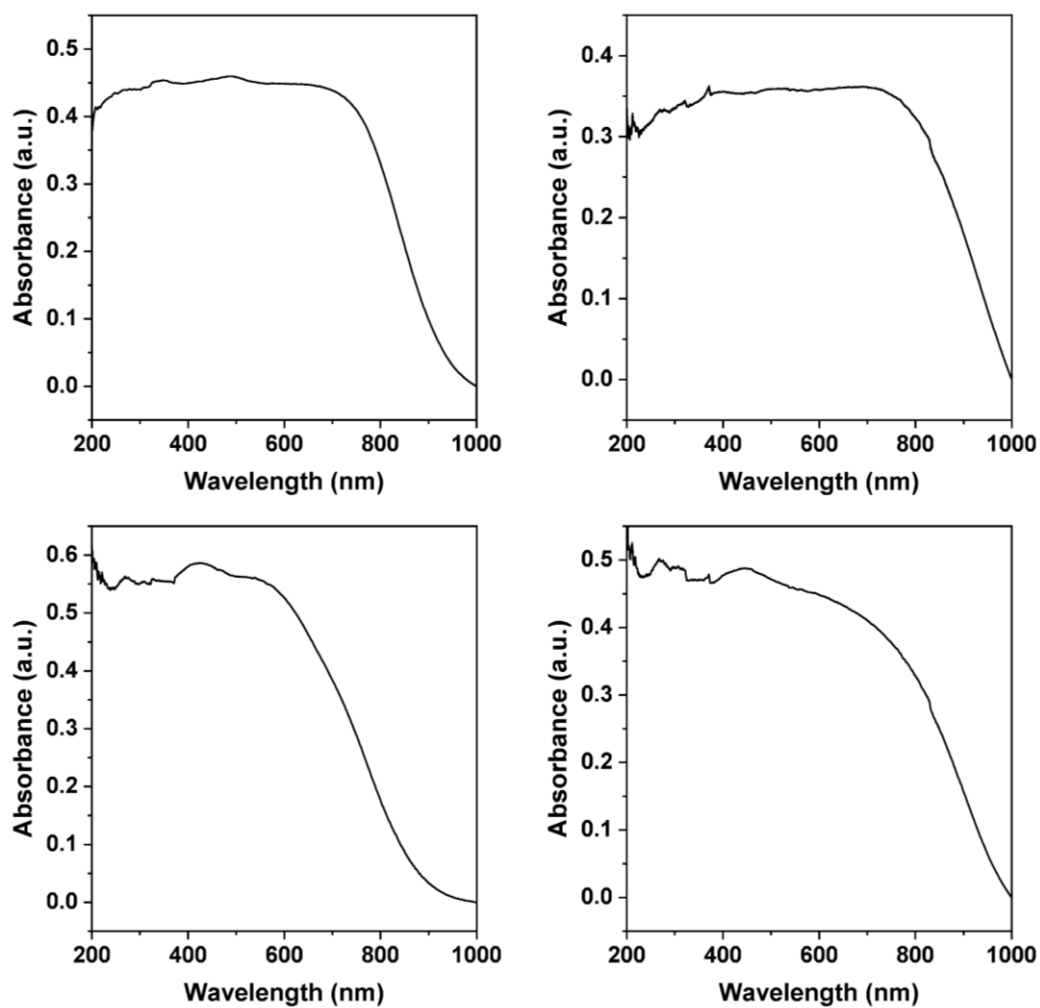


Fig. S41. The UV-Vis spectra of a) TPAPy, b) TPAQu, c) TPACzPy, and d) TPACzQu in the solid state.

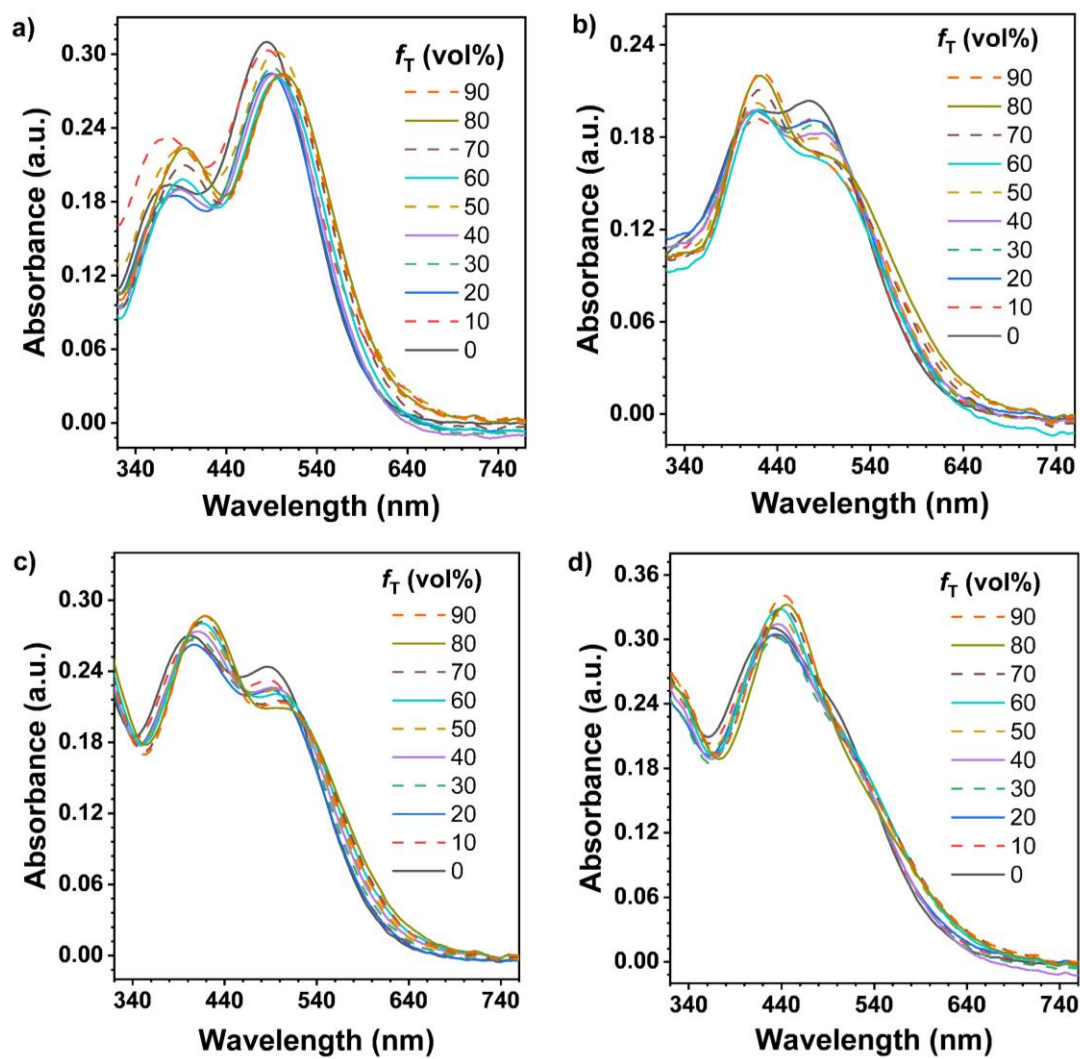


Fig. S42. The UV-Vis spectra of a) TPAPy, b) TPAQu, c) TPACzPy, and d) TPACzQu in the DMSO/toluene mixtures with different toluene fractions (f_T), $c = 10 \mu\text{M}$.

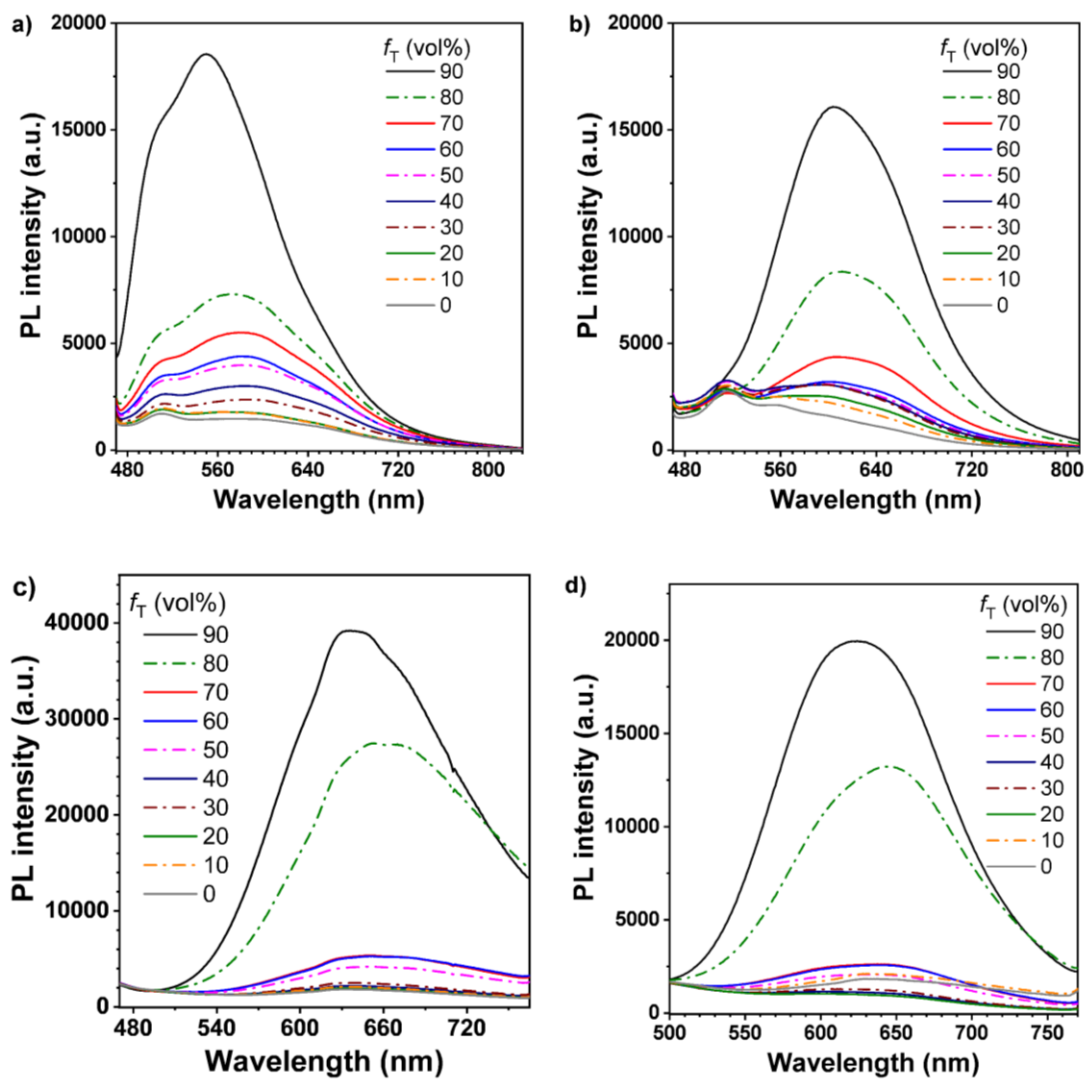


Fig. S43. PL spectra of a) TPAPy, b) TPAQu, c) TPACzPy, and d) TPACzQu in the DMSO/toluene mixtures with different toluene fractions (f_T s), TPAPy: $\lambda_{\text{ex}} = 440$ nm, TPAQu: $\lambda_{\text{ex}} = 440$ nm, TPACzPy: $\lambda_{\text{ex}} = 400$ nm, TPACzQu: $\lambda_{\text{ex}} = 400$ nm. $c = 10$ μM .

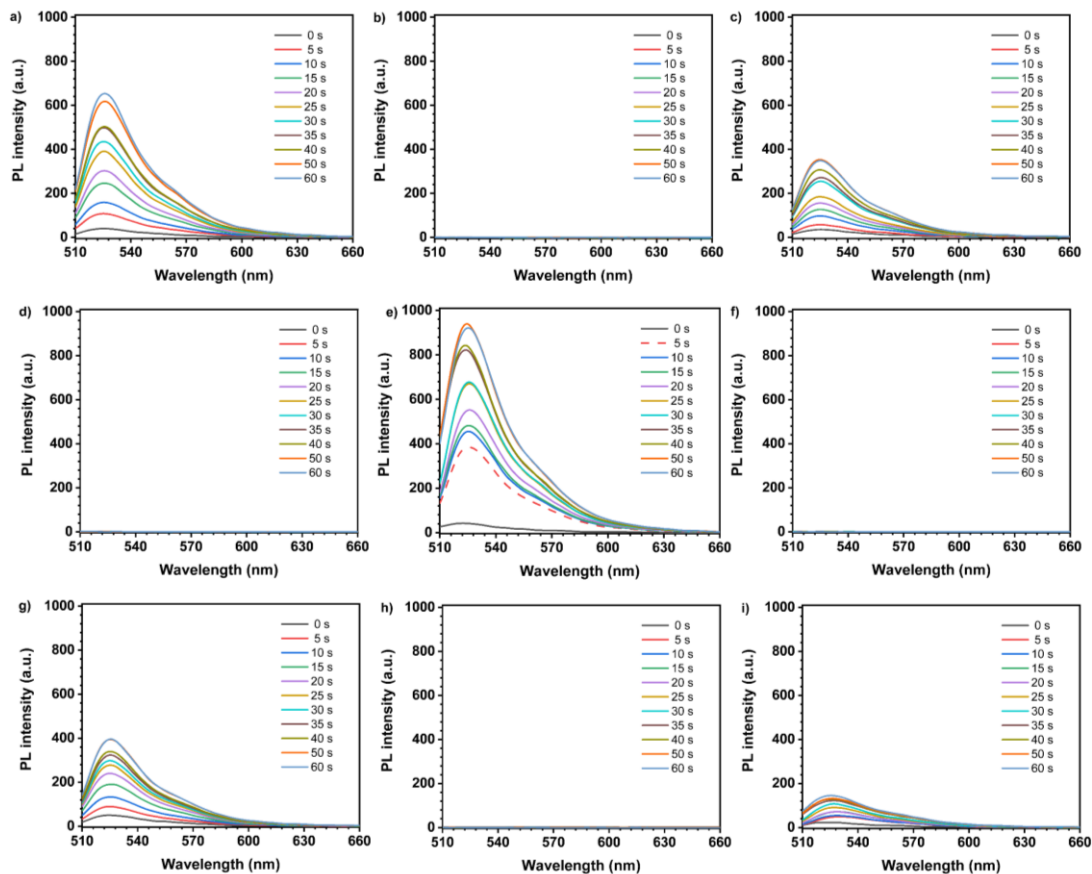


Fig. S44. PL spectra of a) DCFH+TPAPy, b) TPAPy, c) DCFH+TPAQu, d) TPAQu, e) DCFH+TPACzPy, f) TPACzPy, g) DCFH+TPACzQu, h) TPACzQu, and i) DCFH+RB in the DMSO/PBS ($v/v = 2/98$) mixture under the irradiation of white light for different time. $\lambda_{\text{ex}} = 488$ nm.

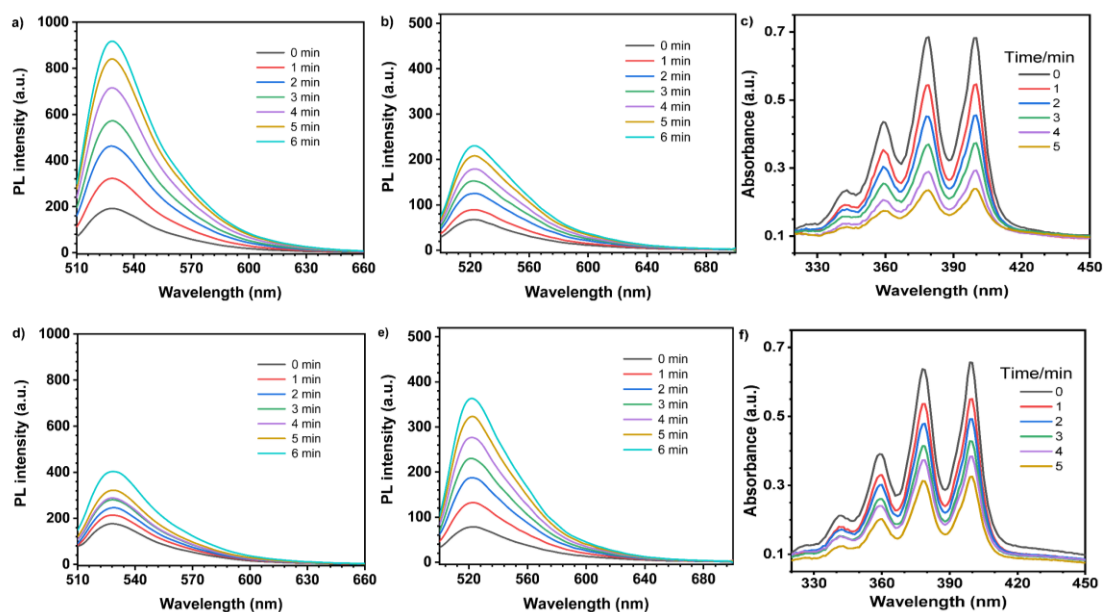


Fig. S45. PL spectra of DHR123 in the presence of a) TPAPy and d) TPAQu in the DMSO/PBS ($v/v = 2/98$) mixture under the white-light irradiation with different time. PL spectra of HPF in the presence of b) TPAPy and e) TPAQu in the DMSO/PBS ($v/v = 2/98$) mixture under the white-light irradiation with different time. The UV-Vis spectra of ABDA in the presence of c) TPAPy and f) TPAQu after being irradiated by white light for different time. DHR123: $\lambda_{ex} = 490$ nm, HPF: $\lambda_{ex} = 480$ nm.

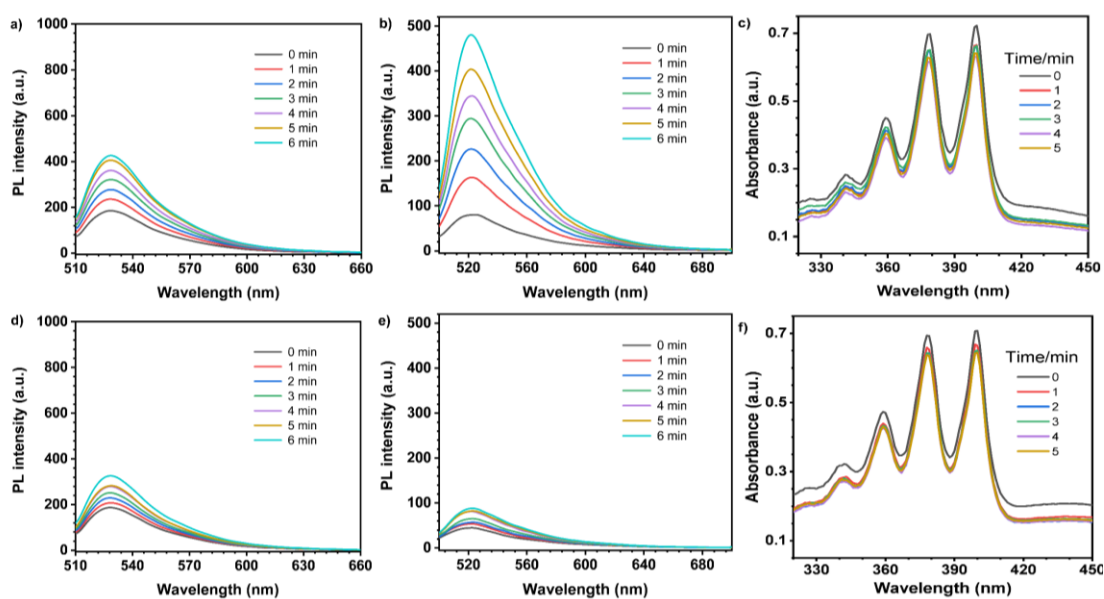


Fig. S46. PL spectra of DHR123 in the presence of a) TPACzPy and d) TPACzQu in the DMSO/PBS ($v/v = 2/98$) mixture under the white-light irradiation with different time. PL spectra of HPF in the presence of b) TPACzPy and e) TPACzQu in the DMSO/PBS ($v/v = 2/98$) mixture under the white-light irradiation with different time. The UV-Vis spectra of ABDA in the presence of c) TPACzPy and f) TPACzQu after being irradiated by white light for different time. DHR123: $\lambda_{ex} = 490$ nm, HPF: $\lambda_{ex} = 480$ nm.

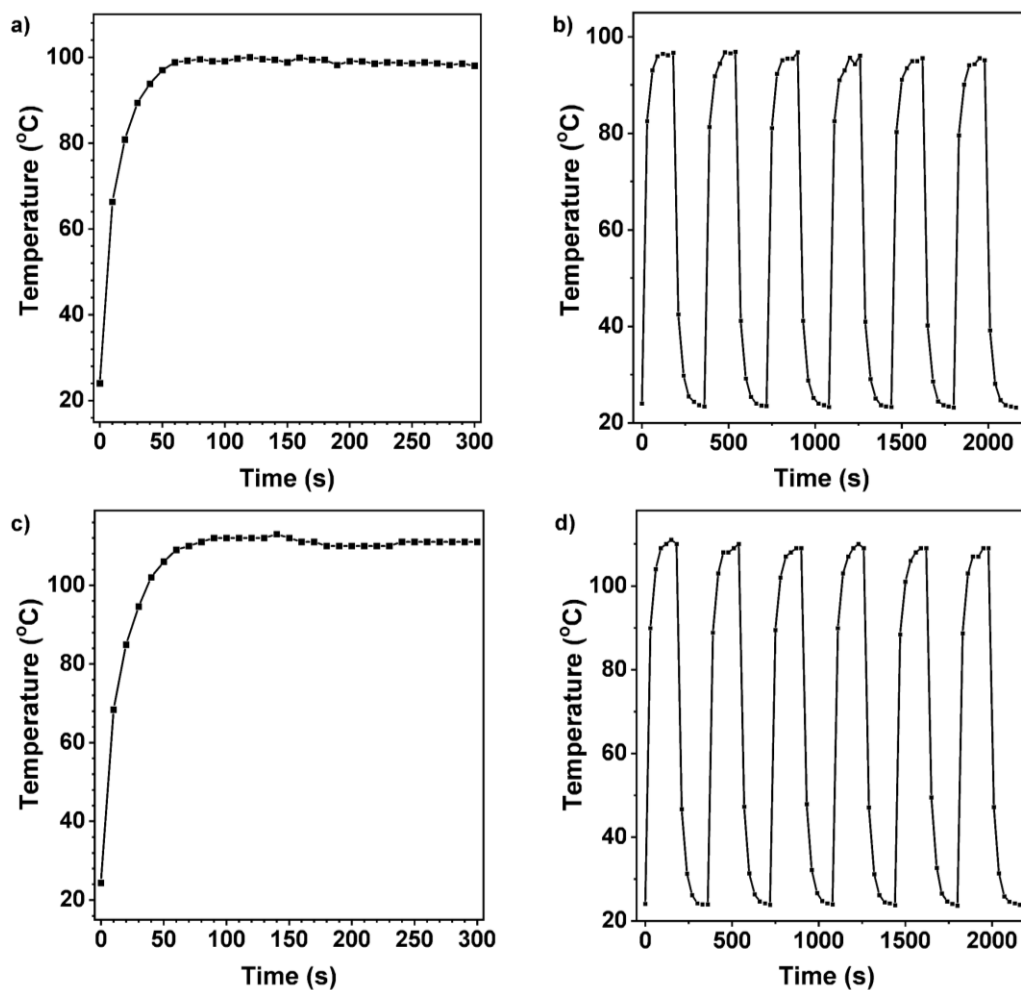


Fig. S47. The temperature variation of the solid-state a) TPAPy and c) TPAQu under the irradiation of a 660 nm-laser (0.70 W/cm^2). The temperature profiles of the solid-state b) TPAPy and d) TPAQu under the irradiation of a 660 nm-laser (0.70 W/cm^2) in six ON/OFF cycles.

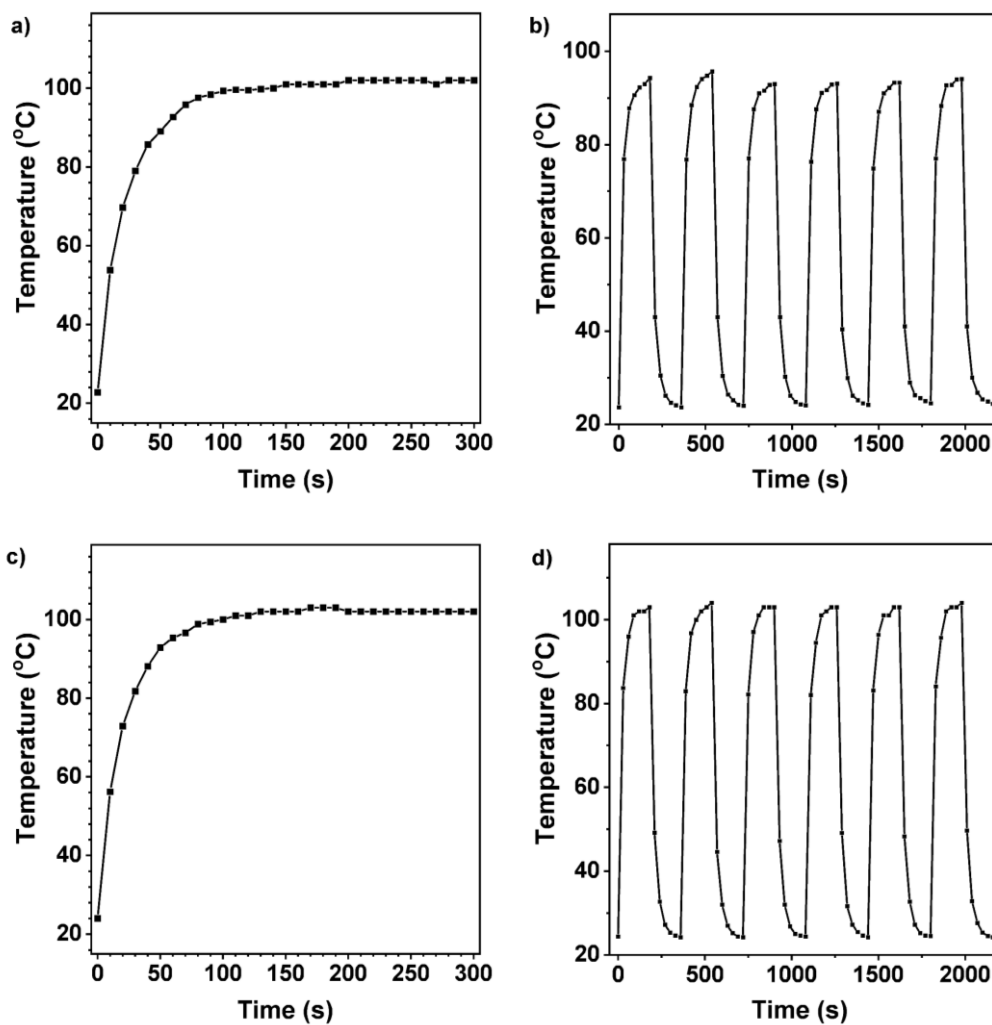


Fig. S48. The temperature variation of the solid-state a) TPACzPy and c) TPACzQu under the irradiation of a 660 nm-laser (0.70 W/cm^2). The temperature profiles of the solid-state b) TPACzPy and d) TPACzQu under the irradiation of a 660 nm-laser (0.70 W/cm^2) in six ON/OFF cycles.

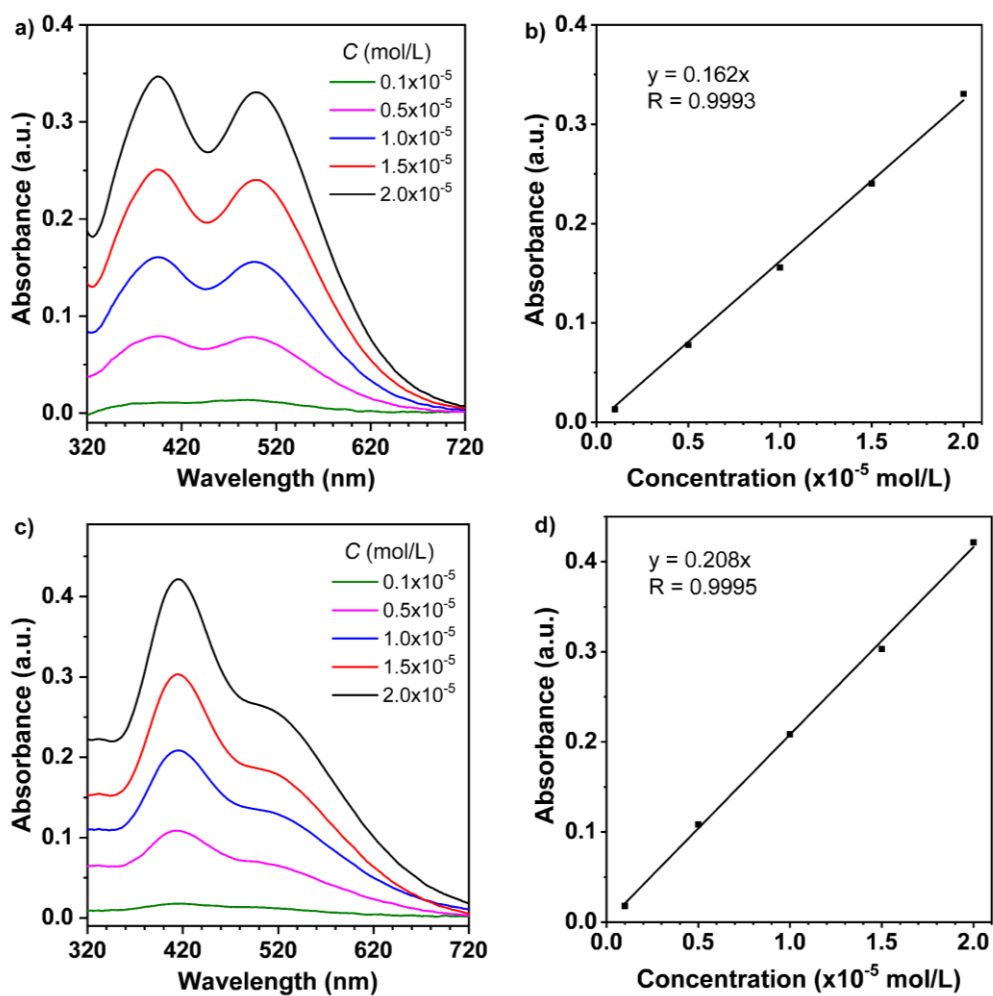


Fig. S49. The UV-Vis spectra of a) TPAPy and c) TPAQu solutions at different concentrations. The linear relationship between the absorbance and concentration of b) TPAPy and d) TPAQu.

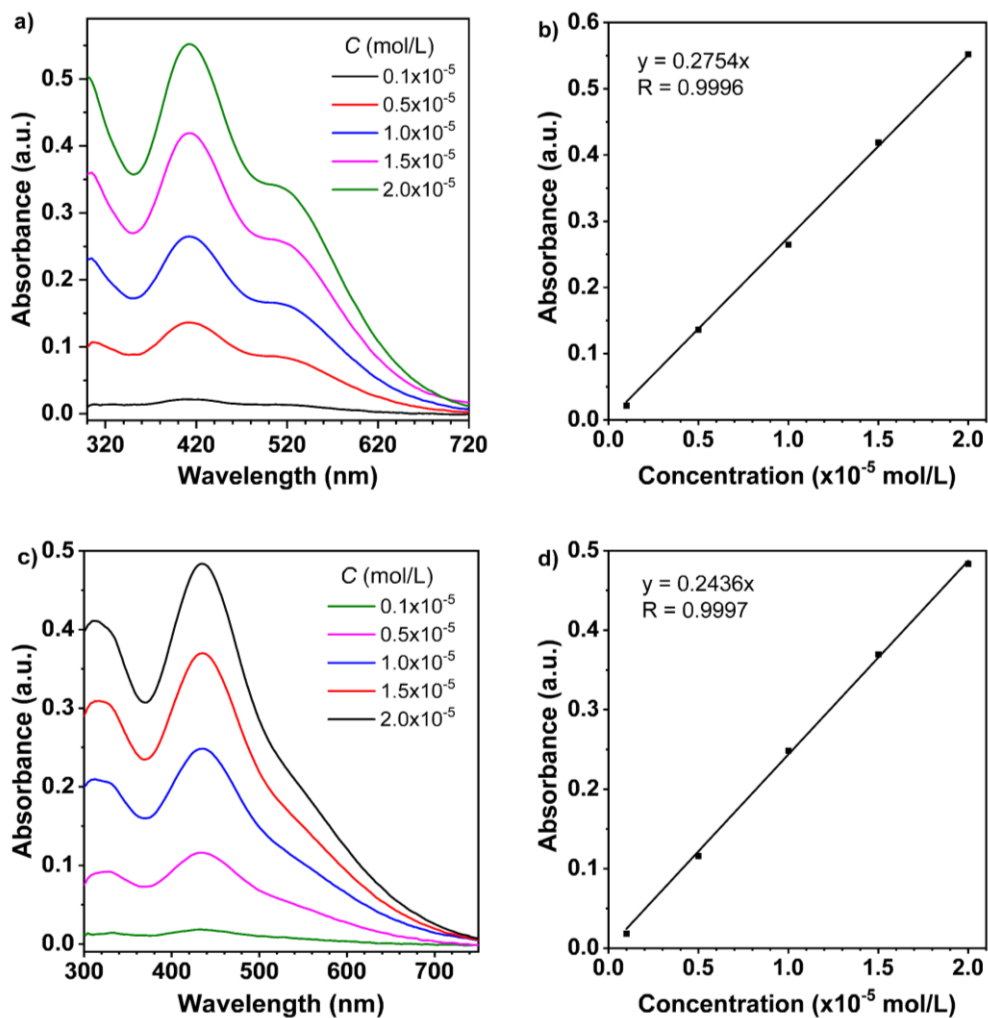


Fig. S50. The UV-Vis spectra of a) TPACzPy and c) TPACzQu solutions at different concentrations. The linear relationship between absorbance and concentration of b) TPACzPy and d) TPACzQu.

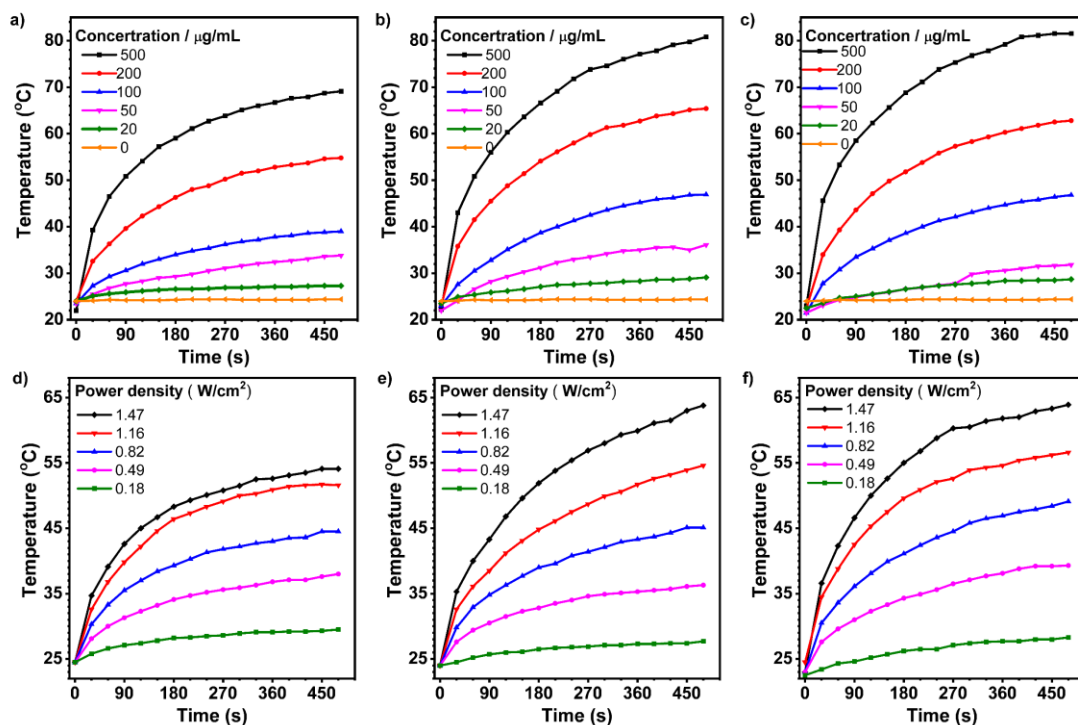


Fig. S51. Photothermal behaviors of a) TPAPy, b) TPAQu, and c) TPACzQu NPs at different concentrations (660 nm, 1.47 W/cm^2). Photothermal behaviors of d) TPAPy, e) TPAQu, and f) TPACzQu NPs at different power densities (660 nm, 200 $\mu\text{g/mL}$).

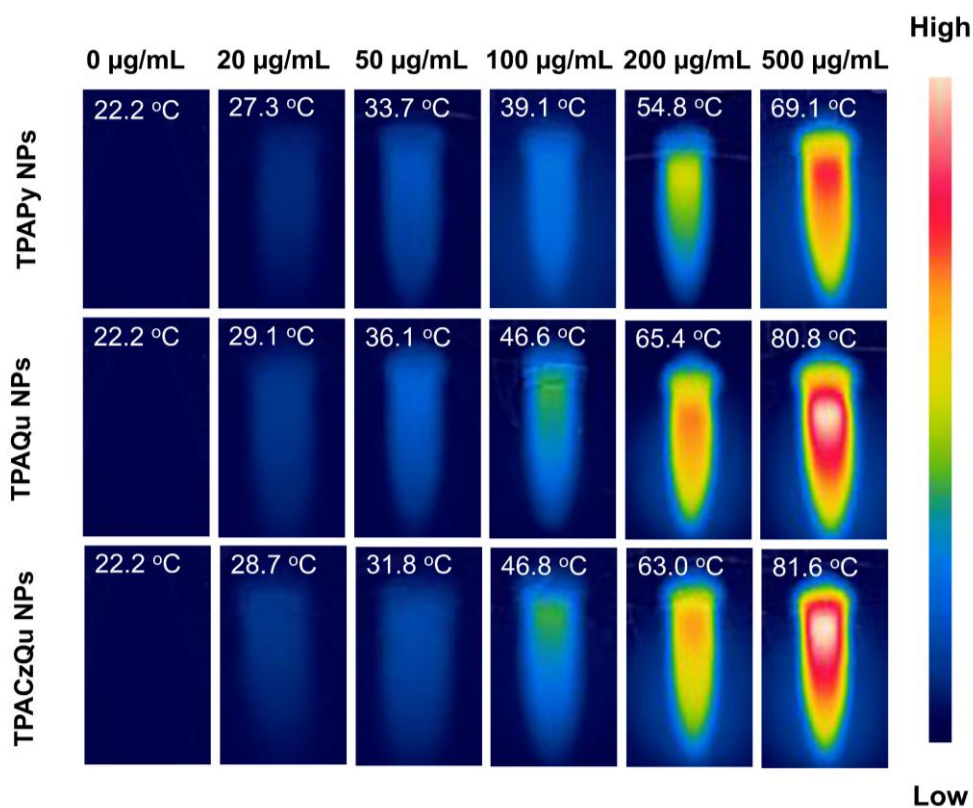


Fig. S52. Photothermal images of TPAPy NPs, TPAQu NPs, and TPACzQu NPs (at different concentrations) when irradiated with 660 nm laser for 8 minutes (1.47 W/cm^2).

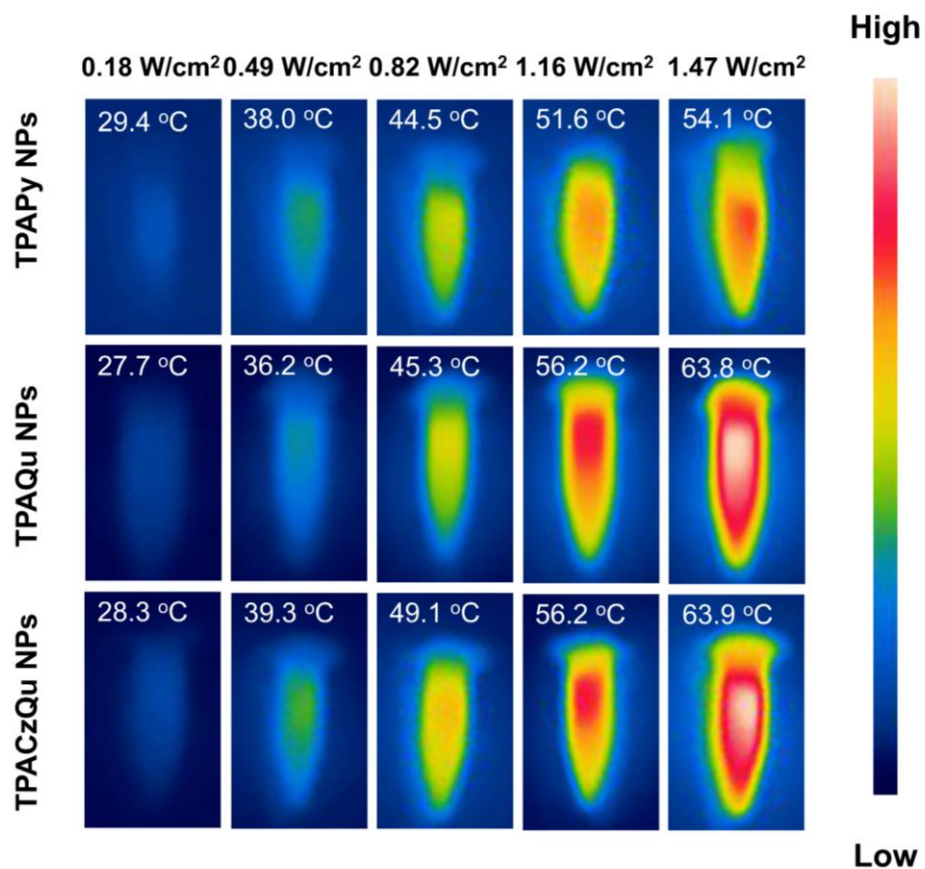


Fig. S53. Photothermal images of TPAPy NPs, TPAQu NPs and TPACzQu NPs when irradiated with 660 nm laser (at different power densities) for 8 minutes (200 μ g/mL).

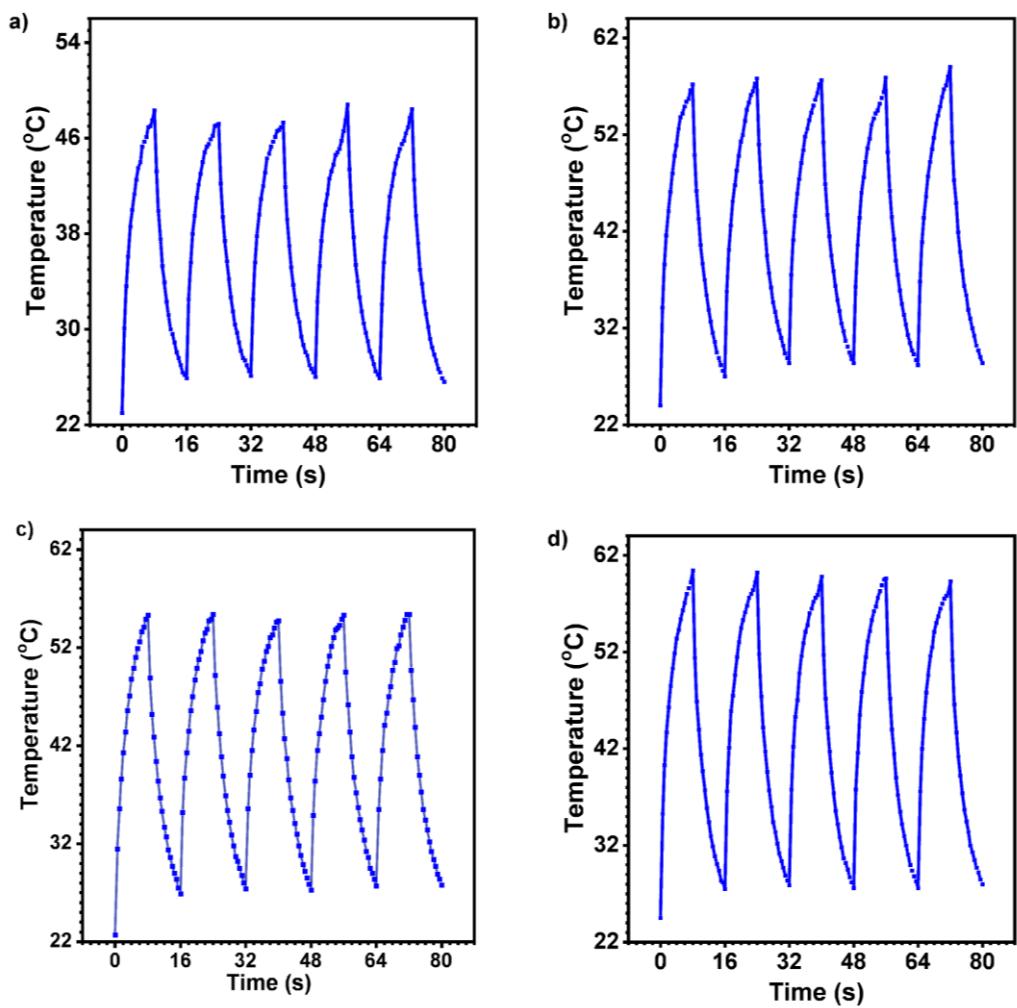


Fig. S54. The Photothermal stability of a) TPAPy, b) TPAQu, c) TPACzPy, and d) TPACzQu (660 nm, 1.16 W/cm², 200 µg/mL).

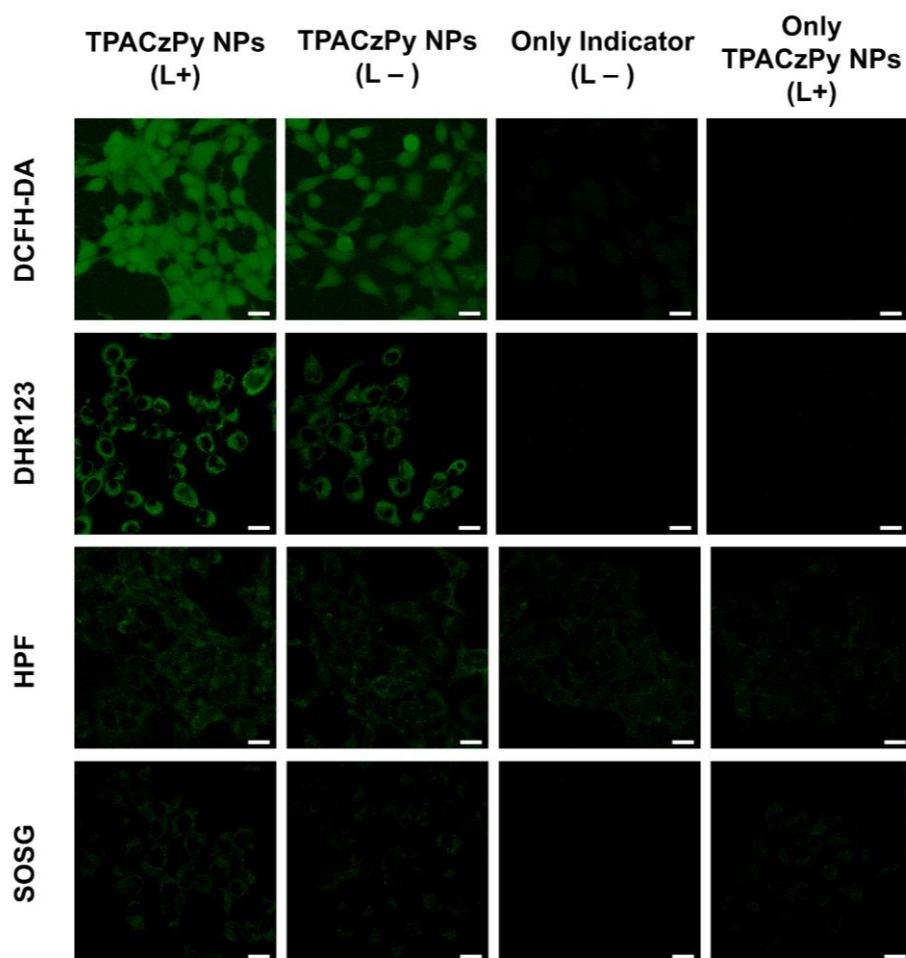


Fig. S55. Intracellular ROS, $O_2^{\cdot-}$, $\cdot OH$ and 1O_2 detection of TPACzPy NPs (4T1 cells), accessed by DCFH-DA, DHR123, HPF, and SOSG, respectively. DCFH-DA: λ_{ex} = 480 nm, λ_{em} = 490–550 nm, DHR123: λ_{ex} = 480 nm, λ_{em} = 500–550 nm, HPF: λ_{ex} = 495 nm, λ_{em} = 490–600 nm, SOSG: λ_{ex} = 480 nm, λ_{em} = 490–550 nm. Scale bar = 20 μm .

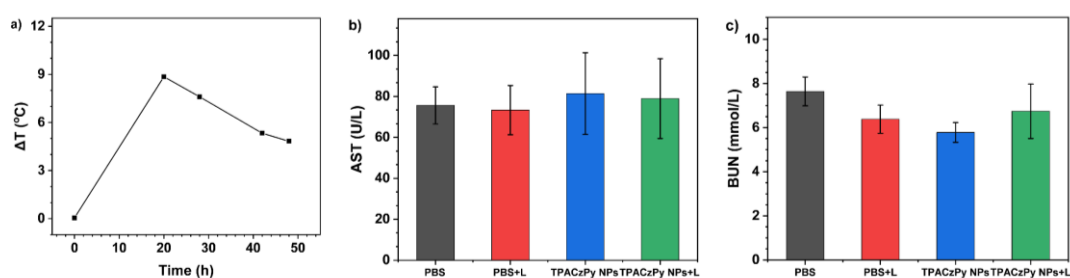


Fig. S56. a) The temperature difference between the mice injected with TPACzPy NPs and PBS for 20 h using 660 nm laser at the tumor site for two minutes. b, c) Blood biochemistry indices (aspartate aminotransferase (AST) and blood urea nitrogen (BUN) of the mice obtained at day 7 after treatment.

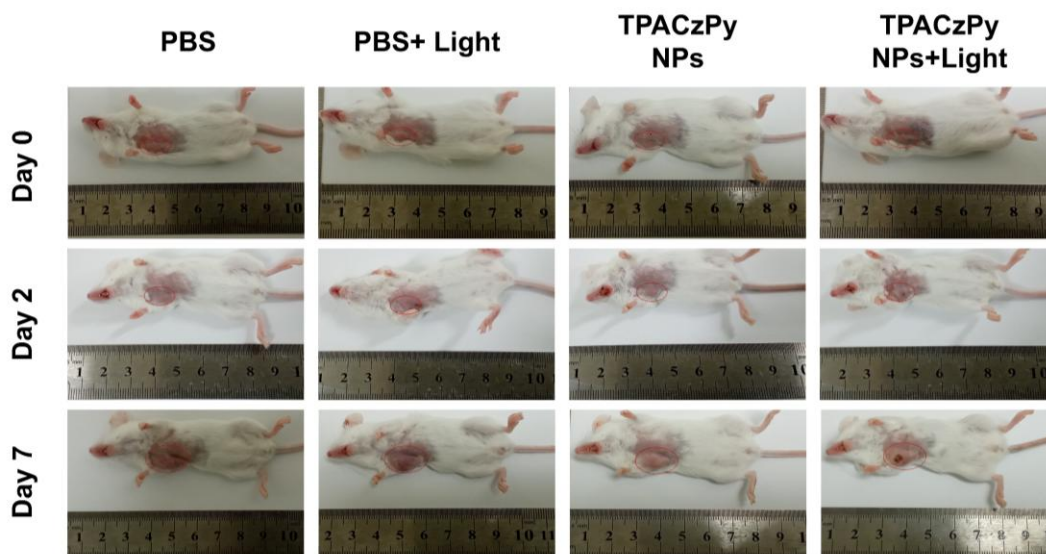


Fig. S57. Photographs of 4T1 tumor-bearing mice in different groups on day 0, 2 and 7 during the treatment process.

Reference

S1 Gaussian 16, Revision C.01, M. J. Frisch, G. W. Trucks, H. B. Schlegel, G. E. Scuseria, M. A. Robb, J. R. Cheeseman, G. Scalmani, V. Barone, G. A. Petersson, H. Nakatsuji, X. Li, M. Caricato, A. V. Marenich, J. Bloino, B. G. Janesko, R. Gomperts, B. Mennucci, H. P. Hratchian, J. V. Ortiz, A. F. Izmaylov, J. L. Sonnenberg, D. Williams-Young, F. Ding, F. Lipparini, F. Egidi, J. Goings, B. Peng, A. Petrone, T. Henderson, D. Ranasinghe, V. G. Zakrzewski, J. Gao, N. Rega, G. Zheng, W. Liang, M. Hada, M. Ehara, K. Toyota, R. Fukuda, J. Hasegawa, M. Ishida, T. Nakajima, Y. Honda, O. Kitao, H. Nakai, T. Vreven, K. Throssell, J. A. Montgomery, Jr., J. E. Peralta, F. Ogliaro, M. J. Bearpark, J. J. Heyd, E. N. Brothers, K. N. Kudin, V. N. Staroverov, T. A. Keith, R. Kobayashi, J. Normand, K. Raghavachari, A. P. Rendell, J. C. Burant, S. S. Iyengar, J. Tomasi, M. Cossi, J. M. Millam, M. Klene, C. Adamo, R. Cammi, J. W. Ochterski, R. L. Martin, K. Morokuma, O. Farkas, J. B. Foresman and D. J. Fox, Gaussian, Inc., Wallingford CT, 2019.